Portland State University

PDXScholar

7-22-2022

Orthotrichum lyellii as an Active Moss Biomonitor: Examining the Interplay between Ambient PM$_{10}$, Bulk Deposition and Heavy Metals in an Urban Environment

Scott Bradley Kiel
Portland State University

Orthotrichum lyellii as an Active Moss Biomonitor: Examining the Interplay

between Ambient PM_{10}, Bulk Deposition and Heavy Metals in an Urban

Environment

by

Scott Bradley Kiel

A thesis submitted in partial fulfilment of the
requirements for the degree of

Master of Science
in
Biology

Thesis Committee:
Todd N. Rosenstiel, Chair
Sarah M. Eppley
Linda A. George
Sarah E. Jovan

Portland State University
2022

Abstract

The importance of monitoring and preventing pollution in the environment is a globally recognized issue. Of the criteria pollutants outlined by the United States Environmental Protection Agency, particulate matter is among these least understood in relation to toxicity and most wide-spread. Many governments have employed continuous air quality monitoring networks to track ambient levels of particulate matter, but are often too widespread to capture the heterogeneity of the urban environment, especially for heavy metal deposition. In Portland, OR, the epiphytic moss *Orthotrichum lyellii* was successfully used as a low-cost passive biomonitor to increase the spatial resolution of pollution around the city, identifying previously unknown heavy metal pollution "hotspots". Though informative, the relationship between environmental concentrations and metal accumulation in moss tissue is still poorly understood. As part of a larger calibration experiment, this study used *O. lyellii* as an active biomonitor deployed across eight experimental sites around Portland, OR along with co-located bulk deposition and PM_{10} monitors over a period of 48 weeks. In addition, an *S. palustre* clone, considered a "gold standard" as an active biomonitor moss, was installed alongside *O. lyellii* under matched conditions and exposed in eight-week intervals over the course of the study. Bulk deposition, PM_{10} and co-located moss tissue for both species were collected and analyzed for 24 elements: Al, As, B, Ba, Ca, Cd, Co, Cr, Cu, Fe, K, Mg, Mn, Mo, Na, Ni, P, Pb, S, Se, Si, Sr, Ti, V & Zn. Results indicate that *O. lyellii* can be successfully used as an active biomonitor and provide quantitative information about the surrounding environment. Significant enrichment of Zn was observed in *O. lyellii* in over 60% of the

i

sites and a significant enrichment of Ni at some sites was identified, confirming the possibility of ongoing exposure at previously identified areas of concern within the city. Unsurprisingly, *S. palustre* showed a greater uptake capacity and greater sensitivity to almost all elements analyzed, especially heavy metals. Spearman correlations were used to compare both species relationship to bulk deposition and PM_{10}, showing significant correlations for multiple metals with both measurements. Both species showed significant correlations with P and B in PM_{10} while *O. lyellii* uniquely correlated with Ca. *S. palustre* had additional significant correlations with K, S, Mn, Fe, Cu, Zn, B, V, Na, Ba, Al and Ti, suggesting a particular sensitivity to PM_{10} deposition on mosses derived from roadways and vehicular traffic. No correlations were seen in either species with heavy metal concentrations in PM_{10}, although longer exposure times may result in better correlations with Cd. Both species showed significant correlations with Al and Co in bulk deposition while *O. lyellii* alone correlated with Cr. Additional correlations were seen in *S. palustre* for Ca, Mn, Fe, Ni, Cu, Zn, V, Sr, Ba and Pb. The results show that *O. lyellii* is uniquely suited to detect Cr in bulk deposition, highlighting species-specific difference in moss metal exchange dynamics. This thesis will further discuss the implications of these results and provide an in-depth analysis that can serve as an informational model for guiding future urban-focused active moss biomonitoring studies.

Table of Contents

List of Tables

iv

List of Figures

1. Introduction

The importance of monitoring and preventing air pollution has become a global issue, as exemplified by legislation and treaties ratified in the US and globally (U.S. Environmental Protection Agency 1963; European Parliament, Council of the European Union 2008; United Nations 2016). Government agencies use an integrated air quality index (AQI) to determine human health safety thresholds. Many criteria pollutants have been identified as having a negative impact on air quality including ozone (O_3), carbon monoxide (CO), sulfur dioxide (SO_2), nitrogen dioxide (NO_2), course particulate matter ($PM_{2.5}$) and fine particulate matter (PM_{10}). Of these pollutants, $PM_{2.5}$ and PM_{10} have a complex relationship to human health since the particles can be fractionally composed of toxic heavy metals—such as Zn, Cr, Ni, As, Cd and Pb—especially in urban area where anthropogenic activity is abundant (Liu et al. 2018). Typically, heavy metal sources occur naturally from degradation of the earth's crust, but human activities greatly increase exposure through industrial effluents, sewage discharge and urban run-off (Jaishankar et al. 2014) . In addition to the many negative effects on human health, heavy metals have a significant effect on ecological, evolutionary and nutritional systems (Nagajyoti, Lee, and Sreekanth 2010) . In most natural systems, heavy metals usually occur at only trace levels and thus require accurate, standardized techniques to ensure data are comparable across all related experiments.

Increased human activity from transportation, industrial processing, and wood fired heating in densely populated areas lead to higher levels of particulate matter in urban environments. Heavy metals can become trapped by aerosols, which eventually deposit

1

back to urban surfaces as dry particulates. Particulate matter is especially concerning to human health due to deposition in the lungs. PM_{10} refers to all particles that have an aerodynamic diameter $\leq 10\mu m$, which are small enough to penetrate deep into human lungs, leading to damage in both the lower and the upper respiratory system (Valavanidis, Fiotakis, and Vlachogianni 2008). Ultra-fine particulate matter $PM_{0.1}$—commonly emitted from vehicular combustion, power plants and forest fires—are small enough to breach the air-blood barrier and enter the blood stream (Shimada et al. 2006; Dean E. Schraufnagel 2020). Therefore, not only does chronic exposure to particulate matter result in a variety of respiratory and cardiovascular diseases, such as asthma or even lung cancer (Russell A. Brunekreef 2009), it can affect almost every organ in the body (D. E. Schraufnagel et al. 2019; Dean E. Schraufnagel et al. 2019).

Acquiring data on heavy metal pollution is labor intensive and expensive because of the equipment needed (Wolterbeek 2002). These limitations also make it difficult to establish a well-dispersed, comprehensive network of air quality monitoring stations, leading to data that is only informative for a relatively small area. Although technology is improving, current methods are woefully inadequate for understanding variation in trace metals exposures across an urban environment, especially in lower income neighborhoods (Lombi 2018). To increase both the spatial-resolution of air quality measures and minimize overall cost, the use of biomonitoring—organisms used to obtain information about surrounding environment quality—has been established as a reliable technique in natural ecosystems (Markert et al. 1999). Some notable biomonitoring studies include the use of moss biomonitoring for: multiple heavy metals (Couto et al.

2

2004; Nickel and Schröder 2017), nitrogen deposition (Harmens et al. 2011), polyaromatic hydrocarbons (Foan et al. 2015; Jovan et al. 2021) and wide array of other trace metals including biologically important cations (Aydogan, Erdag, and Yildiz Aktas 2017; Natali et al. 2016).

The field of biomonitoring can be seen as both a qualitative and quantitative approach to determine environmental quality and monitor pollution (Environment Agency 2007). There are multiple terms used to in the literature to describe biomonitoring organisms including bioindicators, biomonitors and bioaccumulators, Bioindicators provide qualitative information about the environment quality or ecosystem health and can be compared with an instrument measurement. This approach requires a plant to respond to a particular pollutant in order to see how the ecosystem may respond. Biomonitors are also bioindicators, but they hold quantitative information on ecosystem health and the eventual impacts on the ecosystem. Bioaccumulates are organisms that accumulate pollutants within their tissues and are typically unaffected by the presence of those pollutants. These organisms can integrate exposure over time and demonstrate pathways in which pollutants move through an ecosystem. Moss exhibits characteristics for each of these categories and mosses are often referred to as a "bioindicator" or a "biomonitor" depending on the study. For experiments measuring metal concentrations in relation to environmental quality, biomonitor is the more apt and regularly used term because metals are quantified from digested tissue using analytical instrumentation. Biomonitors are generally classified as either passive - organisms collected from sites of natural growth - or active - organisms harvested and exposed under defined conditions.

Both moss and lichen have been used extensively as biomonitors for measuring heavy metals in the environment (Gerdol et al. 2014; Nickel et al. 2014; Owczarek et al. 2001). Unlike vascular plants, mosses lack a root system, have no developed waxy cuticle layer, and have a high cation exchange capacity (Boquete et al. 2013). In addition, mosses can retain particulate matter deposited on their surface (Tyler 1990). These traits allow deposition derived elements to accumulate intracellularly, extracellularly and within vacuoles (Pérez-Llamazares et al. 2011), thus allowing moss to reflect metal concentration in the surrounding environment. A recent study demonstrated the power of this technique by sampling the epiphytic moss *Orthotrichum lyellii* across Portland, OR, revealing previously unknown sources of pollutants too localized to be captured by the current network of air quality equipment (Gatziolis et al. 2016). Though informative, the relationship between environmental concentrations and metal accumulation in moss tissue is still poorly understood due to species differences in biotic regulation, seasonal variation of weather patterns, and cation specific differences in exchange dynamics (Galsomiès et al. 2003). Thus, data acquired through biomonitoring methods are only semi-quantitative, leaving traditional air quality monitoring equipment as the only reliable source of accurate data.

Despite decades of research, there has yet to be a study that finds a direct relationship between environmental deposition and moss tissue concentrations. Although many studies have stated that mosses are good monitors of atmospheric deposition, this is not always the case (Aboal et al. 2010; Boquete et al. 2020). In fact, only 40% of studies comparing bulk deposition—collection of wet deposition (precipitation) and sedimenting

(dry) particles— to moss tissue concentrations have shown significant correlations and many of those correlations are below 0.7 (Boquete et al. 2017). One reason for the lack of clarity in the literature is likely due to the lack of a standardized protocol for the moss technique, leading to research focused on the application of the method rather than the development of the technical aspects (Fernández et al. 2015). In an effort to remedy this, a *Sphagnum palustre* clone was recently isolated for large-scale production of consistent biomass suitable for use as an active biomonitor (Beike et al. 2015). This was a major step forward for the moss bag biomonitoring technique and has led to new research focused on developing a standardized protocol for moss biomonitoring (A. Di Palma et al. 2016; Anna Di Palma et al. 2019). In addition, this has allowed a consistent way to test relative performance of element uptake between different species using this clone of *S. palustre* (Capozzi et al. 2017) as a baseline.

A unified protocol will likely improve our understanding of the potential and limitations of using moss as a biomonitor, however, this does not address the limitation brought about by the complicating issues of moss species-specific difference in uptake and retention of elements. There is just as much variation across studies for biomonitor protocols as there are moss species used in these studies (Ares et al. 2012). Using this standardized *S. palustre* clone would be ideal to limit this variability, but access to this moss tissue is limited, is not yet commercially available, and could be difficult to acquire by municipalities or organizations looking to implement a moss biomonitoring study. Given the limitation of standard moss material for biomonitoring, most moss-based studies utilize locally available/abundant tissue (Fernández et al. 2015). The common

5

epiphytic moss species *Orthotrichum lyellii* has been used extensively for such studies in

Portland, OR and data collected from this species has been used to locate and reduce

emission of heavy metal pollution. Though locally informative (at least with respect to

developing a qualitative spatial understanding of heavy metal abundance) there is still a

poor understanding of how observed concentrations of metals measured in moss tissue

relate to or can inform human exposure.

The overall goal of this study is to significantly improve upon past attempts at

calibrating moss biomonitors by implementing a comprehensive study that co-locates the

S. palustre biomonitoring moss "standard", with a locally abundant biomonitoring

species (*O. lyellii*), adjacent to traditional air quality instrumentation for quantifying

atmospheric heavy metal exposure (PM10 and bulk deposition). In support of this, this

thesis broadly examines three inter-related research questions: 1) How does the

utilization and overall results from *S. palustre* biomonitors in Portland (a relatively clean

urban atmosphere) compare to previous studies? 2) How do two co-located moss species,

S. palustre and *O. lyelli*, compare to each other with respect to the biomonitoring of

heavy metal exposure? 3) How do results from these moss biomonitoring species

compare to results from traditional, instrument-based, measures of atmospheric exposure

to heavy metals?

To explore these questions moss biomonitors, were co-located with bulk deposition

collectors, PM_{10} particle samplers, and micrometeorological stations that were installed at

eight long-term research sites across an urban airshed in Portland, Oregon (USA). Moss

biomonitors were deployed under matched conditions using a standardized moss bag or

"mosspheres"(Capozzi et al. 2016). In order to detect spatial and seasonal variation in heavy metal deposition, both data from the moss biomonitors and air quality instruments were collected frequently during the 48-week experimental period. Finally, this study aims to determine the relative utility of *O. lyellii* as an active biomonitor species, better understand the coherence of the relationship between heavy metal deposition and moss tissue concentrations, as well as the strength of these correlations with direct measurements of deposition both spatially and temporally.

2. Methods

2.1 Site Selection

Initial experimental site locations were selected using a preexisting moss metal content dataset of 346 sites located across the Portland metro area using O. lyellii (Gatziolis et al. 2016). Using this dataset, which showed city-wide distribution of 22 metal Elements, 50 new locations were selected as potential sites for this experiment. During the Summer of 2017, O. lyellii samples were collected within a 10-day period and analyzed for the same 22 elements to ensure that any changes in moss metal content could be accounted for. This new dataset was narrowed down to 8 experimental sites where long-term sampling stations could be established for the course of the study (Figure 1. Map of experimental sites in Portland, OR. Rhombus marker represent sites with low (OES) and high (PWB) urban pollution backgrounds. Square markers represent sites with close proximity of high to moderate traffic (ERL, PFD, UOP). Circle marker represent sites with close proximity to moderate to low traffic (HES, BSP, OHS). Site map was made using an online ArcGIS mapping tool, https://esri.com). Geographic coordinates and description of pollution sources for each site (OES, PWB, HAR, PFD, UOP, HUM, PUM, OHS) are reported in Table 1. It is worth noting that establishing these experimental sites in the city would not have been possible without partnering with community and state organizations. These partnerships allowed for long term access to each site with little disruption to sample collection.

2.2 Experimental Site Setup

For practical reasons and to prevent vandalism, most experimental site housed deposition monitors, a weather station and moss treatments within a 9m^2 coated metal enclosures with 5cm x 5cm gaps as to not impede airflow or particle deposition. Three sites (HAR, HUM, PUM) were housed in larger gated areas and did not need enclosures to be installed. Each site was visited weekly on the same day within a six-hour timeframe over a 48-week period, which included sample collection, maintenance of site conditions and instrument maintenance. Due to difference in sensitivity and collection limitations for each type of measurements, replicates and total number of samples varied per collection period. Additionally, each measurement type was adjusted to match each 8-week moss exposure – referred to as sampling period – for direct comparison between moss and deposition. Table 2 delineates each sampling period, the date range within that period and how each measurement was adjusted to be compared across sampling periods.

2.3 Particulate Matter

Particles with an aerodynamic diameter of $\leq$ 10µm (PM$_{10}$) was collected onto Teflon filters (Tisch Scientific; 2.5µm membrane) using Near Federal Reference Method (N-FRM) sampler (ARA Instruments; Eugene, OR) equipped with a PM$_{10}$ inertial impactor attached to the louvered inlet. PM$_{10}$ was selected over total suspended solids (TSP) because it is more relatable human health and preliminary data showed a large proportion of the elements of interest were found in the PM$_{10}$ fraction. ARA N-FRM monitors were selected as a low-cost alternative to larger scale particulate monitors and have shown to

have high accuracy close to FRM standards (Krug et al. 2021). These battery-operated samplers were set to operate at 16.7L min^{-1} for continuous sampling and data were logged in 5-min intervals, maintaining flow control within ± 2% margin of error. Each sampler was also equipped with a wind anemometer and a particulate counter.

Teflon filters were initially weighed in the lab using an MX5 microbalance (Mettler Toledo) and inserted into a 47mm Teflon filter cassette with an aluminum mesh support designed for the N-FRM sampler. Filters are placed in a cassette holder between the PM_{10} impactor and the monitor inlet for particles to deposit onto. The NFR-M samplers were schedule to run continuously for seven days intervals. Though these samplers are typically used for 24 to 48-hour sampling periods, the longer sampling period in this study did not seem to effect sampling performance (Figure 2). Filters were collected each week by retrieving samples from the intel cassette holder, which was immediately replaced with a clean filter before sampling continued. Exposed filters were stored within machined, aluminum transport cases until the final weight of each filter was measured and sealed in a plastic PetriSlide (Millipore) until chemical analysis. Filters were kept sealed in a controlled environment for 24 hours before the weight was recorded. An unexposed filter (field blank) was carried through the entire collection process to track any potential contamination from the collection procedure. Logged data were also downloaded from each N-FRM sampler each week. On a bi-weekly schedule, sampler inlet components were taken apart and cleaned with DI water mixed with a light detergent (1% (v/v) Liquinox) to removed debris collected on the surfaces of the inlet. Acetone was used for a final rinse to expiated the drying process before components were

reassembled and installed. During this time, an FTS Flow Calibrator (ARA Instruments) was used to ensure sampler flow stayed within 16.7Lpm ± 5% accuracy. If flowrate fell outside of that range, a multipoint flow calibration was performed in the field to correct the error. After 3000hrs of runtime, monitors were sent back for factory recalibration before being redeployed to ensure consistent performance throughout the experiment.

2.4 Bulk Deposition

Bulk deposition – wet and dry deposition – was collected in triplicates using clear, acrylic rain gauges (Cole-Parmer) with a plastic mesh ($3mm^2$) over the inlet funnel to keep out debris. Additionally, plastic spikes were added around the rim to prevent interference from birds. Each rain gauge consisted of an inner measurement tube and an outer tube meant to hold any overfill during heavier rain events. Double reflective insulating wrap was placed around the outside surface of the rain gauge to prevent ultraviolet, visible and infrared light from interacting with the elements in the rai nwater and prevent microbe growth. These monitors where installed on a tripod crossarm (2m height) along with an electronic HOBO logging rain gauge (Onset, RG3) as a reference to control for any evaporation. A solar shielded humidity sensor (Onset, S-THB-M002) was also added to monitor microclimate variation between sites. Both sensors were hooked up to a USB micro weather station and datalogger (Onset, H21-USB).

Bulk precipitation was collected from rain gauges on a bi-weekly schedule. Samples were collected by removing the inner measuring tube, replacing the funnel on the outer overflow tube and pouring the contents back through the funnel and plastic mesh to rinse

through any particles adhered to the outside of the inlet. The contents in the outer container were then swirled and poured into a precleaned high density polyethylene (HDPE) container in a turning motion to catch any condensation on the sides of the container. Bulk deposition samples consisted of primality wet deposition, but small amounts of dry deposition that could land on the rain gauge inlet. During periods of no rainfall ($\leq$ 20ml collection volume), 25ml of bi-distilled water (Resistivity >18 MΩ·cm), acidified with TraceMetal™ grade HNO_3 (Fischer Scientific) to 1% (v/v), was added to the sample before collection. The addition of this volume allowed for collection and chemical testing even when collectors contained primarily dry deposition.

After sample collection was complete, all parts of the rain gauge were rinsed with bi-distilled water acidified to 5% TraceMetal™ gradevHNO_3 (v/v) and air dried before being replaced on the tripod. Samples were brought to the laboratory on the same day within an 8hr timeframe. Collection volume was measured and each sample was acidified to 1% (v/v) with TraceMetal™ grade 70% HNO_3 to preserve the sample and break up larger particles or aggregates within the solution. After a 24hr period, samples were shaken vigorously and aliquoted into an 60ml all plastic syringe with an attached with a 0.45μm 30mm nylon syringe filter. Samples were filtered to remove fine particles from the solution and stored in metal-free HDPE 50mL falcon tubes (Labcon) until analysis.

2.5 Moss Collection and Mossphere Construction

Two moss species were used as material for active biomonitor deployment, *Sphagnum Palustre* (non-local, bioreactor grown) and *O. lyellii* (local, grown naturally).

S. Palustre clone was sourced from the University of Santiago de Compostela, Spain, Department of Functional Biology. The *S. palustre* clone was grown in a photo-bioreactors as described in (Beike et al. 2015) and (Reski et al. 2016). Previous studies have shown the *S. palustre* clone to have low initial metal content within its tissues and high metal uptake capacity, making it an ideal material for active environmental biomonitoring (Capozzi et al. 2017). *O. lyellii* is an epiphytic moss that can be found in British Columbia, Washington, Idaho California and Oregon. *O. lyellii* primarily grows on hardwood trees in large tufts on trunks and branches and is the most common epiphytic moss on street trees found in Portland, OR. These characteristics make *O. lyellii* an ideal biomonitor species for use in Portland, OR. To obtain enough material needed for use in a passive biomonitor apparatus, *O. lyellii* was collected from a single tree in a small patch of forest located at the Oregon Episcopal School (45°28'38.79" N, -122° 45'20.01" W). All materials were collected and stored on the same day to ensure no temporal variation occurred in initial elemental content of the moss tissue.

The *S. palustre* clone material used in this experiment required no cleaning or processing before being packed into mosspheres (spherical shaped, moss weight/bag surface area ratio 10mg cm^{-2}, 2mm mesh size, $\emptyset$ = 11cm) for exposure. The material came packaged, devitalized and pre-cleaned, ready for immediate use. Since *O. lyellii* was collected in natural conditions and has district morphological differences from *S. palustre*, gametophytes were trimmed, cleaned and devitalized before exposure. Using a Petri dish, forceps and scissors sterilized with 70% ethanol, fresh green tissue was removed from each gametophyte according to (Gatziolis et al. 2016). This ensured that

moss tissue used in this experiment was consistent and biologically active without potential contamination for tree bark/soil, insects or necrotic/senescent tissue typically found at the base of the moss patches. To remove debris from leaves and reduce initial metal content, trimmed *O. lyellii* tissue was placed into a plastic sieve (0.7cm^2) and washed with bi-distilled water applying the same method used for the *S. palustre* clone, described here (Capozzi et al. 2016). Seven separate washes were performed using a shaker to agitate the mixture: One wash for 20 min with 10mM EDTA solution (12.5 gDW moss/L), Three washes for 20 min each with distilled water (10 gDW/L), and Three washes for 10 min in bi-distilled water (10 gDW moss/L). Material was then spread out on trays, patted dry with filter paper and placed in a drying oven. To devitalize the tissue, the moss was allowed to dry for 24 hours: 8hrs at 50°C, 8hrs at 80°C and 8hrs at 100°C. Dried material was removed and packed into mosspheres within 24hrs. Devitalization ensured moss element content would not be effect by biotic factors (e.g. new tissue growth, changes in uptake capacity).

Devitalized *S. palustre* and *O. lyellii* was packed into mossphere (Figure 3) using 3g (1.5g per hemisphere) of dry tissue and stored in individual plastic bags prior to exposure. Three mosspheres filled with *S. palustre* were installed at each site. *O. lyellii* was only installed at four of the eight sites (OES, HAR, PWB, PUM) due to the limitation of available moss tissue and the cumbersome, time-consuming steps needed to properly process the moss tissue for an experiment of this scale. Mosspheres were attached to polyvinyl chloride (PVC) pipes and hung at a height of two meters. Exposure took place over 8-week periods for total of 6 total collections over the course of the study. At the

end of each 8-week exposure period, mosspheres were removed from experimental enclosures, exposed moss tissue was removed and stored in kapak bags. Mossphere components were then rinse thoroughly with bi-distilled water and dried before pre-weighed unexposed moss tissue was added and deployed for the next exposure period. On the same day, exposed moss tissue was dried at 40°C for 24-48 hours depending on the degree of tissue water saturation. Once completely dry, moss tissue was sealed in kapak bags to protect from bacterial or fungal growth and stored at 20°C until chemical analysis could be performed.

2.6 Chemical analysis

PM filter analysis – Filter samples containing PM_{10} collected from particulate samplers each week were combined for each four-week period (four filters total) to ensure that trace element content within PM was in a detectable range. All four filters were removed from PetriSlide containers they were shipped in and placed in the same 50ml Teflon digestion and digested as together as one sample. The microwave-assisted digestion method (reagents and microwave program) is the same for the moss analysis described later in this section. Once digestion was complete, samples were diluted in a 25mL volumetric flask, rinsing with bi-distilled water. Flasks were filled to volume, capped and mixed and transferred to plastic storage bottles for subsequent analysis determination of element concentrations by inductively coupled plasma optical emission spectroscopy (ICP-OES) (iCAP 7000 series). Elements analyzed were aluminum–Al, arsenic–As, boron–B, barium–Ba, calcium–Ca, cadmium–Cd, cobalt–Co, chromium–Cr,

copper–Cu, iron–Fe, potassium–K, magnesium–Mg, manganese–Mn, molybdenum–Mo, sodium–Na, nickel–Ni, phosphorous–P, lead–Pb, sulfur–S, silicon–Si, strontium–Sr, titanium–Ti, vanadium–V & zinc–Zn. Each element can be binned into specific classes shown in Table 3 and how data will be group in this paper. As dictated by established standards, plant-essential macro and secondary nutrients are presented as % by dry weight, however detection limits are all calculated as mg/kg. For quality control purposes, method blanks and 4 quality control standards (Agilent) were analyzed for every ten samples during analysis. Quality control data for QCI-710 and Alpha APS-1070 are shown in Table 4 and Ultra IQC-026 and VHG-IPCqY are shown in Table 5 along with instrument detection limits. Most element were ≤ 10% of the expected value except for Cr, Cd, Mo, Na, Ni & Si. None of these elements performed well at trace concentrations below 200ug/L. However, Si was more accurate at higher concentrations.

Bulk deposition analysis – Inductively coupled plasma mass spectroscopy (ICP-MS) (Agilent 7800 Quadrupole) was used to determine elemental composition of bulk precipitation samples for 22 elements including: Al, As, B, Ba, Ca, Cd, Co, Cr, Cu, Fe, K, Mg, Mn, Mo, Na, Ni, P, Pb, Sr, Ti, V & Zn. For quality control purposes, four analytical standards (SCP science) at two different dilutions were chosen for the selected range and elements measured. Quality control data for EnviroMAT™ high drinking water standard (EP-H, Table 6), EnviroMAT™ low drinking water standard (EP-L, Table 7), Quality control standard no. 4 (QC4, Table 8) and ICP-MS verification standard, Sol. A (Ver, Table 9) are presented with instrument detection limits for each element. In addition, an analytical blank (bi-distilled water), reagent blank (bi-distilled water + 70%

HNO$_3$), a method blank (bi-distilled water collected from a rain gauge stored in the lab + 70% HNO$_3$), and a replicate sample were added to each set of 10 samples. Quality control data showed most elements were ≤ 10% expected values except for P, K, Ca, B, Al and Zn, which did not perform well at trace concentrations. However, these elements showed good reliability at higher concentrations shown in Table 7, except for Ca. Due to polyatomic interferences associated with using ICP-MS, Ca did not perform well below 1000µg/L. High ionization energies for Silicon and Sulfur resulted in poor performance on ICP-MS when measuring a broad range of elements and were omitted from the bulk deposition analysis.

Moss tissue analysis – Moss samples were ground into homogenous powder using a mill (IKA Tube mill), stored in polyethylene containers and dried at 40°C for 24hrs. Each sample was weighed out to 0.5g and added to a 50ml Teflon digestion vessel before 10ml of Trace-metal™ grade HNO3 and 2mL of TraceMetal™ grade HCL was added. Samples were left on a shaker overnight in a fume hood to ensure maximal HNO3-imposed oxidation to occur at ambient temperature. The next day, samples were homogenized using a vortex and microwaved digested (CEM MARS 6 digestion oven) using the general plant digest protocol provided by CEM. Once complete, samples were removed from the oven and allowed to cool before 10mL of reagent grade 30% H$_2$O$_2$ was added to each tube. Using the same oven protocol, the samples were microwaved a second time to ensure complete digestion of the plant tissue occurred. All sample were diluted to a total volume of 50mL with bi-distilled water and stored in acid washed HDPE narrow-mouth bottles.

ICP-OES (iCAP 7000 Series) was used for determination of elemental concentrations from moss digest including: Al, As, B, Ba, Ca, Cd, Co, Cr, Cu, Fe, K, Mg, Mn, Mo, Na, Ni, P, Pb, S, Se, Si, Sr, Ti, V & Zn. In order to control for contamination of digest reagents, every 10 samples were accompanied by a method blank (digest solution with no moss tissue). For quality control, every 10 samples were accompanied by two analytical standards and one replicate sample from the digest set to verify accuracy of the instrument. To determine element recovery from digestion, two Standard reference materials were used: IAEA-336 (epiphytic lichen species *Evernia prunastri*) standard reference standard (Table 10) collected in Portugal (international Atomic Energy Agency 1999) and BCR-482 (epiphytic lichen species *Pseudevernia furfuracea*) standard reference material (Table 11) collected in Axalp, Switzerland (Community Bureau of Reference 1995). BCR-482 is certified for Al, As, Cd, Cr, Cu, Ni, Pb and Zn, all other reported element content values are not recommended reference values and is for information purposes. Recoveries for IAEA-336 were between 73% (P) and 118% (As) except for Ca (36%), Ni (45%) and Cd (65%). Recoveries for BCR-482 were between 69% (Cd) and 98% (As) except for B (33%), Na (43%), Mo (44%) and Ca (61%). IAEA-336 content for P, Mg, Ca, Ni, Cr, Cd and Pb are not recommended references values and are for informational purposes. Neither standard reference material has certified values for Si so recoveries are not reported.

2.7 Data processing

The Limit of quantitation of the technique (LOQ_T) for the moss material was determined for each species to control for the variation in elemental content in unexposed tissue (Couto et al. 2004). This is calculated as follow: $xC_i + 1.96sC_i$ where xC_i is mean concentrations of the unexposed moss and sC_i is the corresponding standard deviation (Ares et al. 2015). Criteria for initial comparison of element uptake between species was chosen such that 60% of all measured concentrations (i.e. 43 out of 72) for each element had to be above the LOQ_T for at least one species as used by (Capozzi et al. 2017). All data was analyzed using Microsoft Excel 2016 and R package version 4.0.3. Non-parametric statistical analyses were used data appeared to be not normally distributed according to Shapiro-Wilk test ($p<0.05$). Thus, the Spearman's rank-order correlation was used to determine the significance of the concentrations within species and the Wilcoxon matched pairs test was used to determine the significance of metal uptake between species. Intra-element correlation coefficients were calculated for each moss species using R package 'corrplot': Visualization of a Correlation Matrix (Version 0.92). Spearman correlation coefficients were calculated for comparing moss tissue concentrations to ambient PM_{10} concentrations and bulk deposition.

19

3. Results

3.1 Pre-exposure moss tissue analysis

Element content was measured in unexposed moss tissue before installment in specialized moss bags (Mosspheres) to establish a baseline for accumulation for each element (Table 12). *S. palustre* moss tissue showed lower initial concertation all elements except for Ca, K, Mg, P and S, which fall into the plant-essential macronutrients and plant-essential secondary nutrients classes. Notably, Al, Ba, Fe, Na, Si, Sr and Ti were all many times higher in the *O. lyellii*, indicating the presence of soil mineral elements despite cleaning the moss tissue. Table 13 shows the effectiveness of cleaning *O. lyellii* tissue before exposure by comparing the percent change in element content. In all cases, there was a reduction in total element content in post-washed *O. lyellii*, except for Ba, Na, P and Si. However, overall reduction in element content was lower than expected, especially for soil mineral elements. Content of P and Na were substantially increased in moss tissue after washing, likely due to those elements being difficult to filter out with ion exchange resins.

3.2 post-exposure moss tissue analysis

Descriptive statistics combining all sites and sampling periods are shown for *O. lyellii* and *S. palustre* in Table 14 and Table 15, respectively. *O. lyellii* was only present at four sites (HAR, OES, PUM, PWB; n = 72) and *S. palustre* was present at all eight sites (n=144). *O. lyellii* tissue concentrations were below detection limit (BDL) for Cd (n=4) and As (n=6). *S. palustre* tissue concentrations were BDL for Co (n=2), Cd (n=33), Pb

(n=1) and As (n=77). Fisher-Pearson Skewness for each element was calculated for both

moss species to identify elements with high relative concentrations—a higher skewness

would indicate more extreme values over the total range. This was also used to compare

species to see if both species showed similar sensitivity to the same element. The total

skewness for O. lyellii ranged from -0.4970 (Na) to 1.6098 (Ca) and the total skewness

for S. palustre ranged from -0.1764 (Pb) to 1.0636 (Mo). Elements with the highest

positive skewness for *O. lyellii* was for Ca (1.61), B (1.42), Mn (1.10), Ni (0.90) and Cu

(0.80). Negative skewness was shown in P, Mg, S, Zn, Na, Ti, Al and Si, indicating

extreme values represent low values. The elements with the highest positive skewness for

S. palustre was Mo (1.06), 1.05 (Na), P (0.93), Cu (0.83) and As (0.81). The only element

negatively skewed was Pb (10.18). Both moss species had relatively low skewness

overall indicating that extremely high or low values did not influence to total distribution

of tissue element concentrations.

   To compare relative sensitivity and total accumulation of elements for both moss

species post-exposure moss tissue was paired according sampling period for each site

where both species were present (OES, HAR, PUM, PWB). Percent of accumulation

(PoA) was calculated for each matched pair using $(C_f - C_0/C_0) * 100$ where C_0 is the

concentration of moss tissue before exposure and C_f is the concentration of moss tissue

after an 8-week exposure period. Table 16 shows the minimum, median and maximum

PoA calculated for each species across all sites and sampling periods. In the post

exposure tissue of *O. lyellii*, only Zn met the 60% criterion used for species comparison

reference in the data processing section. Copper was accumulated above the LOQ_T in

44% of the samples and Ca, Ni & B were accumulated in 33%, 36% & 33% of samples, respectively. All other elements were only present in less than 30% of all samples. Sulfur only accumulated in one sample and Na & P never accumulated. The highest median PoA for *O. lyellii* across all sites and sampling periods was 49% (Cu) with a total range from -99% (Cd; matched pair 31) to 328% (Cu; matched pair 10).

S. palustre met the 60% criterion for all elements expect K, Na & S – 11%, 12% & 18% of samples respectively– and Mo & P – both in 8% of samples. For all other elements – Al, B, Ba, Ca, Co, Cr, Cu, Fe, Mg, Mn, Pb, Si, Sr, Ti, V & Zn – the PoA was positive in for than 60% of total samples and will be used for species comparison. The high median PoA was 15,234% (Ti) and overall PoA ranged from -74% (Mo; matched pair 44) and 39,120% (Ti; matched pair 69). The median PoA across all sites and sampling periods was 157%. Extremely high PoA was seen in *S. palustre* for Ti, Al, Si, V, Co, Cd, indicating that the tissue has high sensitivity to these elements in particular. PoA data for each matched pair is reported in appendix under the supplementary data section (Table S1 through Table S12).

3.3 Species Comparison

It should be noted that there is an apparent absence of direct species comparison studies in the literature and much of the data analysis and analytical basis for comparison was provided by (Capozzi et al. 2017). Furthermore, the sphagnum clone used in this experiment was received from that same research group and has allowed for a direct comparison of moss element uptake in *S. palustre* between studies. This is particularly

valuable to moss biomonitor research because biotic differences between moss species and technical differences in methodologies make it difficult to compare bioaccumulation pattern across studies.

Correlation coefficients were calculated for each element observed in each moss species. *O. lyellii* (Figure 4) and *S. palustre* (Figure 5) had similar element correlations indicating that both species accumulated elements from the same source. The strongest positive correlations (above 0.6) were seen in the plant-essential macro and secondary nutrients as well as the soil mineral elements. In contrast, strong negative correlations were often associated between these groups. Spearman correlations were calculated comparing element tissue concentrations between species (Table 17). Elements with high correlations indicates both species accumulated elements similarly during each exposure period. Significant correlations were found for P, K, Ca, S, Fe, Ni, B, Al, Co and Pb.

Boxplots comparing the total distribution of post-exposure tissue concentrations are shown for plant-essential macronutrients (Figure 6), secondary nutrient (Figure 7), micronutrients (Figure 8 & Figure 9), soil mineral elements (Figure 10) and environmentally important trace elements (Figure 11). LOQ_T values calculated for each element is shown in addition to the Wilcoxon Z score to compare respectively: the range of measurements that were significantly enriched and the difference in uptake between the two biomonitors. *S. palustre* showed a higher sensitivity and uptake capacity than *O. lyellii* in all elements used for species comparison across the whole study. Meeting the 60% criterion, *S. palustre* showed significant enrichment in Al, B, Ba, Ca, Co, Cr, Cu, Fe, Mg, Mn, Ni, Pb, Si, Sr, Ti, V & Zn. *O. lyellii* was only significantly enriched in Zn

23

and to a lesser extent for Cu, Ni. The LOQ_T calculated from pre-exposure O. lyellii was always higher – except Ca – despite matched washing procedures. In some cases, LOQ_T of *O. lyellii* was many times higher than the Sphagnum clone, especially for elements associated with soil mineral elements. For example, Al, Si, & Sr were 125x, 110x & 17x higher in pre-exposure tissue concentrations of *O. lyellii* than *S. palustre*. In addition, *S. palustre* was much more sensitive to most environmentally important trace elements – Co, Cr, Cu, Ni & Pb – though the range of tissue concentrations were much closer between species than with soil elements. Element uptake was significantly similar between species for Fe, Cu, Al, Ti, Si and Cd.

Bar charts comparing tissue element concentrations at sites where both species were present are shown for plant-essential macronutrients (Figure 12), secondary nutrient (Figure 13), micronutrients (Figure 14 & Figure 15), soil mineral elements (Figure 16) and environmentally important trace elements (Figure 17) over 6 sampling periods. LOQ_T values calculated for each element are also included to show when mean element concentrations were significantly enriched in moss tissue. These plots show element uptake for *O. lyellii* and *S. palustre* across a pollution gradient where OES has the lowest proximity to sources of pollution, followed by PUM, HAR and PWB with highest. It should be noted that HAR had the closest proximity to frequent roadway traffic, while PWB was closest to industrial sources. Trends in mean element *S. palustre* uptake following this gradient were seen for Fe, Ni, Zn, B, V, Al, Ba, Ti, Si, Cr, Co and Pb. Although significant uptake was not always seen in *O. lyellii* across sites, trends had a similar pattern to *S. palustre* for Fe, Ni, Zn, B, Cr and Pb. Plant essentially macro and

24

secondary nutrients showed stable concentration across sites. Both species showed high

uptake of Ni and Cu at HAR, while only S. palustre picked up Cr and Co from the same

site. The remaining elements did not follow any particular trend across sites and *O. lyellii*

was less sensitive site-specific difference in deposition.

3.4 Cross-study comparison of S. palustre

Unexposed tissue element concentrations in this study and the first species

comparison study using *S. palustre* clone ((Capozzi et al. 2017) were found to be similar

and consistent (Table 18). The percent deviation between studies ranged from, 11% (Fe)

to 98% (V). Element concentrations were almost always lower in tissue used for this

study except Pb, which was 33% higher. The PoA were compared between studies and

showed similar range for Al, As, Ba, Fe, Sr and Zn. Higher ranges were seen in this study

for Cr, Cu Ni and V, however Pb was had higher range in the Capozzi et al study. Lasty,

spearman correlation coefficients were compared between both studies see if there were

there was similar coherence between species for each study. The Capozzi et al. study

compared the *S. palustre* clone to *Pseudoscleropodium purum,* a pleurocarpous, ground

dwelling moss typically found in urban areas and used extensively as a biomonitor for

heavy metals and nitrogen (Harmens et al. 2010). Similar significant correlations were

seen for Fe, V and Zn and to a lesser extent in Al and Ni. Significant correlation for Pb

between species in this study were much lower (0.403 vs 0.798). Correlations for Ba and

Sr were only significant in the Capozzi study and As, Cr and Cu were not significant in

either study.

3.5 Comparison to co-located deposition monitors

Descriptive statistics for element concentration and measurements below instrument detection limit for PM_{10} are shown in Table 21 Element concentrations in PM_{10} were almost all negatively skewed indicating that extremely high values did not occur often. Element concentrations were above instrument detection limit except for Mo (n=3), Fe (n=1), Ni, (n=5), Ba (n=1), Si, (n=1), V (n=5), Co, (n=3), Pb (n=3) and As (n=1). The majority of measurements BDL were at OES and many were associated with the same sample; these values were adjusted to 0. The highest maximum and median concentrations came from Si (2994 ng/m^3), Na, (896 ng/m^3), Fe (910 ng/m^3), Na (896 ng/m^3) and Ca (607 ng/m^3). Table 22 shows that the lowest concentrations of ambient PM_{10} were measured from OES (average 22.6 ± 3.05 µg/m^3). The highest concentrations came from were measured from OHS (average 34.34 ± 3.99 µg/m^3), followed by PWB (average 32.49 ± 3.36 µg/m^3). Table 23 shows the volume of air collected at each site from ARA samplers used to calculate PM_{10} ambient concentrations.

Descriptive statistics for element concentration and measurements below instrument detection limit for bulk deposition are shown in Table 24. Element loading for bulk deposition was all positively skewed with the highest from Mn (1.5101), Co, (1.4998) and Fe (1.4097). Several elements had measurements below detection limit including P(n=41), K (n=36), Ca (n=6), Mo (n=151), Mn (7), Ni (n=1), Sr (n=1), Ti (n=177), Al (n=10), V (n=14), Cr (n=1), Co, (n=1), Cd (n=3) and As (n=47). Although there were a high number non-detects, these include site associated replicate values (n=3) since detection limits were calculated as concentration (µg/L) before conversion to loading. In

addition, many measurement BDL were associated with periods of no precipitation and were set to 0 when loading was calculated. The highest element loading came from Ca (13282 kg/ha), K (11822 kg/ha), Na (4427 kg/ha), Al (2634 kg/ha) and Mg (2238 kg/ha). The highest median values came from Ca (1903 kg/ha), K (1042 kg/ha), Fe (790 kg/ha), Al (457 kg/ha) and Na (431 kg/ha). Table 25 show mean collection at each site across all sampling periods with lowest perception at OHS (average 819 ± 218 mL) and the highest at UOP (961 ± 262 mL).

Spearman correlation coefficients were calculated for each element for comparison between PM_{10} vs both moss species (Table 26) and bulk deposition vs both moss species (Table 27). These values were calculated by combining all sites and sampling periods to encapsulate the complete urban gradient measured by this study. Since two collection periods (four weeks) occurred for each deposition measurement and moss tissue was exposed for a full sampling period (eight weeks), correlations were calculated for both collection periods (CP1 & CP2) in addition to being summed for a full eight-week comparison (CP1+2). This was done to show if there was any temporal variation in correlations. For example, if an element had low correlation during the first collection period and a high correlation during the second collection period, this would indicate that the element accumulates slowly in the biomonitor.

Overall, S. palustre (n=144) had more significant correlations with PM_{10} than O. lyellii (n = 72). Significant correlations for *S. palustre* included P (0.753), S (0.558), Fe (0.446), B, (0.694), V, (0.453), Na (0.574), Ba (0.634), Al (0.351) and Ti (0.495) while *O. lyellii* included P (0.82), Mg (-0.726) and Ca (0.53) for CP1+2. Significant

correlations during CP 1 and CP2 for *S. palustre* included P, Cu, Zn, and Cd, O. lyellii included K, Zn, and Cd, but did not show significance for CP1+2. Surprisingly, in most cases, correlations were higher in CP1 than CP2, however Cd showed higher correlation during CP2. This could indicate that certain elements derived from PM_{10} accumulate and saturate quickly in moss tissues while others accumulate more slowly.

Significant correlations between bulk deposition and *S. palustre* also occurred for more elements than *O. lyellii.* Significant correlation for *S. palustre* included almost all elements except Mg, Ti, Cr, Cd and As (see Table 27 for coefficients) while *O. lyellii* included Mg (0.434), B (-0.502), Al (0.407), Cr (0.603) and Co (0.583) during CP1+2. All significant correlation were found for *S. palustre* during CP1+2 and at least one of the other collection period, however *O. lyellii* correlated with P and V only during CP2. Most elements for bulk deposition vs *S. palustre* showed higher correlation during CP2, except for Ca, Mn, and Pb as well as vs *O. lyellii* for P, Mg, V and Cr. This is the opposite trend seen for correlations with PM_{10} element concentrations.

Abiotic factors likely play a role in accumulation and correlations are not solely based on moss tissue uptake capacity. Weather data was collected at each site for the duration of the study and the average rainfall relative humidity and temperate is shown in Figure 18, including dashed lines are sperate sampling periods. Deposition data was separated by site and sampling period to determine if correlations between biomonitors and deposition measurement vary spatially and temporally. The tradeoff for this analysis is that sample size decreases drastically, which will decrease the number of significant correlations unless strong correlations are found. To visualize trends between measurements type,

timeseries comparing element concentrations of bulk deposition, PM_{10} and *S. palustre* or *O. lyellii* separated by site can be found in the supplementary data section of appendix A (Figure S1 through Figure S44).

Spearman correlations were determined for each element for PM_{10} vs *S. palustre* (Figure 19) and bulk deposition vs *S. palustre* (Figure 20) separated by sampling period. The number of significant correlations increased during period 2 and 3, were lost during sampling period 4, increased during period 5 and decreased during period 6. There were a higher number of significant correlations found in *S. palustre* vs. bulk deposition than PM_{10} when all sampling periods are combined. The number of significant correlations per sampling period followed a similar pattern to the PM_{10} comparison. Periods 1, 2 and 3 had the same number of significant correlations, decrease during period 4, increased again during period 5 and decreased again during period 6. Spearman correlations were also determined for each element for PM_{10} vs *O. lyellii* (Figure 21) and bulk deposition vs *O. lyellii* (Figure 22Figure 20) separated by sampling period. The number of significant correlations were much lower across all sampling periods for *O. lyellii* (n=4) compared to *S. palustre* (n=8) for both sources of deposition. Significant correlations with PM_{10} stayed mostly consistent for all six sampling periods, especially for period 3, 4, 5, and 6. Significant correlations with bulk deposition increased from period 1 to 2, decreased during period 3, increased to the highest number during period and decreased during period 5 and 6.

Spearman correlations were determined for each element for PM_{10} vs *S. palustre* (Figure 23) and bulk deposition vs *S. palustre* (Figure 24) separated by site. The number

of significant correlations for PM_{10} were highest for HUM followed by UOP and lowest at PUM. Significant correlations for bulk deposition were highest for UOP followed by HAR and lowest for PFD. Spearman correlations were also determined for each element for PM_{10} vs *O. lyellii* (Figure 25) and bulk deposition vs *O. lyellii* (Figure 26) separated by site. The number of significant correlations for PM_{10} were highest for PWB followed lowest at PUM. Significant correlations for bulk deposition were highest for PWB and lowest for OES. Spearman correlations were also determined for each element. Overall, there was likely not a big enough sample size to compare *O. lyellii* by site or sampling period.

4. Discussion

4.1 O. lyellii as an active biomonitor

The primary aim of this study was to test the effectiveness of using the epiphytic moss *O. lyellii* as an active biomonitor and present an in-depth analysis to inform readers about best practices when considering the use of moss biomonitors in urban environments. Previous studies that use *O. lyellii* have only measured atmospheric pollutants from *in situ* moss tissue – passive biomonitoring (Donovan et al. 2016; Jovan et al. 2021). Although this method successfully identified previously unknown sources of pollution in city of Portland, it still not well understood how to relate moss tissue concentrations to local atmospheric deposition or human exposure. This statement is not made to discount previous studies, in fact, subsequent testing in areas of concern revealed that the high levels of Cd and Pb were validated by the Oregon department of environmental quality (Burghard et al., 2016). Clearly, *O. lyellii* is an effective tool for informing where traditional air quality instrumentation could be installed for further study, but the purpose of the research outlined in this thesis was to examine if moss biomonitors such as *O. lyellii* might have utility as a direct proxy for human exposure. Using an active biomonitor has been shown to increase the sensitivity and reliability of element tissue concentration by allowing for the establishment of a baseline signal in the moss before exposure and devitalization removes potential biotic effects (Ares et al. 2012). By implementing this technique with *O. lyellii*, we can improve our understanding of exchange dynamics in the moss tissue and develop more informative methods for moss biomonitor studies.

31

The first step typically used for preparing an active moss biomonitor is to collect *in situ* moss followed by cleaning and devitalization of the tissue. Table 13 shows that washing *O.lyellii* was successful for most elements in reducing tissue concentrations, except for P, Na and to a lesser extent Ba and Si. This is not surprising as both P and Na are difficult to remove using ion exchange resins and was likely absorbed by the moss during the washes. Interestingly, soil mineral elements had the least amount of change from washing, potentially due to larger soil particles staying adhered to moss surfaces. Overall, cleaned tissue showed a reduction in baseline concentrations which was used to determine Percentage of accumulation (PoA) during exposure periods. Percentage of accumulations is simply a way to determine relative element enrichment in moss tissue when compared initial tissue concentrations using the formula using $(C_f - C_0/C_0)*100$ (see methods for full description).

Calculating PoA is a useful measurement because it can be used to clearly interpret the absolute change in tissue concentrations before and after exposure. Table 16 shows the range of PoA seen across four sites (OES, HAR, PUM, PWB) and sampling periods. Median values for most elements are positive, indicating that positive accumulation occurred more often than negative accumulation—or leaching. P and Na never accumulated at any site and this is likely due to the accumulation of these elements during the washing protocol. Since tissue concentrations in these elements were enriched before exposure, they were much more likely to leach out of tissues than accumulate. For all other element, accumulation occurred at some point during the experiment, especially Cu, which had the highest maximum accumulation of the elements measured. Most

median PoA values were positive, meaning that many elements accumulation in over half of the samples collected. Aside from P and Na, elements that did not accumulate in more than half of the samples were K, Cd, S, Mn, B and As, although last four were only slightly negative. These results show that *O. lyellii* can be used as an effective biomonitor, giving quantitative information about environmental deposition over 8-week exposure periods. The moss wasn't sensitive enough show accumulation across all sites and sampling periods, but element did accumulate when background concentrations were more often than not in most cases.

In addition to examining elemental accumulation using PoA, a statistical approach was also used to determine significant enrichment of an element in moss tissues by calculating the limit of quantitation of the technique (LOQ_T). This approach is similar to three sigma method used for determining limits of analytical instruments. The LOQ_T is used to calculate the noise of the moss material by accounting the variance around the mean using the formula $xC_i + 1.96sC_i$ (see data processing section for full description). The LOQ_T for *O. lyellii* is shown in Table 12 for each element. The LOQ_T can be compared to the total distribution of the moss biomonitor measurements for each element in Figure 6 through Figure 11 and can be compared to the mean concentrations across sites in figure 12 through Figure 17. In all cases, the median tissue concentrations for *O. lyellii* were below the LOQ_T except for Zn, which showed significant accumulation for more than 60% of the total measurements. Mean tissue concentrations were significantly enriched in Zn for PUM, HAR and PWB showing the expected trend along the pollution gradient. Uniquely, significant enrichment of B was seen at PWB and significant

33

enrichment of Ni was seen al HAR. These results show that *O. lyellii* is particularly good at accumulating Zn across a pollution gradient, but not for the other elements. In fact, many elements are just as likely to leach out of the tissue than accumulate; this result could be a consequence of devitalization of the tissue and may not reflect exchange dynamics of living *O. lyellii*. Despite the generally low sensitivity for most elements, significant accumulation was still observed at sites that have a particularly high background for an element. Past measurements at HAR have shown high concentrations of Ni in the environment and *O. lyellii* as an active biomonitor is capable of picking up that signal from the area over an 8-week exposure period.

It should be noted that the results using the LOQ_T is not a foolproof way to measure determine the effectiveness of a moss species as a biomonitor. The purpose of this analysis is to better understand how the variability of element concentrations in the initial moss tissue may affect sensitivity to environmental deposition and should be viewed as a supplement to the PoA measurements. *O. lyellii* did show accumulation of many elements more often than not, however high variance in the unexposed tissues make that accumulation difficult to quantify. This data is probably more useful for comparing performance of different moss species – discussed in another subsection – than an absolute determination of a species effectiveness as a biomonitor. This is why it was important include co-located measures of deposition, which will be discussed later in this chapter.

Ideally, an active biomonitor would show positive accumulation across all elements, however, this was not the case for *O. lyellii*. The study was set up to capture the

heterogeneity of pollution in the urban environment, thus sites were not selected

specifically for high pollution *per se*. OES, for example, was selected because of its

relatively clean pollution background. In addition, not all sites will have equal amounts of

element deposition across the gradient used in this experiemnt. Multiple types of

comparisons are used in this study in order to fully explore the usefulness of the *O. lyellii*

as an active biomonitor. Although sensitivity was relatively low and significant

accumulation did not occur consistently across the elements, this does not necessarily

suggest that devitalized *O. lyellii* does not hold important information about the

surrounding environment. For example, Gatziolis et al., 2016 measured *in situ O. lyellii*

from a comparable Portland study location and observed Ni tissue concentrations to be

43.5 mg/kg compared to 1.82 mg/kg measured at the same location. Although the

previous study showed a much higher Ni concentration in the surrounding environment,

the active biomonitor showed similar elevation of Ni outside the normal distribution of

concentrations measured at all other sites (Figure 14). Other factors could effect to

difference in tissue concertation including, exospores time, residency time of elements in

tissue, effects of devitalization and timing of collection. This study took place 2 years

after elevated Ni concentration were confirmed in their area and the lower concentration

could be a result of cleanup effort. Regardless, compared to the screening method

employed by the previous study, the active biomonitor was able to pick up the same high

Ni background with much lower sensitivity and a much lower exposure time. Although

this active biomonitoring technique could be refined, *O. lyellii* appears to be a good

active biomonitor capable of identifying high pollution areas around the city and also

provide unique information about exchange dynamics that cannot be determined with *in situ* measurements alone.

4.2 S. palustre clone analysis

   This is the first American study to utilize a *S. palustre* clone specifically selected for its high element uptake capacity and consistency in absorption, especially for Pb (Anna Di Palma et al. 2019). Sphagnopsida is a class of extremely important organisms for ecosystems and the earth's climate, creating peatlands that uptake and store much of the world's carbon (Clymo and Hayward 1982). Within Sphagnopsida, the genus Sphagnum has been shown to have high cation exchange capacity and is most commonly used moss for active biomonitoring (Clymo 1963; Ares et al. 2012). Because of the widespread use of sphagnum, extensive research has been done to establish axenic *in vitro* cultures of Sphagnum grown from single spores (Beike et al. 2015). There are two major advantages of developing these cultures: 1) culturing allows for tissue to be grown from a single spore in bioreactors quickly and in large amounts and 2) using single genotype grown in a controlled environment means all tissue share the same genetic, physiological and environmental background. The S. palustre clone used in this experiment was specifically selected for an active biomonitor materials and is a major step forward for standardizing the moss active biomonitors technique. Even further efforts have been implemented to characterize the moss on a molecular level and determine the bio-surface properties associated with metal uptake (Di Palma et al. 2016; Di Palma et al. 2019), Here we

discuss the performance of this *S. palustre* as a "gold standard" under matched conditions with *O. lyellii*.

The *S. palustre* clone in this experiment was received from the University of Santiago de Compostela in Spain and is the same clone previously used in other moss biomonitor experiments (Capozzi et al. 2017; Anna Di Palma et al. 2019). The moss tissue came pre-cleaned and Table 12 shows that the moss had an extremely low baseline tissue concentrations, especially for soil elements. Because this moss was grown in a bioreactor, baseline tissue concentrations could be kept to a minimum. Notably, Na was very high in initial tissue concentrations, which may be due to the same factors that affected *O. lyellii*. Table 16 shows that positive accumulation in most elements across the entire study. P, K, S, Mo, Na and As were more likely to leach out of tissues, while the rest of the element were more likely to accumulate based on median values. *S. palustre* showed substantial accumulation of soil elements and most environmentally important elements, especially Co, Cd and Cr. The highest accumulation was seen for Ti, Al and V and accumulation was about 1000% at all times. These elements are common soil minerals and indicate that *S. palustre* is extremely efficient at capturing soil particles from the atmosphere. In addition, *S. palustre* always accumulated Cu and Zn, a common transportation pollutant, likely from brake-wear. Common products of industrial practices, Cr, Co and Cd were also accumulated showing *S. palustre* has a high sensitivity to common sources of urban pollution.

The LOQ_T was below median values for most elements except P, K, S, Mo, Na and As. These results indicate that *S. palustre* has a high sensitivity to elements across each

site and sampling periods and can provide a substantial amount of quantitative information. In addition, *S. palustre* trends across sites that follow the expected pollution gradient for Fe, Zn, V, Ba, Al, Ti and Si. *S. palustre* also picked up uniquely high pollution for Ni Cr, and Co at HAR as well as B and Zn at PWB. Clearly, *S. palustre* can provide an abundance of quantitative deposition data across the city with 8-week exposures, even for OES where the pollution background is relatively low. This is in part due to the low initial tissue concentration, which led to an LOQ_T not much higher than the mean concentration of the unexposed tissues. Primarily, these results show that all the work that went into developing the *S. palustre* clone led to a biomonitor material with remarkable ability to accumulate elemental deposition, especially for environmentally important heavy metals. These results show that *S. palustre* performs as an ideal active biomonitor, truly exhibited qualities of a "gold standard" and is sensitive enough to capture the heterogeneity of the urban environment.

4.3 Species comparison: O. lyellii vs S. palustre

The primary purpose of including S. *palustre* in this experiment was to have a standard to compare *O. lyellii* under matched conditions. One of the most common criticisms of moss biomonitor research is that it is difficult to compare results across studies in a meaningful way. A species comparison using standardized tissue can be a useful way to overcome this limitation since this analysis will give context to exchange dynamics throuhg direct comparison. *O. lyellii* and *S. palustre* showed very different responses as active biomonitors. Ideally, an active biomonitor will always accumulate an

38

element in response to environmental deposition. Unsurprisingly, the *S. palustre* out performed *O. lyellii* in both sensitivity and total uptake capacity during the course of the study. In fact, Zn was the only element met the 60% criterion (outlined in the methods section) for both species compared to *S. palustre* meeting that criterion for all elements except P, S, Mo, Na, K and As. These results show the stark difference between the two mosses and helps in understanding what limitations exist with *O. lyellii*. Concentrations measured from *O. lyellii* represent accumulation across a population compared to *S. palustre*, which consists of a single individual. Initial tissue concentrations certainly play a role in why accumulation was difficult to determine in *O. lyellii*, however, the high variation seen in the blank material could be a result of genetic differences rather than specifically environmental differences.

Percent of accumulation of elements over time differed substantially between the two moss species. Median values were almost always higher in *S. palustre* and minimum values in *O. lyellii* were negative for every element. Maximum PoA of *S. palustre* was almost always higher for each element – except K and Ca – especially for soil elements and heavy trace metals. P and K did not accumulate well in either species, which make sense considering plant tissue was devitalized before deployment. There was also weak accumulation in Mg, Ca and S as negative median values for these elements indicate leaching occurred more often than accumulation in tissues. both species had comparable ranges for Mo, Na and As. Aside from Na, soil mineral elements always accumulated in *S. palustre* and median PoA was many times higher. The difference in drastic PoA is in part due to the high initial concentrations of soil mineral element in *O. lyellii*. the range of

PoA for element Cr, Co, Cd and Pb were also higher in *S. palustre* indicating a higher

sensitivity to heavy metals. The data might suggest that the high initial concentrations in

O. lyellii may have reduced the overall uptake capacity of the *O. lyellii*. In other words, a

higher proportion of the surface area in *O. lyellii* was unavailable for particles to adhere

to compared to *S. palustre*. Although ranges are substantially different, negative PoA

seen in *O. lyellii* indicate that tissue concentrations may be equilibrating with the

surrounding environment. This would mean that accumulation of elements in *O. lyellii*

may not be directly related to deposition, but absolute concentrations may better reflect

patterns of deposition in the surrounding environment. Examining associations between

elements within moss tissue can be used to help determine pollution sources. Strong

positive correlations between elements suggest that element originated from the same

source. Element associations for both species are presented for *O. lyellii* (Figure 4) and *S.*

palustre (Figure 5) and show similar patterns of correlations. Correlations between P and

K were high in both species as well as plant-essential micronutrient elements. This is

unsurprising considering that there is a natural abundance of these elements in plant

tissues. There were also high correlations between Mn and Fe in both species. Both

species also show high correlations between soil mineral elements indicating that both

species accumulated soil particles from the atmosphere. S is a combustion product of

sulfur containing fuels and showed correlations above 0.5 for P, K, Mo, Zn and Na for

both species and Mg for only *O. lyellii*. Mo and Zn could be related to vehicular emission

from brakes pads and tires (Zechmeister et al. 2005). Elements measured in this study

that are commonly emitted from industrial source worldwide include As, Cd, Cr, Co, Cu

Mn, Ni, Pb, Zn and V (Jozef M. Pacyna and Elisabeth G. Pacyna 2001). Of these, both mosses showed high positive correlations between Cr, Co, Cu, Mn and V. Uniquely, *O. lyellii* showed a strong correlation between Cu and Cr. These correlations could be evidence of accumulations from industrials sources, however these metals call also be found in soil background concentrations of the Portland basin (Dietz 2013).

Limit of quantitation of the technique (LOQ_T) was calculated by measuring cleaned, unexposed moss tissue for each species. The LOQ_T method is similar to how quantitation limits are calculated for instrumental analysis. The is an inherent noise associated with material that is related to the variation of element concentrations. The lower the variation around the mean, the lower the noise and the easier it is to determine a quantifiable number. Applying this method to moss tissue is a useful approach that gives a statistical basis for quantifiable accumulation. The LOQ_T for each species can be seen as horizontal in lines in Figure 6 through Figure 11 in comparison to the total distribution of moss tissue concentrations across the entire study. The criterion for species comparison was arbitrarily set such that 60% of all measures needed to be above the LOQ_T in at least one species. *S. palustre* met this criterion for all elements except P and S. *O. lyellii* only met the criteria for Zn. It should be noted that this criterion is used for the basis of a species comparison analysis and does not necessarily reflect that quality of information in relation to environmental deposition. These results simply emphasize that in most cases, these species are not directly relatable and exhibit difference exchange dynamics. These values will be compared to direct measures of deposition to gain a clearer understanding of the relationship for each species.

41

The Wilcoxon test showed significant distributions of elements were significantly different for between species for all elements except Fe, Cu, Al, Ti, Si and Cd. This suggests that both species have similar responses to the presence of soil mineral elements, but do not for other elements. Interestingly, despite *O. lyellii* almost never accumulating Cd, both species showed an even distribution in tissue concentration across sites and sampling periods.

In addition to looking at total distribution across the entire study, mean concentrations of both species were compared across the four experimental sites (OES, HAR, PUM, PWB) to determine if similar trends in accumulation were observed. Of these four sites, OES is expected to always have the lowest moss concentrations since it also had the lowest pollution background throughout the study followed by PUM, HAR and then PWB, which had the highest pollution background. Mean concentrations along with the LOQ_T for both species are compared across sites in Figure 12 through Figure 13. Similar trends in accumulation were observed for both species for multiple elements including Ni, Cu, Zn, and B despite mean concentrations being below the LOQ_T. *S. palustre* showed trend along the gradient for multiple elements showing that metal uptake is sensitive enough to reflect the urban pollution gradient. Both species revealed particularly high Ni concentrations at HAR. As mentioned earlier, comparable measurements at HAR revealed high concentration of Ni at that sight two-year prior. Although there was not significant accumulation in *O. lyellii* both species showed an elevated level of Cr and Co at HAR as well, which were also found to be elevated in this area of Portland two years prior. The source of this pollution was determined to be associated with a nearby metal

42

fabrication company (Precision Castparts), in which Ni, Cr and Co were commonly used in metal alloys (Public Health Division, Oregon Health Authority, Public Health Division 2020). This is direct evidence that *O. lyellii* can be successfully be used as an active biomonitor to identify point sources of anthropogenic pollution.

It is clear from this comparison that exchange dynamics between both species are very different and *O. lyellii* is less sensitive overall to element deposition under matched conditions. However, this moss species comparison also shows that, despite the lack of significant accumulation over this study duration, *O. lyellii* can still provide useful information about the surrounding environment. Under matched conditions, *S. palustre* outperforms *O. lyellii* in accumulation for almost all elements. Comparing the maximum PoA for both species (Table 16), value for *S. palustre* were much higher expect for K and Mo, for which values are comparable. This is especially apparent for most soil mineral elements and heavy metals where accumulation in *S. palustre* substantially higher. Methodological changes may improve the information obtained from *O. lyellii*. Adjusting the washing protocols and increasing exposure times would likely improve element accumulation in the tissues and lead to higher sensitivity. The devitalization process may also cause *O. lyellii* more harm than *S. palustre*, outweighing the benefits gained by halting biological activity. In the cation exchange process, most element accumulation primarily occurs via functional organic groups, such as polyuronic acid, located in cell walls (Blagnytė and Paliulis 2010). The devitalization process could impact these functional groups depending on the species and result in a reduction of the cation exchange capacity. Previous studies of show that living *O. lyellii* can have a high uptake

capacity in polluted areas (Gatziolis et al. 2016; Donovan et al. 2016). While that may be due in part to longer exposure, it cannot be ruled that living tissue (unlike devitalized tissue used here) may also be involved in facilitating the high accumulation observed as well. Adjustments to the devitalization protocol or removing it all together should be tested with *O. lyellii* to better determine the effects of this pretreatment on accumulation and sensitivity. Overall, these species do not prove a one-to-one comparison and reveal just how species-specific differences may impact the performance of active moss biomonitors. Although *S. palustre* is much more useful in terms of providing quantitative information about element uptake, this does not necessarily translate to a better correlation with atmospheric element deposition. To investigate this, each moss species was compared to direct measures of deposition co-located at each site.

4.4 Cross study comparisons

Concentrations measured in this studied were compared to (Capozzi et al. 2017)) using the same *S. palustre* clone. This is the first study utilizing the *S. palustre* clone in the United States and the first effort to compare the performance of this specific biomonitor between two long-term urban field studies. Pre-exposure tissue concentrations showed consistent low concentrations for elements measured between the two studies. Mean elemental concentrations in this study were found to be slightly lower, however these differences are minimal when considering the range of accumulation observed in post-exposure tissue. PoA between studies showed a similar range, though should be noted that our exposure time were two weeks longer and our studies covers a much

smaller spatial distribution. Zero or negative Poa was seen in both studies for As, Cr and Ni, which could indicate that *S. palustre* clone does not hold on to these metals well under certain conditions. The rest of the elements always accumulated in studies, except for Zn, which showed a small negative accumulation at -6%. There were similar ranges of accumulation from soil mineral elements, however PoA for V was many times higher. The is likely due to the lower initial concentration determined in this study, but also indicates that Portland may have high V from emission or soil particulates. Higher PoA of Cr, Cu and Ni may be evidence of industrial emission since the study focused only on urban areas. The (Capozzi et al. 2017)) paper showed stronger correlations between *S. palustre* and *Pseudoscleropodium purum* than with *O. lyellii*, which is not surprising since *P. purum* is more similar to *S. palustre* in structure and, unlike *O. lyellii* had much lower initial elemental concentrations. Regardless, both species comparisons showed significant correlations for Al, Fe, Ni, Pb, V and Zn, but not for Ba or Sr. this suggests that all three species accumulate deposition for the same metals. However, *O. lyellii* clearly has a distinct mechanism of exchange and response for Ba and Sr.

4.5 Species comparison to bulk deposition

    The most common measurement used to understand the relationship between moss biomonitors and environmental deposition is bulk deposition. Although most studies do not generally reveal strong correlations between the two measurements (Fernández et al. 2015), it is still a useful tool for understanding element exchange dynamics in mosses, especially for species that have not been used for active biomonitoring. There are also

many different methods to collect and compare overall rates of bulk deposition and much

effort was put into this experiment design to mitigate the impacts from extraneous

variables. Although high correlations would, of course, be the most useful for using moss

to predict bulk deposition, any correlation, or even no correlation, can still give valuable

information about how a particular moss species may exchange elements with their

environments. It should be noted that when comparing deposition data, *S. palustre* was

deployed at all 8 sites, while *O. lyellii* was only deployed at 4 sites due to limitations in

available moss tissue. Because of this, comparisons of *S. palustre* had a larger sample

size and represents a higher spatial resolution across the city.

Spearman's correlations between bulk deposition and both moss species are shown in

Table 27 for all elements. Spearman's correlations were used to determine correlations

and coefficients are based on monotonic relationships rather than linear relationships. To

increase overall deposition measurements, two 4-week collection periods were summed

to represent the full 8-week exposure (CP1+CP2). Correlations were also calculated for

collection period individually to see if there were any differences in the timing of

measurements (refer to table 2 for detailed information on collection periods for each

deposition measurement). Significant positive correlations between *O. lyellii* and the 8-

week bulk deposition sum (CP1+CP2) was found for Mg, Al, Cr, and Co with the

strongest correlations seen in Cr and Co. Significant positive correlations appeared in *S.*

palustre for Ca, Mn, Fe, Ni, Cu, Zn, V, Sr, Ba, Al, Co and Pb, the highest of which were

shown for Ba and Fe. Overall, *O. lyellii* did not show strong correlations between soil

mineral elements and bulk deposition compared to results from *S. palustre,* which shows

significant correlation for each element except Na. This is not surprising considering that *O. lyellii* had high initial concentrations of soil mineral elements, likely from localized growth impacts on tissue concentration or because a greater background of larger soil particles adhered to these field-collected tissues. *S. palustre*, however, exhibited very low initial tissue concentrations and was able to accumulate soil mineral elements and show greater sensitivity than *O. lyellii*. These results indicate that both species can provide information related to bulk deposition across all sites and sampling periods. *S. palustre* correlates with more elements, but *O. lyellii* shows comparable correlations with *S. palustre* for Co and uniquely correlates with Mg and Cr. Both species are able to provide some useful information about heavy metals in bulk deposition. Despite *O. lyellii* not showing significant accumulation with these elements, strong correlations were found which suggests that measurable accumulation isn't solely an indicator of a good biomonitor. Ultimately, a biomonitor is more useful if it reflects deposition in the environment than just having a high cation uptake capacity. Despite the low relative accumulation of Cr, *O. lyellii* was found to have a high significant correlation with Cr and *S. palustre* did not. These results suggest that *O. lyellii* is uniquely suited for determining Cr from bulk deposition and is a species-specific ability.

4.6 Species comparison to PM$_{10}$

A useful measurement of environment deposition relevant to human exposure and associated health risks is PM$_{10}$. These coarse particulates have an aerodynamic diameter $\leq 10\mu m$, can penetrate deep into lung tissue, and with chronic exposure can result in

adverse health effects. In Portland, *O. lyellii* has already been used as a proxy to human exposure, but no study to our knowledge has ever directly measured the correlation between environmental PM_{10} and metal accumulation by an active moss biomonitor under matched conditions. Bulk deposition collectors capture particles in the wet deposition and sedementing particulates that land in the container. The major limitation of this type of measurement is that fine particulates are typically not captured because they are less likely to deposit into the collector or are easily dislodged from the collector by wind gusts. Previous studies have showed that moss surfaces entrap particulate matter, over 95% percent of which are particles in the inhalable fraction (PM $\leq$ 10µm) (Tretiach et al. 2011; Anna Di Palma et al. 2017). Although indirectly, moss biomonitors have been correlated to heavy metals in particulate matter associated with traffic, agriculture and industry (Spagnuolo et al. 2013; Limo et al. 2018; Betsou et al. 2021). In addition, moss biomonitors were shown to coincide with mathematical models of air pollution, including PM_{10} (Svozilík et al. 2021). Thus, measuring PM_{10} alongside active biomonitors will give us a direct measurement of particles often missed by bulk deposition and is much more informative in context to human exposure.

Spearman's correlations between both species and PM_{10} on *O. lyellii* and PM_{10} are shown in table 27. For the full 8-week sum (CP1+CP2), *O. lyellii* showed significant positive correlations with P, Ca, and B while *S. palustre* showed significant positive correlations with P, K, S, Mn, Fe, Cu, Zn, B, V, Na, Ba, Al and Ti. Both species had a high correlation between P, B and PM_{10} and although not always significant with *O. lyellii*, K as well. P, K and B are all found in high concentrations in soils and both species

48

appear to accumulate these from coarse particulate matter as opposed to bulk deposition where all three of those elements were negatively correlated. *S. palustre* had high correlations between PM_{10} and soil mineral elements, especially Na and Ba. Interestingly, Ni did not show significant correlations with PM_{10} even though Ni showed high accumulation in both mosses at HAR. In fact, Ni concentration did not appear to be abnormally in PM_{10} or bulk deposition measurements at that site. Further, only weak correlations (~0.4) were observed between Ni content and bulk dep in *S. palustre*. Taken together, these results suggests that Ni may be primarily deposited to the moss biomonitors as particles larger than PM_{10}.

From a biological perspective, the relationship between P and K in in both mosses show a similar trend. Both mosses show high significant correlations with PM_{10} for P (above 0.7) and to a lesser K. However, these patterns flip in bulk deposition, showing a significant negative correlation in both species. Both of these elements are considered essential nutrients for plants and this may be the first evidence that mosses primary receive these nutrients the coarse particle deposition. This pattern is particularly interesting for *O. lyellii* as it is an epiphytic moss with no direct contact with soils.

Looking at the trends seen across the four sampling sites compared in this study, an interesting pattern is seen with *S. palustre* for B, Zn, V, Mn, Fe, Ba and Ti. each of these metals show a similar trend across sites with increasing proximity to traffic. All of these elements can be associated with stone faction and binder found in assault (Lindgren 1998). Although these metals can be found in other sources of deposition, such as soil crust degradation and industrial processes, many of these elements show similar

49

correlations with PM$_{10}$ in *S. palustre*. These results indicate that moss biomonitors may be especially suited for monitoring human exsposure to roadway derived pollutants.

4.7 Collection period and weather patterns

Comparing the correlations across different collection periods shows that metal uptake for each element is different for both species and both deposition measurements. Moss tissue concentrations and both deposition measurements showed that correlations were almost always better during CP2 than CP1 (Table 26). In some cases, significant positive correlations were only seen during CP2 and were lost when both collection periods were added together. There was a positive correlation between bulk deposition and *O. lyellii* for V during CP2, but not for CP1. Positive correlations were also seen between *O. lyellii* and PM$_{10}$ for K and Zn during CP2 but not CP1. Both species showed a significant correlation for Cd with PM$_{10}$, during CP2, but not CP1. This highlights the importance of taking into account variability in weather patterns during periods of exposure. The relationship between elements derived from dry and wet deposition is complicated and is one of the most difficult challenges to overcome in moss biomonitor research. These results highlight that complicated relationship by showing that there may be an inverse relationship between accumulation in moss tissue between wet and dry deposition. Not just rain events, but the intensity of rain events probably play the biggest role in this relationship because dry particles are more easily removed from moss surface the harder it rains. Additional complications arise since each region or city will have different weather patterns. To improve consistency of tissue concentrations, the type of

deposition should first be considered and exposure periods should be synced up with the weather patterns. Measure of dry deposition, for example, could improve with shorter exposure times and during dry periods.

To determine any effects from seasonal patterns correlations were determined by separating data by site or by sampling period. The limitation of this analysis is that it lowers the sample size and makes it harder to identify significant correlations. Weather data is shown in figure 18 to show seasonal variation across sampling periods. A typical Portland trend is seen where the summer is dry and precipitation steadily increases during the fall, continues through the winter and start to decrease in the spring. Notably, sampling period 1 is the driest and sampling period 3 and 4 was the wettest. An important distinction is that sampling period 3 had multiple smaller rain events while sampling 4 for had to two rain events during the season that much more intense. Strong rain events were found to reduce the number of significant correlations in *S. palustre* with PM_{10} and bulk deposition. This suggests that elements in moss tissues leach at the highest rates during storms and may reduce their reliability as a biomonitor. Interestingly, a similar pattern was not observed for *O. lyellii*, which could indicate that this species is better at retaining elements during a storm event. This could be another feature of an epiphytic moss that has more to lose from heavy rainfall, however, high initial tissue concentrations make *O. lyellii* less reliable for this type of analysis.

4.8 Conclusion

This study presents an in-depth analysis of *O. lyellii* as an active biomonitor in comparison with an emerging "gold standard" moss biomonitoring clone and with direct atmospheric deposition measurements. This is the first American study to use the *S. palustre* clone and tests its performance against another species in a fine scale urban landscape. In addition, this is the first study to test active moss biomonitors as a proxy for human exposure through PM_{10}. The first aim of this study was to assess the usefulness of *O. lyellii* as an active biomonitor. The results here confirm that *O. lyellii* does accumulate elements in tissue in areas with high levels of pollution and that these values can provide quantitative information about atmospheric deposition in those areas. This can be seen clearly for Ni as *O. lyellii* significantly accumulated this element at HAR throughout the experiment. The next aim was to assess the performance of *O. lyellii* as an active biomonitor by comparing it to an *S. palustre* clone under matched field conditions. Unsurprisingly, *S. palustre* outperformed *O. lyellii* in uptake capacity for all elements and had a much higher sensitivity to element deposition, potentially due to lower initial tissue concentrations and differences in absorptivity kinetics. These results show that the two species may have completely different cation exchange dynamics and respond differently as an active biomonitor. More research needs to be done to determine better cleaning methods for *O. lyellii* to reduce initial tissue concentrations and to see if devitalization may negatively impact element uptake in the tissues.

Importantly, this study is one of the first we are aware of to attempt to link moss biomonitors with both bulk deposition and PM10. Our high-resolution *S. palustre* clone

showed a greater number of significant positive correlations with both measures of deposition, suggesting this species is useful for determining multiple sources of deposition. Overall, tissue concentrations in *O. lyellii* also showed significant correlations with bulk deposition, though to a lesser degree than *S. palustre,* and especially for the environmentally important heavy metals Cr and Co. These results may, in part, help to explain the previous success of using this moss species to identify important neighborhood-scale patterns of Cr and Co accumulation from industrial pollution (Gatziolis et al. 2016). These results, plus the observation that soil particles may be a key source of element exposure in moss biomonitors suggests that there are likely to be long-term and persistent exposure from legacy pollutants, despite cleanup efforts (Oregon Health Authority, 2020). This highlights the need to consider best practices for sediment and dust/dirt abatement and dust control in neighborhoods with legacy exposures.

As researchers work to refine the robustness of moss-based biomonitoring studies, results from this work identified the importance of monitoring weather patterns and the negative effect they can have on the effective of biomonitors. The data also suggests that *O. lyellii* may be better at retaining metals during heavy rainfall, but more tested is needed to confirm this. The results found in the study will greatly improve our understanding of the information provided by *O. lyellii* tissue concentrations and provides an active biomonitor approach which, once improved, can provide direct quantifiable element concentrations related to environmental deposition and human exposure. These finding will be applied to results from a much larger associated study that includes additional moss treatments in an ultimate effort to calibrate *O. lyellii* as a cheap

alternative for the quantification of urban-based pollution. Results from these complimentary studies will further explore the role of additional moss treatments including the utility of *in situ* measurements (passive biomonitor) and reciprocal transplants in studying the relationship between metal exposure and metal accumulation in *O. lyellii*. Overall, results from this study will broadly inform moss biomonitor research and help push the moss biomonitor technique in a reliable and widely-used methods for measuring pollution, especially with respect to establishing robust and reproducible sampling methodologies that can be deployed in urban landscapes.

As previously mention, this study is a part of a larger experiment to further calibrate *O. lyellii* as a biomonitor. This study highlights its use an a active biomonitor, but other moss treatments were employed to broaden our understanding of the relationship between tissue concentrations and environmental pollution. Future work will focus on comparing this data to *in situ* measurements of *O. lyellii* collected from the same locations and reciprocal transplant to better understand the long-term exchange dynamics of this species. *O. lyellii* is abundant and well distributed throughout Portland, OR and other cities in the Pacific Northwest. Because of this, *O. lyellii* will continue to be used in this region as a low-cost pollution biomonitor. Further work should include active biomonitor to some degree as it will give unique information about surrounding deposition with in a fixed timescale. One of the major limitations seen in this study is that even with co-located deposition measurements, it is difficult to discern the source of the elements found in the moss tissue. Overall, this study attempts to consolidate many techniques seen across moss biomonitoring literature and present a unified approach to analyzing a

54

potential moss biomonitor species. This research can be used as a guideline for research or organizations that aim to employ this technique, but don't know where to start. Improvements still need to be made to this technique to improve our understanding of how quantitative data from moss tissue can be applied to directly to air pollution, however, this research shows that the utilization of moss biomonitors can be a reliable proxy for human exposure.

Figures and Tables

Figure 1. Map of experimental sites in Portland, OR. Rhombus marker represent sites with low (OES) and high (PWB) urban pollution backgrounds. Square markers represent sites with close proximity of high to moderate traffic (ERL, PFD, UOP). Circle marker represent sites with close proximity to moderate to low traffic (HES, BSP, OHS). Site map was made using an online ArcGIS mapping tool, https://esri.com

Table 1. Coordinates and description of local pollution sources for experimental sites in Portland, OR.

Site ID	Site Name	Sites Description	Latitude	Longitude
OES	Oregon Episcopal School	Low pollution urban background	45°28'25.59" N	-122°45'15.67" W
PWB	Portland Water Bureau	High pollution urban background	45°32'11.36" N	-122°40'21.78" W
HAR	Errol Heights City Park	High roadway traffic	45°27'45.68" N	-122°36'53.36" W
PFD	Portland Forestry Division	High highway traffic	45°36'01.22" N	-122°40'59.07" W
UOP	University of Portland	Moderate to high roadway traffic	45°34'21.73" N	-122°43'22.03" W
HUM	Humboldt Elementary School	Moderate roadway traffic	45°33'29.37" N	-122°40'15.76" W
PUM	Bryant St. Pumphouse	Low roadway traffic	45°34'23.61" N	-122°35'46.30" W
OHS	Oregon Humane Society	Moderate to low roadway traffic	45°34'52.01" N	-122°39'08.39" W

57

Table 2. Sampling period, date range and measurement adjustments used to match up PM_{10} and bulk deposition to moss exposure period.

Sampling Period	Collection period	Start Date	Collection Date	PM_{10} measurements per period	Bulk deposition measurements per period	Exposed moss measurements per period
1	1	7/17/2018	8/14/2018			
	2	8/14/2018	9/11/2018			
2	3	9/11/2018	10/9/2018	n=2	n=4	n=3
	4	10/9/2018	11/6/2018			
3	5	11/6/2018	12/4/2018	Filters collected weekly then 4 filters were combined for analysis for each collection period. Filter were summed for each sampling period.	Bulk deposition samples were collected bi-weekly in triplicates. Mean bi-weekly values were summed for each sampling period.	Moss material collected after an 8-week exposure represented by sampling period. All other measurement were adjusted to match this period for comparison purposes.
	6	12/4/2018	1/2/2019			
4	7	1/2/2019	1/29/2019			
	8	1/29/2019	2/26/2019			
5	9	2/26/2019	3/26/2019			
	10	3/26/2019	4/23/2019			
6	11	4/23/2019	5/21/2019			
	12	5/21/2019	6/18/2019			
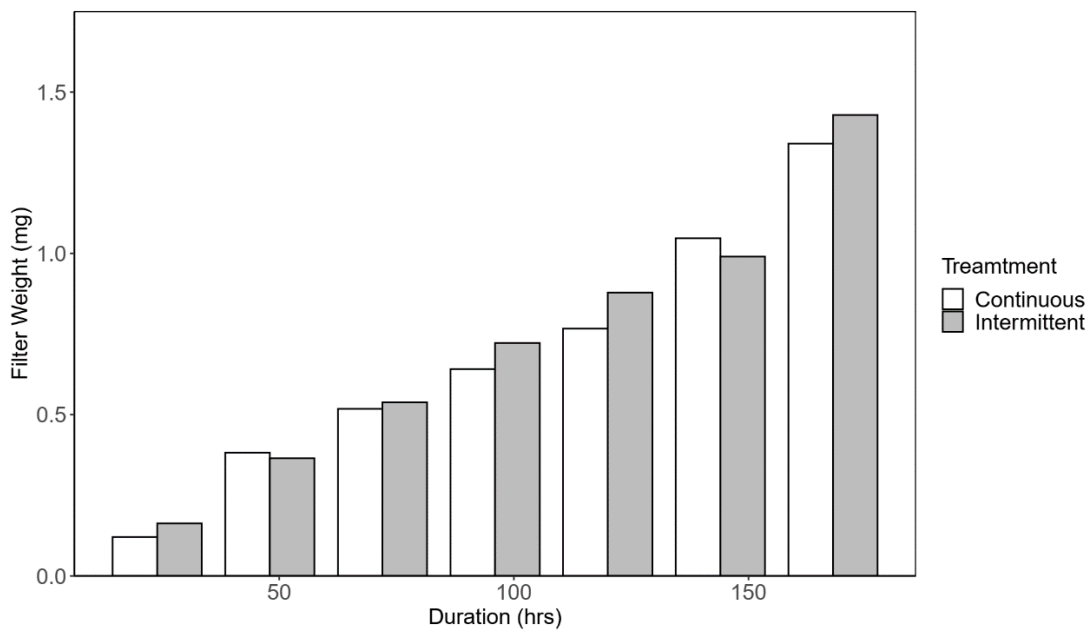
Figure 2. Comparison of filter weights for continuous and intermittent PM_{10} sampling. The white bar represents filter weights measured from a single filter every 24 hours. The gray bar represents seven different filters that were measured at 24, 48, 72, 96, 120, 144, 168, 192 hours.

Figure 3. Mossphere design and assembly

Table 3. Element name and units used for moss tissue concentrations presented in this study. Class column is used to organize elements based on likely relationships in plant tissues.

Element	Symbol	Class
Phosphorus	P (%)	Plant-essential macronutrients
Potassium	K (%)	
Magnesium	Mg (%)	Plant-essential secondary nutrients
Calcium	Ca (%)	
Sulfur	S (%)	
Molybdenum	Mo (mg/kg)	Plant-essential micronutrients
Manganese	Mn (mg/kg)	
Iron	Fe (mg/kg)	
Nickel	Ni (mg/kg)	
Copper	Cu (mg/kg)	
Zinc	Zn (mg/kg)	
Boron	B (mg/kg)	
Vanadium	V (mg/kg)	
Sodium	Na (mg/kg)	Soil mineral elements
Strontium	Sr (mg/kg)	
Barium	Ba (mg/kg)	
Aluminum	Al (mg/kg)	
Titanium	Ti (mg/kg)	
Silicon	Si (mg/kg)	
Chromium	Cr (mg/kg)	Environmentally important trace elements
Cobalt	Co (mg/kg)	
Cadmium	Cd (mg/kg)	
Lead	Pb (mg/kg)	
Arsenic	As (mg/kg)	

Table 4. Quality control data for inductively coupled plasma optical emission spectroscopy as µg/L for quality control standard QCI-710 (n=10) and Alpha APS-1070 (n=12). Detection limits shown as ug/L and the dilution factor (DF) used is shown for each standard.

Element	QCI-710 (DF=5)			Alpha APS-1070 (DF=100)			Detection limit (ug/L)
	Measured mean ± std err	Expected value	Percent Deviation	Measured mean ± std err	Expected value	Percent Deviation	
P	--	--	--	99.2 ± 1.7	100	1%	0.155
K	6919 ± 121	6780	2%	2086 ± 17	2100	1%	0.510
Mg	--	--	--	783 ± 7	800	2%	0.004
Ca	--	--	--	1245 ± 13	1250	0%	0.002
S	2975 ± 76	2710	10%	--	--	--	0.105
Mo	--	--	--	--	--	--	0.038
Mn	--	--	--	1003 ± 10	1000	0%	0.007
Fe	--	--	--	3558 ± 55.9	3500	2%	0.025
Ni	--	--	--	0.973 ± 0.177	2	51%	0.036
Cu	--	--	--	29.4 ± 0.3	30	2%	0.039
Zn	--	--	--	687 ± 12.3	700	2%	0.019
B	--	--	--	--	--	--	0.069
Na	14882 ± 162	15100	1%	1169 ± 41	1000	17%	0.037
Sr	--	--	--	--	--	--	0.001
Ba	--	--	--	67.6 ± 0.8	70	3%	0.003
Ti	--	--	--	--	--	--	0.030
Al	--	--	--	6643 ± 41	7000	5%	0.151
Si	--	--	--	30082 ± 706	30000	0%	0.720
V	--	--	--	7.63 ± 0.08	8	5%	0.023
Cr	--	--	--	6.34 ± 0.22	4	58%	0.021
Co	--	--	--	1.01 ± 0.07	1	1%	0.051
Cd	--	--	--	5.09 ± 0.62	2	155%	0.007
Pb	--	--	--	597 ± 10	600	0%	0.106
As	--	--	--	61.9 ± 3.6	60	3%	0.143
Se	--	--	--	--	--	--	0.305

Table 5. Quality control data for inductively coupled plasma optical emission spectroscopy as µg/L for quality control standard IQC-026 (n=12) and VHG-IPCqY (n=14). Detection limits shown as ug/L and the dilution factor (DF) used is shown for each standard.

Element	Ultra IQC-026 (DF=500)			VHG-IPCqY (DF= 500)			Detection limit (ug/L)
	Measured mean ± std err	Expected value	Percent Deviation	Measured mean ± std err	Expected value	Percent Deviation	
P	--	--	--	1017 ± 25	1000	2%	0.155
K	2063 ± 30	2000	3%	990 ± 49	1000	1%	0.510
Mg	210 ± 4	200	5%	207 ± 2	200	3%	0.004
Ca	213 ± 7	200	7%	204 ± 2	200	2%	0.002
S	--	--	--	--	--	--	0.105
Mo	223 ± 4	200	11%	--	--	--	0.038
Mn	214 ± 1	200	7%	214 ± 2	200.7077	7%	0.007
Fe	184 ± 8	200	8%	--	--	--	0.025
Ni	205 ± 3	200	3%	213 ± 4	200	6%	0.036
Cu	206 ± 2	200	3%	208 ± 5	200	4%	0.039
Zn	215 ± 5	200	7%	216 ± 5	200	8%	0.019
B	194 ± 5	200	3%	196 ± 3	200	2%	0.069
Na	243 ± 8	200	21%	--	--	--	0.037
Sr	--	--	--	212 ± 2	200	6%	0.001
Ba	206 ± 3	200	3%	203 ± 3	200	2%	0.003
Ti	217 ± 2	200	8%	--	--	--	0.030
Al	215 ± 4	200	8%	--	--	--	0.151
Si	138 ± 14	100	38%	--	--	--	0.720
V	217 ± 2	200	8%	217 ± 2	200	9%	0.023
Cr	193 ± 2	200	4%	196 ± 3	200	2%	0.021
Co	210 ± 2	200	5%	220 ± 2	200	10%	0.051
Cd	190 ± 2	200	5%	188 ± 2	200	6%	0.007
Pb	214 ± 4	200	7%	213 ± 4	200	7%	0.106
As	202 ± 4	200	1%	207 ± 3	200	4%	0.143
Se	217 ± 4	200	9%	216 ± 6	200	8%	0.305

Table 6. Quality control data for inductively coupled plasma mass spectroscopy analysis as µg/L for EnviroMAT™ high drinking water standard (n=10). Detection limits calculated from analytical blanks are shown as kg/ha (n=20). Dilution factor (DF) is shown for each standard.

Element	EP-H (DF=1000)			EP-H (DF=10000)			Detection limit[a] (ug/L)
	Measured mean ± std err	Expected value	Percent Deviation	Measured mean ± std err	Expected value	Percent Deviation	
P	25.4 ± 7.8	22.7	12%	8.13 ± 4.30	2.27	258%	18.96[a]
K	748 ± 55	721	4%	114 ± 52	72.1	58%	19.32[a]
Mg	381 ± 5	379	1%	37.9 ± 1.7	37.9	0%	1.94
Ca	1068 ± 73	1160	8%	85.5 ± 23.4	116	26%	77.13
Mo	19.7 ± 0.6	19.8	0%	2.07 ± 0.07	1.98	5%	0.059[a]
Mn	11.3 ± 0.2	10.9	4%	1.210 ± 09	1.09	11%	0.171
Fe	51.5 ± 0.9	48.8	5%	4.76 ± 0.27	4.88	2%	0.625
Ni	26.3 ± 0.5	24.9	5%	2.62 ± 0.10	2.49	5%	0.080
Cu	52.7 ± 1.1	48.6	8%	5.18 ± 0.14	4.86	6%	0.030
Zn	254 ± 5	249	2%	22.9 ± 0.5	24.9	8%	0.513
B	310 ± 19	345	10%	38.6 ± 1.4	34.5	12%	0.77[a]
Na	764 ± 12	754	1%	75.9 ± 3.0	75.4	1%	5.09
Sr	40.1 ± 1.2	37.5	7%	4.53 ± 0.31	3.75	21%	0.076
Ba	80.1 ± 1.7	82.3	3%	8.52 ± 0.29	8.23	4%	0.085
Ti	--	--	--	--	--	--	1.67[a]
Al	19.1 ± 4.0	30.3	37%	5.50 ± 2.78	3.03	82%	4.42[a]
V	39.9 ± 0.7	38.6	3%	3.88 ± 0.09	3.86	0%	0.007[a]
Cr	25.5 ± 0.5	25	2%	2.52 ± 0.09	2.5	1%	0.063[a]
Co	4.01 ± 0.08	3.77	6%	0.385 ± 0.007	0.377	2%	0.011
Cd	4.98 ± 0.06	4.95	1%	0.492 ± 0.012	0.495	1%	0.004[a]
Pb	20.2 ± 0.2	20.4	1%	2.00 ± 0.03	2.04	2%	0.034
As	12.2 ± 0.4	11.8	3%	1.25 ± 0.06	1.18	6%	0.15[a]

[a]Limit of detection was halved (LOD/2) for elements with high numbers of measurements BDL.

Table 7. Quality control data for inductively coupled plasma mass spectroscopy analysis as µg/L for EnviroMAT™ low drinking water standard (n=10). Detection limits calculated from analytical blanks are shown as kg/ha (n=20). Dilution factor (DF) is shown for each standard.

Element	EP-L 1 (DF=1000)			EP-L (DF=10000)			Detection limit[a] (ug/L)
	Measured mean ± std err	Expected value	Percent Deviation	Measured mean ± std err	Expected value	Percent Deviation	
P	25.1 ± 7.5	21	20%	7.77 ± 3.06	2.1	270%	18.96[a]
K	452 ± 62	410	10%	117 ± 59	41	185%	19.32[a]
Mg	43.9 ± 1.5	41	7%	5.15 ± 0.80	4.1	26%	1.94
Ca	584 ± 44	430	36%	64.2 ± 20.9	43	49%	77.13
Mo	24.1 ± 0.4	23	5%	2.54 ± 0.09	2.3	11%	0.059[a]
Mn	6.04 ± 0.19	6	1%	0.567 ± 0.068	0.6	6%	0.171
Fe	29.6 ± 0.5	28	6%	3.16 ± 0.39	2.8	13%	0.625
Ni	21.6 ± 0.4	20	8%	2.15 ± 0.09	2	7%	0.080
Cu	17.5 ± 0.3	16	10%	1.67 ± 0.05	1.6	4%	0.030
Zn	42.7 ± 0.7	43	1%	2.40 ± 0.43	4.3	44%	0.513
B	75.2 ± 4.3	80	6%	9.76 ± 0.83	8	22%	0.77[a]
Na	245 ± 5	230	6%	27.1 ± 2.4	23	18%	5.09
Sr	148 ± 2	140	6%	15.1 ± 0.7	14	8%	0.076
Ba	8.37 ± 0.32	8	5%	0.757 ± 0.088	0.8	5%	0.085
Ti	--	--	--	--	--	--	1.67[a]
Al	110 ± 7	100	10%	15.3 ± 4.9	10	53%	4.42[a]
V	14.6 ± 0.2	14	4%	1.47 ± 0.04	1.4	5%	0.007[a]
Cr	13.6 ± 0.2	13	4%	1.39 ± 0.05	1.3	7%	0.063[a]
Co	10.6 ± 0.2	10	6%	1.08 ± 0.15	1	8%	0.011
Cd	2.17 ± 0.04	2	8%	0.214 ± 0.014	0.2	7%	0.004[a]
Pb	4.15 ± 0.04	4	4%	0.427 ± 0.012	0.4	7%	0.034
As	10.4 ± 0.2	10	4%	1.03 ± 0.04	1	3%	0.0.15[a]

[a]Limit of detection was halved (LOD/2) for elements with high numbers of measurements BDL

Table 8. Quality control data for inductively coupled plasma mass spectroscopy analysis as µg/L for quality control standard no. 4 (n=10). Detection limits calculated from analytical blanks are shown as kg/ha (n=20). Dilution factor (DF) is shown for each standard.

Element	QC4 (DF=1000)			QC4 (DF=10000)			Detection limit[a] (ug/L)
	Measured mean ± std err	Expected value	Percent Deviation	Measured mean ± std err	Expected value	Percent Deviation	
P	--	--	--	9.0 ± 4.0	--	--	18.96[a]
K	963 ± 53	1000	4%	151 ± 53	100	51%	19.32[a]
Mg	100 ± 2	100	0%	10.7 ± 0.7	10	7%	1.94
Ca	59.6 ± 14.8	100	40%	5.9 ± 3.6	10	41%	77.13
Mo	97.5 ± 2.0	100	2%	10.6 ± 0.4	10	6%	0.059[a]
Mn	97.9 ± 2.3	100	2%	10.0 ± 0.17	10	0%	0.171
Fe	99.1 ± 1.9	100	1%	10.1 ± 0.4	10	1%	0.625
Ni	102 ± 2	100	2%	10.3 ± 0.1	10	3%	0.080
Cu	103 ± 2	100	3%	10.6 ± 0.2	10	6%	0.030
Zn	97.2 ± 2.0	100	3%	8.2 ± 0.5	10	18%	0.513
B	89.6 ± 3.7	100	10%	10.8 ± 0.3	10	8%	0.77[a]
Na	98.5 ± 3.3	100	1%	9.6 ± 1.8	10	4%	5.09
Sr	--	--	--	--	--	--	0.076
Ba	98.9 ± 2.4	100	1%	10.0 ± 0.2	10	0%	0.085
Ti	97.2 ± 2.8	100	3%	9.9 ± 1.1	10	1%	1.67[a]
Al	98.7 ± 8.4	100	1%	5.5 ± 1.7	10	45%	4.42[a]
V	98.7 ± 1.6	100	1%	10.0 ± 0.2	10	0%	0.007[a]
Cr	98.9 ± 1.7	100	1%	9.9 ± 0.2	10	1%	0.063[a]
Co	100 ± 2	100	1%	10.1 ± 0.2	10	1%	0.011
Cd	98.8 ± 1.3	100	1%	9.9 ± 0.1	10	1%	0.004[a]
Pb	98.1 ± 1.5	100	2%	9.8 ± 0.1	10	2%	0.034
As	99.6 ± 1.6	100	0%	9.7 ± 0.2	10	3%	0.0.15[a]

[a]Limit of detection was halved (LOD/2) for elements with high numbers of measurements BDL

Table 9. Quality control data for inductively coupled plasma mass spectroscopy analysis as µg/L for ICP-MS verification standard, sol. A (n=10). Detection limits calculated from analytical blanks are shown as kg/ha (n=20). Dilution factor (DF) is shown for each standard.

Element	Ver (DF=100)			Ver (DF=1000)			Detection limit[a] (ug/L)
	Measured mean ± std err	Expected value	Percent Deviation	Measured mean ± std err	Expected value	Percent Deviation	
P	--	--	--	--	--	--	18.96[a]
K	132 ± 51	100	32%	92.5 ± 57.1	10	825%	19.32[a]
Mg	102 ± 2	100	2%	10.2 ± 0.7	10	2%	1.94
Ca	230 ± 22	100	130%	27.6 ± 10.2	10	176%	77.13
Mo	--	--	--	--	--	--	0.059[a]
Mn	101 ± 1	100	1%	10.7 ± 0.4	10	7%	0.171
Fe	102 ± 2	100	2%	10.4 ± 0.3	10	4%	0.625
Ni	103 ± 2	100	3%	10.9 ± 0.2	10	9%	0.080
Cu	104 ± 2	100	4%	11.6 ± 0.2	10	11%	0.030
Zn	101 ± 2	100	1%	8.3 ± 0.4	10	17%	0.513
B	--	--	--	--	--	--	0.77[a]
Na	98.4 ± 2.0	100	2%	13.1 ± 2.7	10	30%	5.09
Sr	101 ± 2	100	1%	10.4 ± 0.3	10	4%	0.076
Ba	103 ± 1	100	3%	10.4 ± 0.2	10	4%	0.085
Ti	--	--	--	--	--	--	1.67[a]
Al	86.2 ± 7.7	100	14%	6.1 ± 2.4	10	39%	4.42[a]
V	101 ± 1	100	1%	10.5 ± 0.2	10	5%	0.007[a]
Cr	101 ± 1	100	1%	10.4 ± 0.3	10	4%	0.063[a]
Co	102 ± 1	100	2%	10.6 ± 0.2	10	6%	0.011
Cd	102 ± 1	100	2%	10.4 ± 0.1	10	4%	0.004[a]
Pb	96.5 ± 1.3	100	3%	9.6 ± 0.1	10	6%	0.034
As	101 ± 2	100	1%	10.5 ± 0.2	10	5%	0.15[a]

[a]Limit of detection was halved (LOD/2) for elements with high numbers of measurements BDL

67

Table 10. Quality control data for inductively coupled plasma optical emission spectroscopy for element analysis of IAEA-336 *Pseudevernia furfuracea* standard reference material (n = 27). Instrument detection limit for each element is mg/kg.

Element	IAEA-336				
	IAEA value (95% CI)	Measured Range	Measured mean ± std err	Recovery	Detection limit (mg/kg)
P (%)	0.061 (0.0490-0.0730)	0.039-0.50	0.045 ± 0.001	73%	0.155
K (%)	0.184 (0.164-0.204)	0.148-0.182	0.164 ± 0.002	89%	0.255
Mg (%)	0.058	0.046-0.055	0.052 ± 0.001	90%	0.004
Ca (%)	0.282	0.049-2.74	0.099 ± 0.003	36%	0.002
S (%)	None listed	0.046-0.274	0.190 ± 0.001	-	0.105
Mo (mg/kg)	None listed	0.005-0.073	0.043 ± 0.002	-	0.038
Mn (mg/kg)	63 (56-70)	54-62	58.2 ± 0.6	92%	0.007
Fe (mg/kg)	430 (380-480)	348-417	393 ± 5.0	92%	0.025
Ni (mg/kg)	1.65	0.53-2.32	0.74 ± 0.01	45%	0.036
Cu (mg/kg)	3.6 (3.1-4.1)	2.5-3.5	2.9 ± 0.04	81%	0.039
Zn (mg/kg)	30.4 (27.0-33.8)	21.5-26.1	24.5 ± 0.25	80%	0.019
B (mg/kg)	None listed	1.1-2.6	1.54 ± 0.07	-	0.069
Na (mg/kg)	320 (280-360)	210-275	257 ± 4.0	80%	0.037
Sr (mg/kg)	9.3 (8.2-10.4)	7.1-8.7	8.1 ± 0.01	87%	0.001
Ba (mg/kg)	6.4 (5.3-7.5)	4.3-6.9	5.3 ± 0.2	83%	0.003
Ti (mg/kg)	None listed	7.0-32.4	16.1 ± 2.1	-	0.030
Al (mg/kg)	680 (570-790)	385-742	538 ± 25	79%	0.151
Si (mg/kg)	None listed	420-1097	717 ± 51	-	0.72
V (mg/kg)	1.47 (1.25-1.69)	0.94-1.573	1.23 ± 0.05	83%	0.023
Cr (mg/kg)	1.06 (0.89-1.23)	0.8-1.3	1.06 ± 0.04	100%	0.021
Co (mg/kg)	0.29 (0.24-0.34)	0.20-0.30	0.24 ± 0.01	84%	0.051
Cd (mg/kg)	0.117 (0.100-0.134)	0.002-0.126	0.074 ± 0.002	65%	0.007
Pb (mg/kg)	4.9 (4.3-5.5)	3.7-5.7	4.9 ± 0.1	99%	0.106
As (mg/kg)	0.63 (0.55-0.71)	0.54-0.99	0.73 ± 0.02	118%	0.143

Table 11. Quality control data for inductively coupled plasma optical emission spectroscopy for element analysis of IAEA-336 *Evernia prunastri* standard reference material (n = 27). Instrument detection limit for each element is mg/kg.

Element	BCR-482				
	BCR value (95% CI)	Measured mean ± std err	Measured range	Recovery	Detection limit (mg/kg)
P (%)	0.069	0.054 ± 0.001	0.046-0.063	78%	0.155
K (%)	0.39	0.335 ± 0.003	0.291-0.048	86%	0.255
Mg (%)	0.0578	0.0453 ± 0.001	0.039-0.049	78%	0.004
Ca (%)	0.2624	0.160 ± 0.001	0.130-0.224	61%	0.002
S (%)	0.2166	0.192 ± 0.002	0.126-0.232	88%	0.105
Mo (mg/kg)	0.85	0.370 ± 0.011	0.314-0.481	44%	0.038
Mn (mg/kg)	33	26.2 ± 0.1	23.8-27.8	79%	0.007
Fe (mg/kg)	804	707 ± 3	644-763	88%	0.025
Ni (mg/kg)	2.47	1.88 ± 0.06	1.62-2.32	76%	0.036
Cu (mg/kg)	7.03	6.63 ± 0.08	5.40-9.08	94%	0.039
Zn (mg/kg)	100.6	76.3 ± 0.04	69.0-93.6	76%	0.019
B (mg/kg)	4.3	1.41 ± 0.04	1.12-2.04	33%	0.069
Na (mg/kg)	119	51.3 ± 2.6	40.2-70.5	43%	0.037
Sr (mg/kg)	10.35	8.91 ± 0.08	8.02-9.60	86%	0.001
Ba (mg/kg)	14.9	10.5 ± 0.1	9.16-12.54	71%	0.003
Ti (mg/kg)	34.2	30.4 ± 2.0	14.1-57.6	89%	0.030
Al (mg/kg)	1103	778 ± 7	450-952	71%	0.151
Si (mg/kg)	Not listed	972 ± 434	214-1834	-	0.720
V (mg/kg)	3.74	3.35 ± 0.02	3.07-3.72	89%	0.023
Cr (mg/kg)	4.12	3.37 ± 0.08	2.83-4.07	82%	0.021
Co (mg/kg)	0.32	0.286 ± 0.004	0.226-0.343	89%	0.051
Cd (mg/kg)	0.56	0.385 ± 0.005	0.315-0.467	69%	0.007
Pb (mg/kg)	40.9	32.1 ± 0.24	29.2-35.7	78%	0.106
As (mg/kg)	0.85	0.832 ± 0.021	0.588-1.29	98%	0.143

Table 12. Mean elemental concentrations with standard deviation in unexposed moss tissue shown as mg/kg (n= 20) and LOQ_T shown as mg/kg (n=20) for both species.

Element	Mean ± std err		LOQ_T	
	O. Lyellii	*S. palustre*	*O. Lyellii*	*S. palustre*
P	0.14 ± 0.01	0.16 ± 0.01	0.16	0.18
K	0.30 ± 0.02	1.08 ± 0.03	0.33	1.15
Mg	0.10 ± 0.01	0.101 ± 0.004	0.11	0.11
Ca	0.18 ± 0.04	0.27 ± 0.02	0.25	0.32
S	0.06 ± 0.01	0.08 ± 0.004	0.07	0.08
Mo	0.35 ± 0.07	2.90 ± 0.26	0.49	3.41
Mn	17.01 ± 5.49	6.56 ± 0.51	27.77	7.55
Fe	557.33 ± 122.00	96.08 ± 12.22	796.45	120.04
Ni	0.62 ± 0.15	0.45 ± 0.07	0.92	0.59
Cu	5.85 ± 1.61	1.52 ± 1.10	9.01	1.88
Zn	12.21 ± 1.70	9.62 ± 0.57	15.54	10.73
B	1.33 ± 0.18	0.23 ± 0.12	1.68	0.46
Na	1988.29 ± 556.67	1793.87 ± 122.90	3079.35	2034.75
Sr	31.97 ± 2.15	1.85 ± 0.08	36.19	2.00
Ba	39.37 ± 7.07	0.39 ± 0.15	53.23	0.69
Ti	60.11 ± 15.16	0.03 ± 0.07	89.82	0.17
Al	447.77 ± 106.05	3.59 ± 1.27	655.62	6.08
Si	801.69 ± 216.63	7.30 ± 3.50	1226.28	14.16
V	1.92 ± 0.44	0.006 ± 0.009	2.79	0.02
Cr	1.68 ± 0.42	0.08 ± 0.08	2.51	0.24
Co	0.27 ± 0.05	0.007 ± 0.009	0.37	0.02
Cd	0.08 ± 0.07	0.002 ± 0.004	0.21	0.01
Pb	1.50 ± 0.45	0.40 ± 0.26	2.38	0.91
As	0.29 ± 0.12	0.20 ± 0.12	0.52	0.44

Table 13. Mean element content (mg/kg) of pre-wash *O. lyellii* (n=8) and post-wash *O. lyellii* (n=20) for 24 elements.

Element	Pre-wash O. Lyellii	Post-wash O. Lyellii	Percent Change
P	0.01 ± 0.02	0.14 ± 0.01	1300%
K	0.94 ± 0.34	0.30 ± 0.02	-68%
Mg	0.18 ± 0.04	0.10 ± 0.01	-44%
Ca	0.42 ± 0.06	0.18 ± 0.04	-57%
S	0.08 ± 0.02	0.06 ± 0.01	-25%
Mo	1.45 ± 2.92	0.35 ± 0.07	-76%
Mn	27.67 ± 3.70	17.01 ± 5.49	-39%
Fe	664.57 ± 104.56	557.33 ± 122.00	-16%
Ni	3.34 ± 6.78	0.62 ± 0.15	-81%
Cu	7.32 ± 1.42	5.85 ± 1.61	-20%
Zn	27.75 ± 3.77	12.21 ± 1.70	-56%
B	6.86 ± 3.31	1.33 ± 0.18	-81%
Na	288.95 ± 70.33	1988.29 ± 556.67	588%
Sr	39.04 ± 6.22	31.97 ± 2.15	-18%
Ba	37.39 ± 6.45	39.37 ± 7.07	5%
Ti	81.46 ± 10.24	60.11 ± 15.16	-26%
Al	477.79 ± 60.36	447.77 ± 106.05	-6%
Si	749.89 ± 115.90	801.69 ± 216.63	7%
V	2.43 ± 0.39	1.92 ± 0.44	-21%
Cr	2.14 ± 1.62	1.68 ± 0.42	-21%
Co	0.39 ± 0.06	0.27 ± 0.05	-31%
Cd	0.11 ± 0.03	0.08 ± 0.07	-27%
Pb	3.12 ± 0.34	1.50 ± 0.45	-52%
As	0.34 ± 0.17	0.29 ± 0.12	-15%

Table 14. Descriptive statistics for post exposure *O. lyellii* across all sampling periods and sites (HAR, OES, PUM, PWB), n=72.

Element	Minimum	Maximum	Mean	Median	Fisher-Pearson Skewness coefficient	Samples below detection limit
P	0.0446	0.1435	0.0911	0.0920	-0.1032	0
K	0.1334	0.5033	0.2199	0.1986	0.8860	0
Mg	0.0633	0.1303	0.1075	0.1087	-0.3027	0
Ca	0.1376	0.3775	0.2427	0.2020	1.6098	0
S	0.0436	0.0716	0.0599	0.0601	-0.1320	0
Mo	0.2240	0.5995	0.3939	0.3843	0.3709	0
Mn	11.5949	28.6484	18.3766	16.5672	1.1028	0
Fe	352.2391	1032.9283	610.8041	605.8291	0.1063	0
Ni	0.4110	1.8210	0.8904	0.8030	0.9027	0
Cu	4.5656	25.0109	9.7634	8.6888	0.8032	0
Zn	11.2929	22.2621	16.7779	16.8631	-0.0972	0
B	0.6215	4.5973	1.7634	1.3061	1.4201	0
Na	125.0240	1655.6174	926.6330	1019.0805	-0.4970	0
Sr	22.5152	39.9090	34.1939	34.0273	0.1718	0
Ba	33.1622	56.0197	42.0339	41.0217	0.4910	0
Ti	16.3464	125.8733	67.1709	68.3645	-0.1709	0
Al	198.2077	707.5322	478.9548	497.4194	-0.4855	0
Si	33.5330	1264.3945	804.1570	839.3226	-0.4514	0
V	1.1200	3.3309	2.0583	2.0409	0.1173	0
Cr	0.8520	3.2214	1.9104	1.8808	0.1776	0
Co	0.1818	3.0500	0.3632	0.3109	0.4767	0
Cd	0.0005	0.2289	0.0774	0.0662	0.6321	4
Pb	0.5462	3.2531	1.8625	1.8190	0.2471	0
As	0.0055	0.7284	0.3040	0.2864	0.3946	5

72

Table 15. Descriptive statistics for post exposure *S. palustre* across all sampling periods and sites (OES, PWB, HAR, PFD, UOP, HUM, PUM, OHS), n=144.

Element	Minimum	Maximum	Mean	Median	Fisher-Pearson Skewness coefficient	Samples below detection limit
P	0.0642	0.2315	0.1024	0.0920	0.9311	0
K	0.3733	1.7276	0.6829	0.6204	0.6512	0
Mg	0.0954	0.1979	0.1355	0.1335	0.3356	0
Ca	0.2857	0.5851	0.4224	0.4185	0.1932	0
S	0.0542	0.1261	0.0739	0.0719	0.4447	0
Mo	0.7430	4.5557	1.9433	1.6015	1.0636	0
Mn	7.9079	27.2152	14.3617	13.6819	0.6574	0
Fe	160.7526	743.2083	352.1792	333.1681	0.4914	0
Ni	0.2101	19.1956	0.9902	0.6202	0.6516	0
Cu	1.9903	16.4665	5.4793	4.7343	0.8257	0
Zn	11.6548	36.5005	20.0762	19.1175	0.5789	0
B	0.0463	3.9709	0.8748	0.7018	0.8333	0
Na	570.4022	2943.5776	1151.2644	976.9003	1.0550	0
Sr	2.4283	10.4457	4.6352	4.3107	0.6560	0
Ba	1.3447	11.0113	4.6746	4.2821	0.6157	0
Ti	6.0477	66.9113	24.9410	23.5951	0.3249	0
Al	56.9247	433.9541	201.4874	190.1452	0.4089	0
Si	36.9802	685.0439	321.1974	300.0699	0.4427	0
V	0.2204	1.6851	0.7217	0.6795	0.3813	0
Cr	0.0829	3.7117	1.1074	0.9836	0.5708	0
Co	0.0468	0.7358	0.1611	0.1352	0.7448	2
Cd	-0.0007	1.4045	0.0495	0.0309	0.4446	33
Pb	-0.2668	3.3151	1.2835	1.3137	-0.1764	1
As	-0.1048	1.1783	0.1760	0.1304	0.8102	76

73

Table 16. Minimum, median and maximum percent of accumulations in *O. lyellii* (O) and *S. palustre* (S) for all sites and sampling periods.

Element	Min O	Median O	Max O	Min S	Median S	Max S
P	-69%	-36%	0%	-59%	-43%	42%
K	-55%	-33%	70%	-65%	-40%	60%
Mg	-37%	8%	29%	1%	42%	97%
Ca	-22%	14%	113%	6%	55%	103%
S	-31%	-5%	13%	-23%	-6%	67%
Mo	-37%	8%	69%	-74%	-45%	45%
Mn	-32%	-3%	68%	21%	103%	315%
Fe	-37%	9%	85%	67%	237%	674%
Ni	-34%	29%	193%	-54%	45%	834%
Cu	-22%	49%	328%	82%	346%	1033%
Zn	-8%	38%	82%	21%	94%	280%
B	-53%	-1%	247%	5%	214%	1611%
Na	-94%	-49%	-17%	-64%	-44%	64%
Sr	-30%	6%	25%	32%	147%	466%
Ba	-16%	4%	42%	242%	917%	2704%
Ti	-73%	14%	109%	3675%	15234%	39120%
Al	-56%	11%	58%	1486%	5300%	11987%
Si	-96%	5%	58%	407%	4138%	9284%
V	-42%	6%	73%	3774%	12196%	28219%
Cr	-49%	12%	91%	0%	1294%	4370%
Co	-33%	14%	129%	566%	2160%	10359%
Cd	-99%	-17%	187%	-100%	798%	9164%
Pb	-64%	21%	117%	52%	253%	730%
As	-98%	-1%	152%	-100%	-8%	220%

Figure 4. Correlation matrix of element concentrations in post-exposure *O. lyellii*. Colors represents correlation coefficient thresholds set at 0-0.2 (light grey), 0.2-0.6 (dark grey), and 0.6-1.0 (black). The same colors scheme is used for negative correlation coefficients.

Figure 5. Correlation matrix of element concentrations in post-exposure *S. palustre*. Colors represents correlation coefficient thresholds set at 0-0.2 (light grey), 0.2-0.6 (dark grey), and 0.6-1.0 (black). The same colors scheme is used for negative correlation coefficients.

Table 17. Spearman correlation coefficients for elements concentrations in *O. lyellii* and *S. palustre.* *p < 0.05, **p < 0.01, ***p < 0.001., n = 72.

Element	Spearman coefficient
P	0.904***
K	0.672***
Mg	-0.156
Ca	0.408*
S	0.561**
Mo	0.271
Mn	-0.116
Fe	0.412*
Ni	0.438*
Cu	0.245
Zn	0.400*
B	0.665***
V	0.474*
Na	-0.129
Sr	0.055
Ba	-0.009
Al	0.489*
Ti	0.370
Si	0.355
Cr	0.386
Co	0.562**
Cd	0.145
Pb	0.403*
As	-0.087
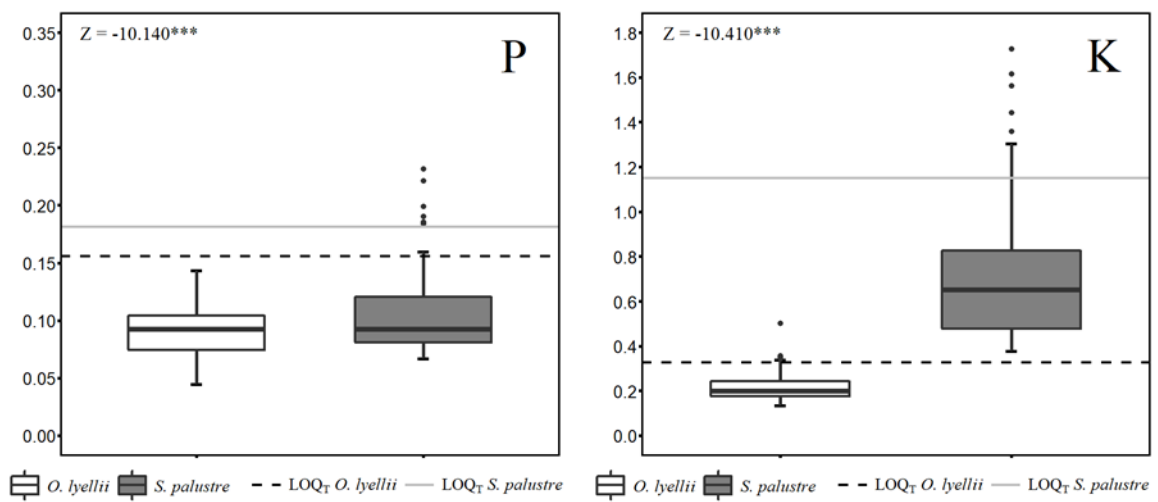
Figure 6. Boxplots of post-exposure moss tissue concentration (mg/kg) for plant-essential macronutrients across all matched pair sites (HAR, OES, PUM, PWB) and all sampling periods for *O. lyellii* (white) and *S. palustre* (grey), n=72. LOQ_T is represented by the dashed black line (*O. lyellii*) and the grey (*S. palustre*). Boxes show median, 1st and 3rd quantiles; whiskers show ±1.5 x Interquartile range (IQR). Significance of accumulation was calculated from Wilcoxon matched pair test (top-right).
*p < 0.05, **p < 0.01, ***p < 0.001.
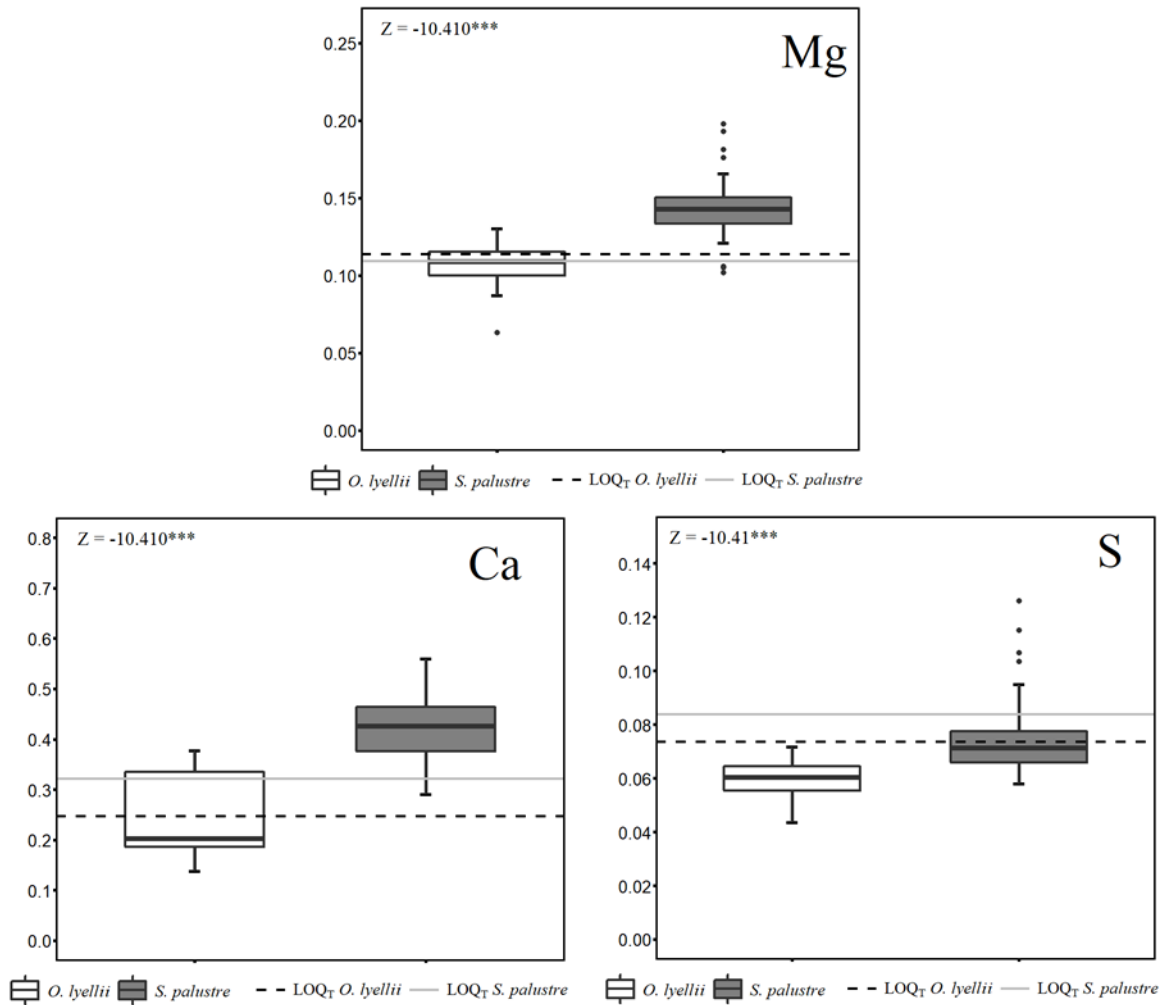
Figure 7. Boxplots of post-exposure moss tissue concentration (mg/kg) for plant-essential secondary nutrients across all matched pair sites (HAR, OES, PUM, PWB) and all sampling periods for *O. lyellii* (white) and *S. palustre* (grey), n=72. LOQ_T is represented by the dashed black line (*O. lyellii*) and the grey (*S. palustre*). Boxes show median, 1st and 3rd quantiles; whiskers show ±1.5 x Interquartile range (IQR). Significance of accumulation was calculated from Wilcoxon matched pair test (top-right). *p < 0.05, **p < 0.01, ***p < 0.001.
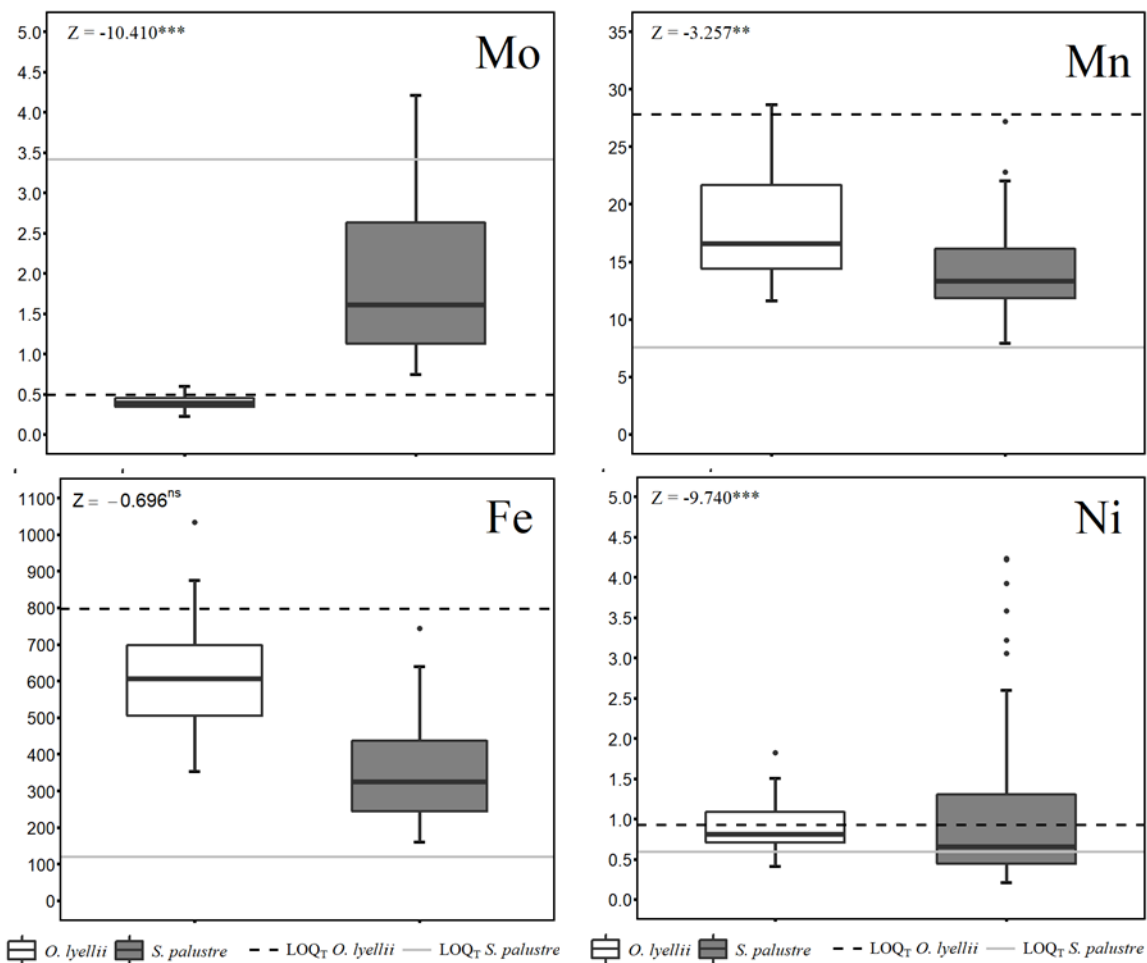
Figure 8a. Boxplots of post-exposure moss tissue concentration (mg/kg) for plant-essential micronutrients (Mo, Mn, Fe & Ni) across all matched pair sites (HAR, OES, PUM, PWB) and all sampling periods for *O. lyellii* (white) and *S. palustre* (grey), n=72. LOQ_T is represented by the dashed black line (*O. lyellii*) and the grey (*S. palustre*). Boxes show median, 1st and 3rd quantiles; whiskers show ±1.5 x Interquartile range (IQR). Significance of accumulation was calculated from Wilcoxon matched pair test (top-right).
*p < 0.05, **p < 0.01, ***p < 0.001.
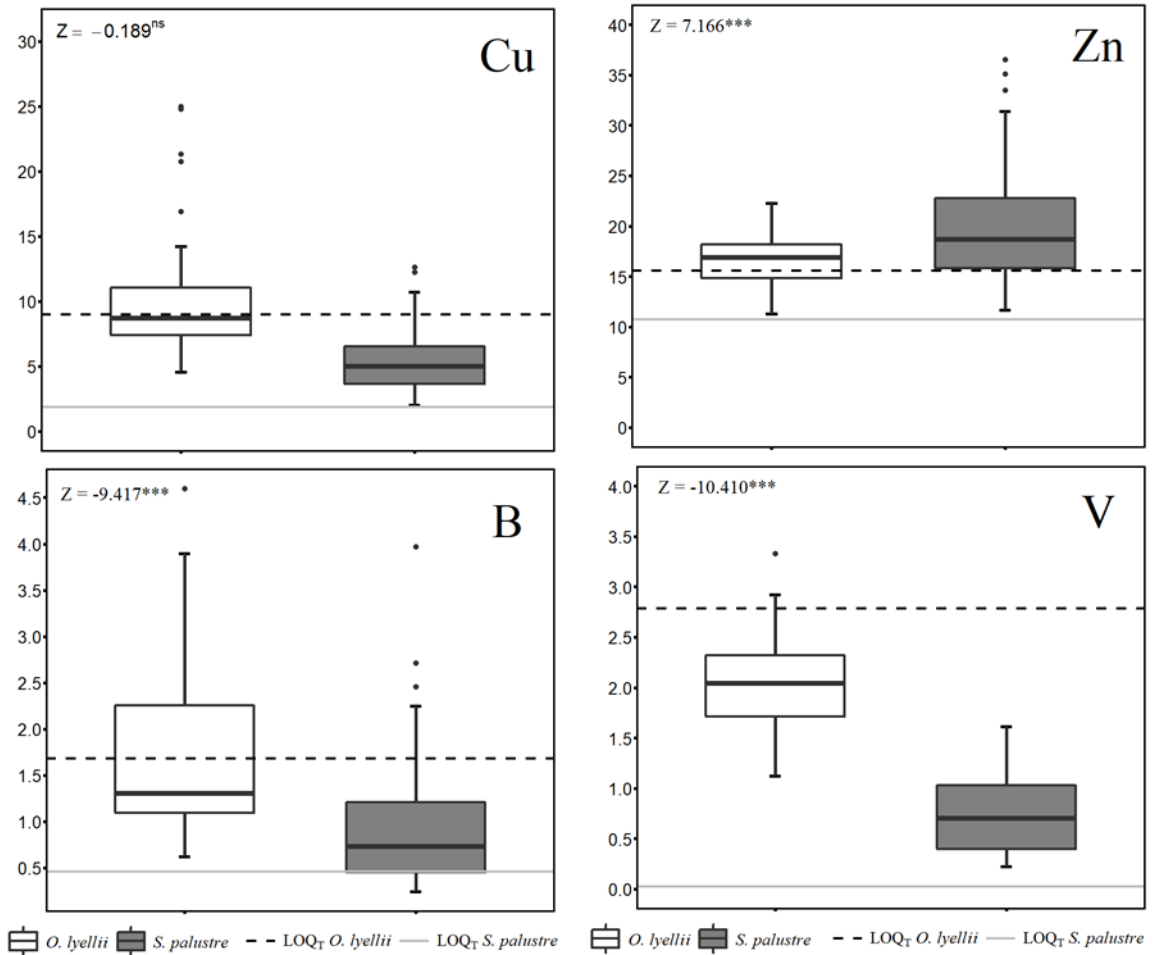
Figure 9. Boxplots of post-exposure moss tissue concentration (mg/kg) for plant-essential micronutrients (Cu, Zn, B &V) across all matched pair sites (HAR, OES, PUM, PWB) and all sampling periods for *O. lyellii* (white) and *S. palustre* (grey), n=72. LOQ_T is represented by the dashed black line (*O. lyellii*) and the grey (*S. palustre*). Boxes show median, 1st and 3rd quantiles; whiskers show ±1.5 x Interquartile range (IQR). Significance of accumulation was calculated from Wilcoxon matched pair test (top-right). *p < 0.05, **p < 0.01, ***p < 0.001.
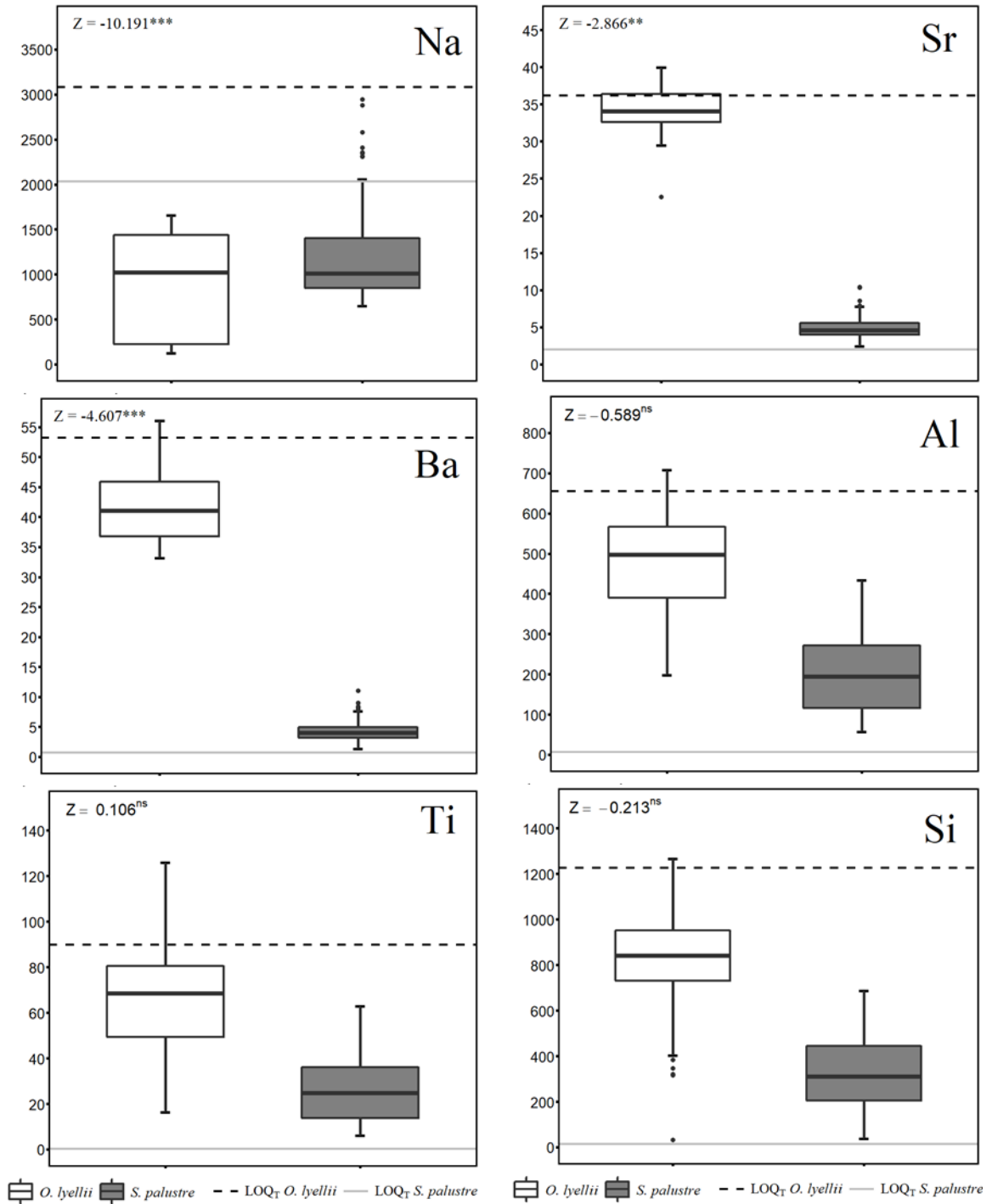
Figure 10. Boxplots of post-exposure moss tissue concentration (mg/kg) for soil mineral elements across all matched pair sites (HAR, OES, PUM, PWB) and all sampling periods for *O. lyellii* (white) and *S. palustre* (grey), n=72. LOQ_T is represented by the dashed black line (*O. lyellii*) and the grey (*S. palustre*). Boxes show median, 1st and 3rd quantiles; whiskers show ±1.5 x Interquartile range (IQR). Significance of accumulation was calculated from Wilcoxon matched pair test (top-right).
*p < 0.05, **p < 0.01, ***p < 0.001.
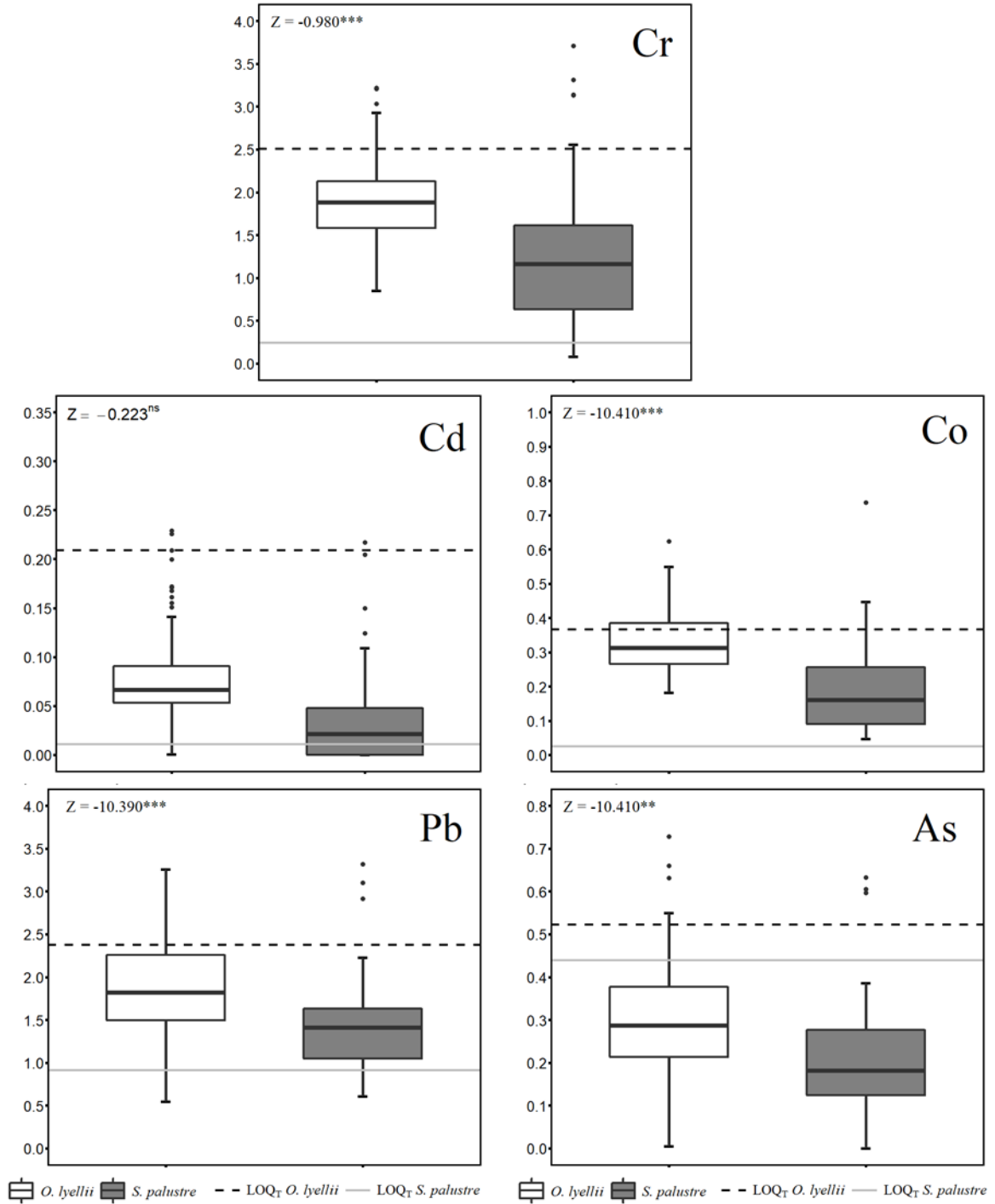
Figure 11. Boxplots of post-exposure moss tissue concentration (mg/kg) for environmentally important trace metals across all matched pair sites (HAR, OES, PUM, PWB) and all sampling periods for *O. lyellii* (white) and *S. palustre* (grey), n=72. LOQ_T is represented by the dashed black line (*O. lyellii*) and the grey (*S. palustre*). Boxes show median, 1st and 3rd quantiles; whiskers show ±1.5 x Interquartile range (IQR). Significance of accumulation was calculated from Wilcoxon matched pair test (top-right). *p < 0.05, **p < 0.01, ***p < 0.001.
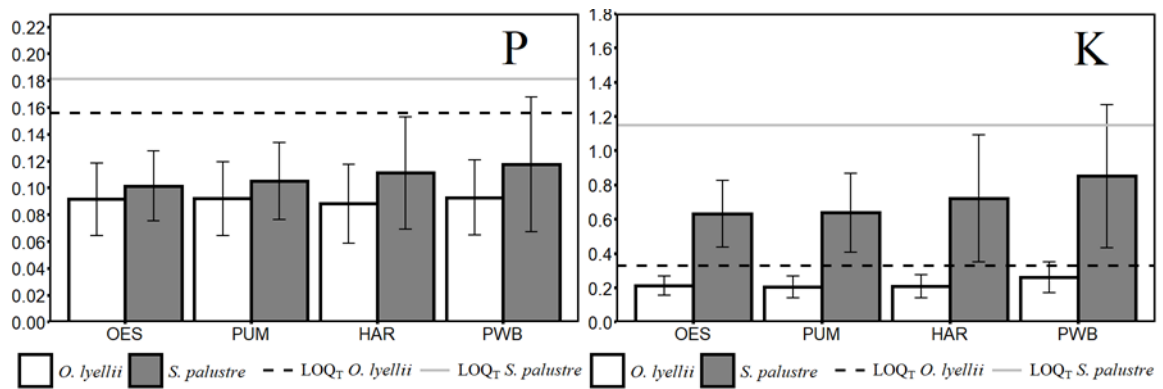
Figure 12. Bar charts showing post-exposure moss tissue concentration (mg/kg) for plant essential macronutrients separated by site for *O. lyellii* (white) and *S. palustre* (grey). n=72. LOQ_T is represented by the dashed black line (*O. lyellii*) and the grey (*S. palustre*). All six sampling periods are combined for each mean. Bars represent mean concentration and the error bar show standard deviation.
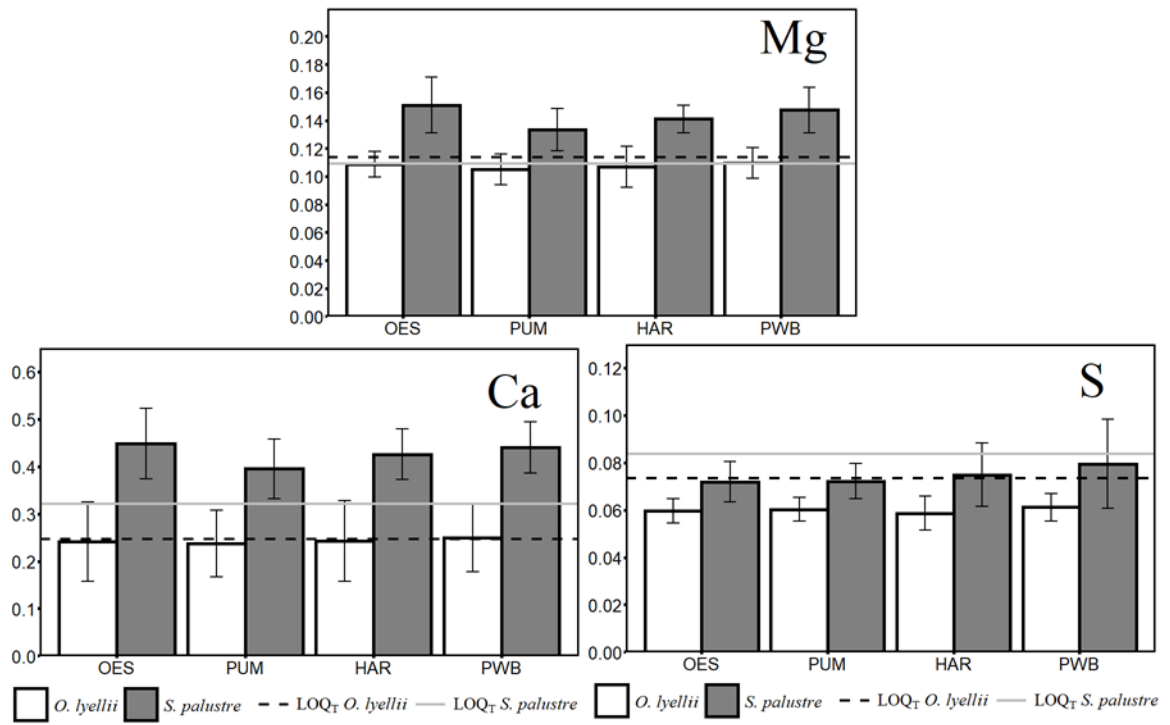
Figure 13 Bar charts showing post-exposure moss tissue concentration (mg/kg) for plant essential secondary nutrients separated by site for *O. lyellii* (white) and S. palustre (grey). n=72. LOQ_T is represented by the dashed black line (*O. lyellii*) and the grey (*S. palustre*). All six sampling periods are combined for each mean. Bars represent mean concentration and the error bar show standard deviation.
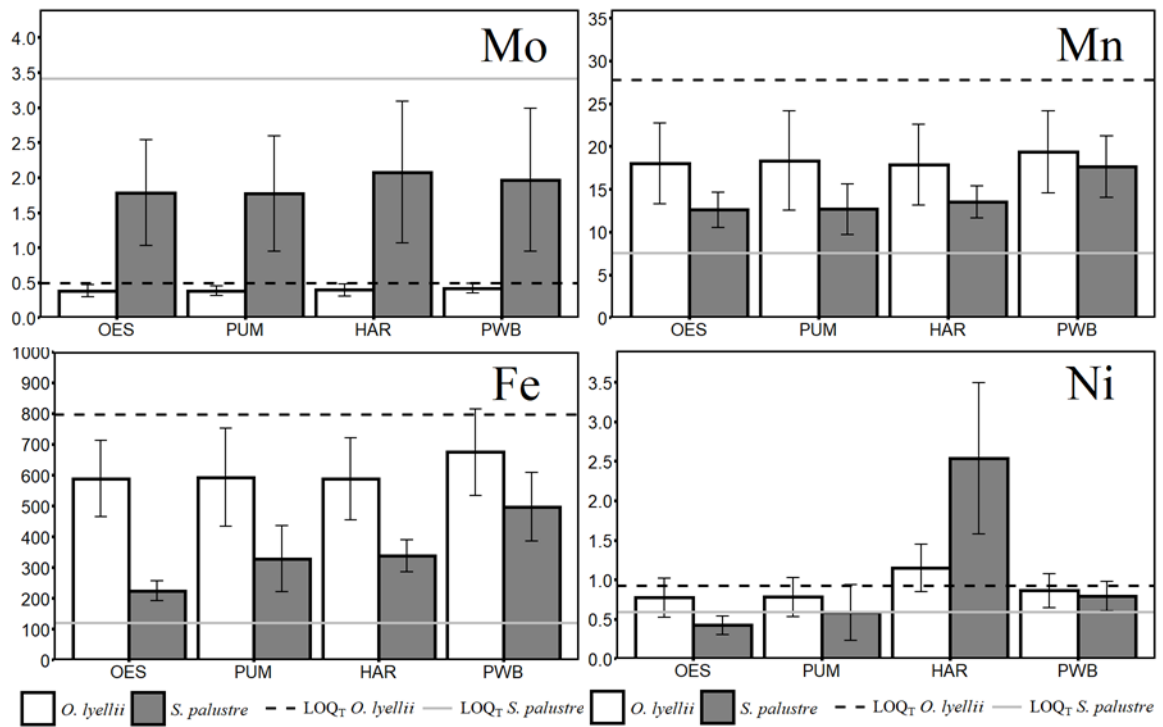
Figure 14. Bar charts showing post-exposure moss tissue concentration (mg/kg) for plant essential micronutrients (Mo, Mn, Fe, Ni) separated by site for *O. lyellii* (white) and *S. palustre* (grey). n=72. LOQ_T is represented by the dashed black line (*O. lyellii*) and the grey (*S. palustre*). All six sampling periods are combined for each mean. Bars represent mean concentration and the error bar show standard deviation.
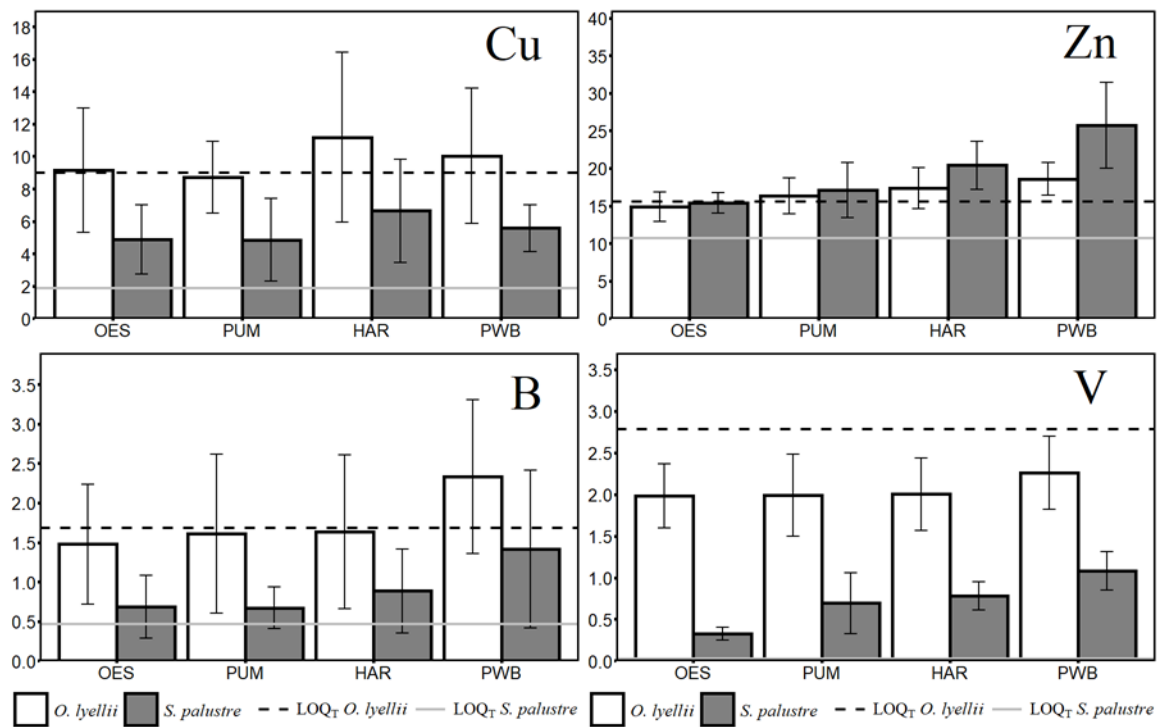
Figure 15. Bar charts showing post-exposure moss tissue concentration (mg/kg) for plant essential micronutrients (Cu, Zn, B & V) separated by site for *O. lyellii* (white) and *S. palustre* (grey). n=72. LOQ_T is represented by the dashed black line (*O. lyellii*) and the grey (*S. palustre*). All six sampling periods are combined for each mean. Bars represent mean concentration and the error bar show standard deviation.

87
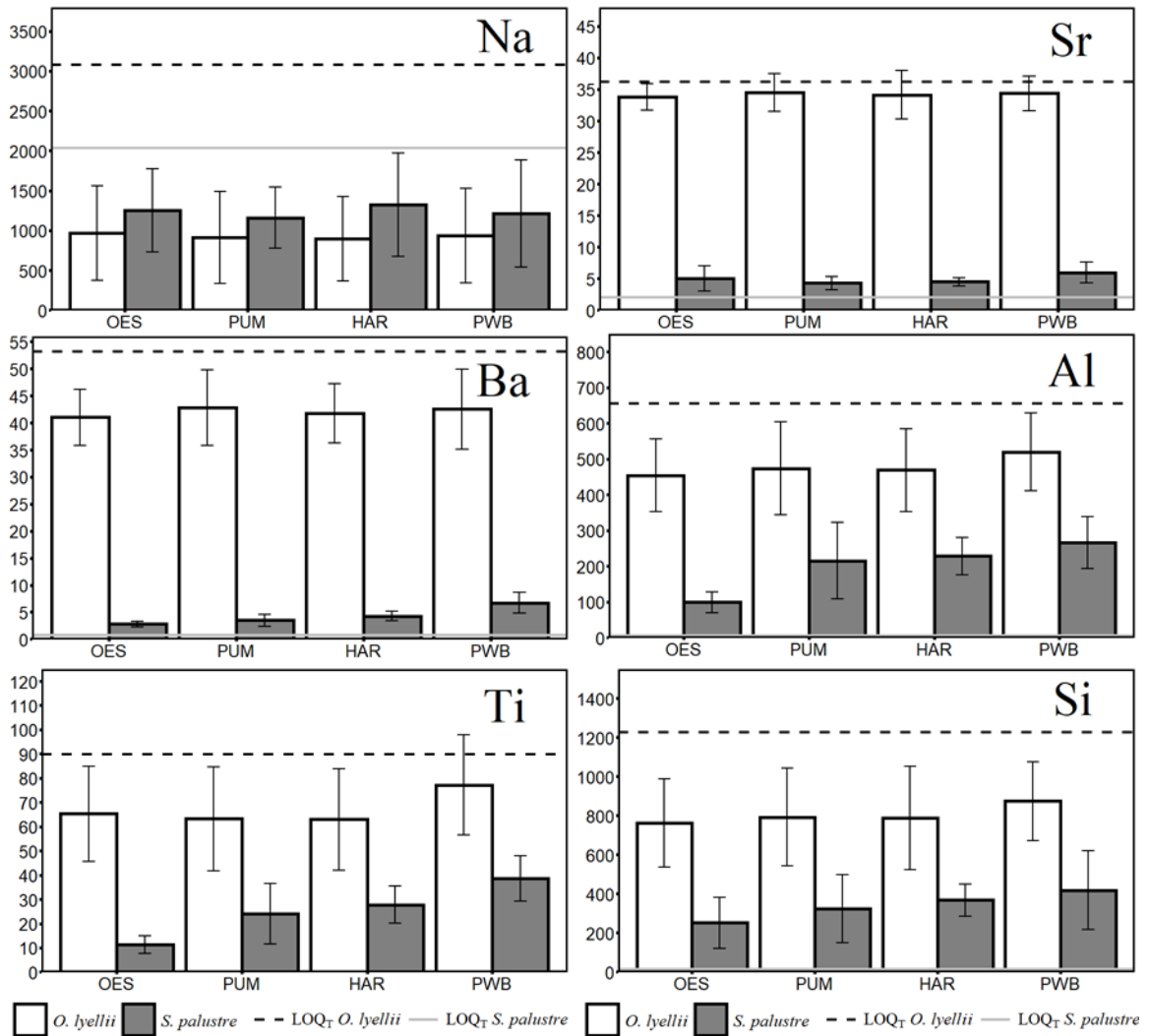
Figure 16. Bar charts showing post-exposure moss tissue concentration (mg/kg) for soil mineral elements separated by site for *O. lyellii* (white) and *S. palustre* (grey). n=72. LOQ$_T$ is represented by the dashed black line (*O. lyellii*) and the grey (*S. palustre*). All six sampling periods are combined for each mean. Bars represent mean concentration and the error bar show standard deviation.
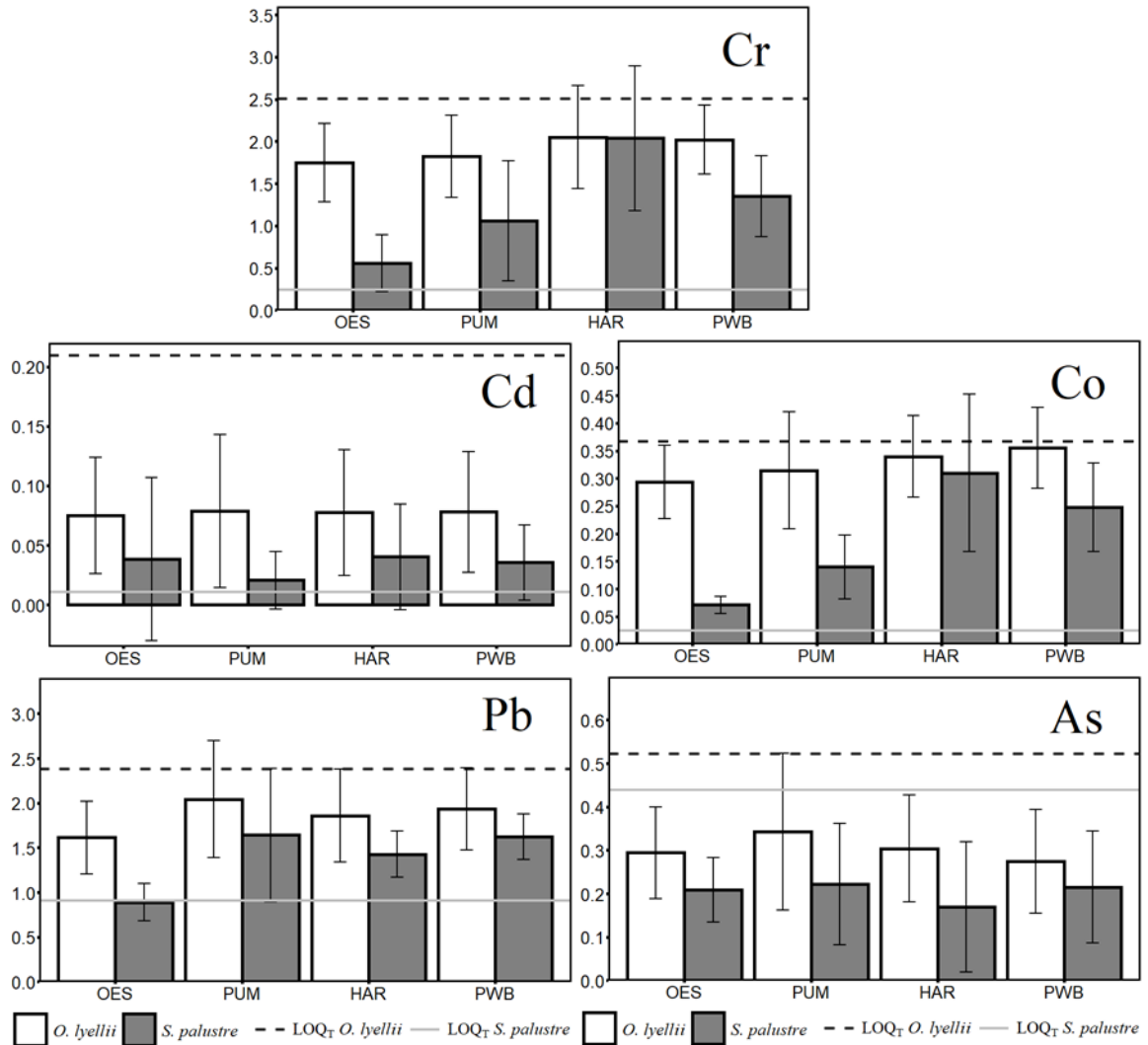
Figure 17 Bar charts showing post-exposure moss tissue concentration (mg/kg) for environmentally important trace elements separated by site for *O. lyellii* (white) and *S. palustre* (grey). n=72. LOQ_T is represented by the dashed black line (*O. lyellii*) and the grey (*S. palustre*). All six sampling periods are combined for each mean. Bars represent mean concentration and the error bar show standard deviation.

Table 18. Comparison of unexposed tissue element concentrations in
S. palustre clone determined for this study (n=20) and the Capozzi et
al. study (n=10).

Element	This study (United States)	Capozzi et al. (2017) study (Spain/Italy)	Percent deviation
Al	3.59 ± 1.27	16 ± 3.54	78%
As	0.20 ± 0.12	0.3 ± 0.07	33%
Ba	0.39 ± 0.15	0.65 ± 0.11	40%
Cr	0.08 ± 0.08	0.52 ± 0.04	85%
Cu	1.52 ± 1.10	1.94 ± 0.67	22%
Fe	96.08 ± 12.22	108.35 ± 13.49	11%
Ni	0.45 ± 0.07	2.25 ± 1.4	80%
Pb	0.40 ± 0.26	0.3 ± 0.07	33%
Sr	1.85 ± 0.08	2.2 ± 0.26	16%
V	0.006 ± 0.009	0.25 ± 0.12	98%
Zn	9.62 ± 0.57	17.05 ± 3.46	44%

Table 19. Comparison of percentage of accumulation per element in *S. palustre* clone
determined for this study (n=72) and the Capozzi et al. study (n=30).

Element	This study (United States)			Capozzi et al. (2017) study (Spain/Italy)		
	Min	Median	Max	Min	Median	Max
Al	1486%	5300%	11987%	663%	2966%	10194%
As	-100%	-8%	220%	-67%	0%	433%
Ba	242%	917%	2704%	421%	1332%	2963%
Cr	0%	1294%	2921%	-4%	160%	804%
Cu	82%	346%	1033%	19%	137%	570%
Fe	67%	237%	674%	85%	296%	899%
Ni	-54%	45%	834%	-51%	-16%	100%
Pb	52%	253%	730%	33%	417%	4233%
Sr	32%	147%	466%	59%	196%	401%
V	3774%	8926%	26937%	0%	260%	1100%
Zn	21%	94%	280%	-6%	99%	387%

Table 20. Comparison of Spearman correlation coefficients per element for *S. palustre* clone vs *O. lyellii* determined in this study (n=72) and *S. palustre* clone vs *Pseudoscleropodium purum* in the Capozzi et al. study (n=30).

Element	This study (United States)	Capozzi et al. (2017) study (Spain/Italy)
Al	0.489*	0.682***
As	-0.087	0.006
Ba	-0.009	0.532**
Cr	0.386	0.282
Cu	0.245	0.044
Fe	0.412*	0.468**
Ni	0.438*	0.572***
Pb	0.403*	0.789***
Sr	0.055	0.515**
V	0.474*	0.499**
Zn	0.400*	0.404*

Table 21. Descriptive statistics for element concentrations in ambient PM_{10} (ng/m^3) for all sites and sampling periods.

Element	Minimum	Maximum	Mean	Median	Fisher-Pearson Skewness coefficient	Samples below detection limit
P	0.6554	101.5016	17.2532	20.7853	-0.7371	0
K	7.7592	257.8192	76.1336	85.7245	-0.7729	0
Mg	0.9452	240.1095	69.4701	82.8355	-0.8112	0
Ca	0.7787	607.9786	148.2297	191.8325	-0.9604	0
S	0.9856	399.5498	193.1774	199.9603	-0.2853	0
Mo	0.0000	5.6062	0.5953	0.6810	-0.4208	3
Mn	0.0122	39.1228	11.3450	13.0434	-0.6005	0
Fe	0.0000	910.5340	321.8615	355.1010	-0.5398	1
Ni	0.0000	11.3501	1.0436	1.3941	-0.6943	5
Cu	0.0147	19.3779	5.9490	6.5334	-0.5318	0
Zn	1.5711	91.2101	11.4701	12.7688	-0.3946	0
B	0.1026	4.0135	0.8419	1.0393	-0.8621	0
Na	1.1933	896.0999	280.0705	316.2909	-0.6299	0
Sr	0.0032	6.6316	1.2380	1.5038	-0.8354	0
Ba	0.0000	33.0541	9.4262	10.2138	-0.4423	1
Ti	0.8982	95.8154	17.3675	21.8246	-0.8103	0
Al	2.8957	912.2894	86.4165	140.2050	-1.0839	0
Si	0.0000	2993.9125	92.2595	582.7970	-1.8795	1
V	0.0000	2.9344	0.5758	0.7323	-0.8389	1
Cr	0.0000	9.7743	1.8242	2.1077	-0.5187	5
Co	0.0000	1.3420	0.1944	0.2266	-0.5093	3
Cd	0.0038	0.4831	0.0513	0.0577	-0.3994	0
Pb	0.0000	3.5347	1.9439	1.9639	-0.0689	3
As	0.0000	2.2823	0.5920	0.8000	-1.0835	1

Table 22. Mean ambient PM_{10} concentrations (ug/m^3) determine for each site across six sampling periods with mean and standard error.

Site	1	2	3	4	5	6	Mean ± std err
OES	36.42	23.84	22.83	17.87	15.32	19.32	22.6 ± 3.05
UOP	36.37	29.36	29.03	19.86	20.40	24.24	26.55 ± 2.57
PUM	40.03	32.57	28.81	19.88	21.26	26.98	28.25 ± 3.05
HUM	49.79	34.34	26.03	19.62	18.89	27.70	29.39 ± 4.69
HAR	45.47	33.53	34.76	24.51	22.22	26.96	31.24 ± 3.49
PFD	50.01	34.46	29.90	24.89	26.73	28.30	32.38 ± 3.77
PWB	47.05	35.06	30.63	22.91	27.56	31.71	32.49 ± 3.36
OHS	50.16	37.93	32.17	21.69	27.67	36.41	34.34 ± 3.99

Table 23.Total collection volume (L) from ARA PM samplers for each site across six sampling periods with mean and standard error.

Site	1	2	3	4	5	6	Mean ± std err
OES	1274.26	1031.58	1368.79	1321.13	1344.18	1105.07	1241 ± 52
UOP	1307.80	1346.65	1261.92	1321.27	1343.10	1345.11	1321 ± 12
PUM	1327.96	1203.78	1119.61	1321.31	1325.43	1337.08	1273 ± 34
HUM	1251.09	1189.55	1351.84	1320.60	1279.97	1213.90	1268 ± 23
HAR	1167.90	1308.00	1174.06	1288.18	1285.92	1344.27	1261 ± 27
PFD	1276.40	1335.36	1314.00	1320.86	1343.87	1344.54	1323 ± 10
PWB	1295.43	1340.30	1346.97	1321.13	1301.99	1344.41	1325 ± 8
OHS	1326.93	1336.13	1262.61	1290.83	1343.53	1175.71	1289 ± 24

Table 24. Descriptive statistics of element concentrations in bulk deposition (kg/ha) for all sites and sampling periods.

Element	Minimum	Maximum	Mean	Median	Fisher-Pearson Skewness coefficient	Samples below detection limit
P	2.5599	2310.1779	198.9495	242.6921	1.0432	41
K	0.0000	11821.8714	798.2660	1042.1645	0.5206	36
Mg	36.2668	2338.1964	301.0839	322.6128	1.3330	0
Ca	21.7660	13282.4877	1251.4463	1903.0877	1.2286	6
S	--	--	--	--	--	--
Mo	0.0082	10.6726	0.2521	0.7805	0.5504	151
Mn	0.1960	206.3819	34.0569	42.7354	1.5101	7
Fe	14.5704	4638.1889	607.2900	790.0995	1.4097	0
Ni	0.2370	72.7256	3.1856	5.8018	0.7053	1
Cu	1.5642	119.7642	18.5219	18.5921	1.3309	0
Zn	4.4578	539.8006	94.2922	102.6787	1.2815	0
B	0.8110	59.2196	5.4510	6.1363	0.8699	0
V	0.0016	203.4476	2.3249	14.6463	0.3667	0
Na	165.7173	4426.7137	606.3642	431.8637	0.7652	1
Sr	0.3649	128.3982	9.8049	16.3408	1.1026	0
Ba	0.6286	202.0309	19.0869	25.7147	1.2548	177
Al	5.3961	2633.9188	352.7540	457.1071	1.4082	10
Ti	0.0000	120.7895	14.7583	20.8877	1.2615	--
Si	--	--	--	--	--	14
Cr	0.0000	18.6534	1.7387	2.6414	1.0753	24
Co	0.0219	3.5183	0.5559	0.6633	1.4498	1
Cd	0.0224	3.8252	0.4795	0.5422	1.1216	3
Pb	0.1923	31.9029	4.9472	6.4525	1.4044	0
As	0.0000	2.0371	0.2984	0.3132	0.9147	47

Table 25. Total bulk deposition collector volume (mL) measured for each site across six sampling periods with mean and standard error.

Site	1	2	3	4	5	6	Mean ± std err
OHS	10	855	1450	1448	837	311	819 ± 218
PFD	14	923	1586	1580	866	390	893 ± 234
OES	0	1012	1726	1377	1011	284	901 ± 243
PUM	3	923	1690	1497	974	337	904 ± 242
PWB	17	958	1725	1542	1045	337	937 ± 248
HAR	12	1047	1695	1512	1073	342	947 ± 244
HUM	44	953	1707	1682	984	372	957 ± 251
UOP	19	885	1674	1782	1063	344	961 ± 262

Table 26. Spearman correlation coefficients for element concertation in ambient PM_{10} (ng/m^3) compared to *O. lyellii* and *S. palustre* for two 4-week measurement periods. *p < 0.05, **p < 0.01, ***p < 0.001., n =72 (*O. lyellii*) and n= 144 (*S. palustre*). CP1 is the first 4-week collection period and CP2 is the second 4-week collection period. CP1+2 combines both collection periods to match 8-week moss exposure.

Element	*O. Lyellii*			*S. palustre*		
	CP1	CP2	CP1+2	CP1	CP2	CP1+2
P	0.82***	0.671***	0.756***	0.753***	0.670***	0.733***
K	0.263	0.411*	0.368	0.262	0.486***	0.491***
Mg	-0.726***	-0.605**	-0.711***	-0.141	-0.054	-0.114
Ca	0.530**	0.730***	0.656***	0.061	0.147	0.111
S	0.243	0.227	0.283	0.558***	0.591***	0.644***
Mo	-0.234	0.266	0.075	-0.034	-0.017	0.01
Mn	0.249	-0.089	0.044	0.221	0.355*	0.296*
Fe	0.375	0.017	0.223	0.446**	0.474***	0.471***
Ni	-0.033	0.297	-0.035	0.127	0.159	0.057
Cu	0.244	0.016	0.216	0.18	0.403**	0.357*
Zn	-0.007	0.415*	0.282	0.267	0.545***	0.427**
B	0.397	0.560**	0.668***	0.694***	0.529***	0.777***
V	0.293	0.084	0.157	0.453**	0.318*	0.446**
Na	-0.22	-0.049	00.01	0.574***	0.686***	0.713***
Sr	0.008	0.065	0.044	0.102	0.125	0.135
Ba	-0.065	-0.410*	-0.287	0.634***	0.587***	0.679***
Al	0.254	-0.097	0.114	0.351*	0.189	0.304*
Ti	0.361	-0.044	0.178	0.495***	0.352*	0.477***
Si	0.054	0.186	0.202	0.281	0.103	0.278
Cr	0.050	0.170	-0.047	0.075	0.157	0.008
Co	-0.123	-0.054	-0.152	0.168	0.106	0.112
Cd	0.140	0.416*	0.298	0.024	0.302*	0.199
Pb	0.206	0.033	0.110	0.096	0.176	0.12
As	-0.002	0.070	0.067	-0.127	-0.028	-0.072

Table 27. Spearman correlation coefficients for element concertation in ambient bulk deposition (kg/ha) compared to *O. lyellii* and *S. palustre* for two 4-week measurement periods. *p < 0.05, **p < 0.01, ***p < 0.001., n =72 (*O. lyellii*) and n= 144 (*S. palustre).* CP1 is the first 4-week collection period and CP2 is the second 4-week collection period. CP1+2 combines both collection t periods to match 8-week moss exposure.

Element	*O. Lyellii*			*S. palustre*		
	CP1	CP2	CP1+2	CP1	CP2	CP1+2
P	-0.251	-0.542**	-0.399	-0.121	-0.463***	-0.382**
K	-0.221	-0.137	-0.175	-0.301*	-0.2	-0.291*
Mg	0.221	0.574**	0.434*	0.23	0.14	0.189
Ca	-0.141	0.385	0.073	0.449**	0.333*	0.468***
S	--	--	--	--	--	--
Mo	0.141	0.014	0.063	-0.382**	-0.565***	-0.55***
Mn	-0.012	0.355	0.092	0.53***	0.383**	0.628***
Fe	0.349	0.303	0.343	0.494***	0.616***	0.671***
Ni	-0.064	0.035	-0.011	0.324*	0.413**	0.43**
Cu	-0.169	0.15	-0.051	0.372**	0.484***	0.462***
Zn	-0.285	0.136	-0.089	0.269	0.675***	0.521***
B	-0.431*	-0.433*	-0.502*	-0.398**	-0.405**	-0.436**
V	0.119	0.517**	0.298	0.336*	0.648***	0.605***
Na	-0.132	0.025	-0.042	-0.698***	-0.687***	-0.704***
Sr	-0.127	-0.088	-0.104	0.314*	0.303*	0.374**
Ba	-0.233	-0.178	-0.197	0.6***	0.783***	0.786***
Al	0.298	0.507*	0.407*	0.361*	0.604***	0.588***
Ti	-0.338	0.221	-0.169	0.037	0.372**	0.279
Si	--	--	--	--	--	--
Cr	0.289	0.658***	0.603**	0.281	0.276	0.259
Co	0.523	0.521**	0.583**	0.414**	0.634***	0.597***
Cd	-0.099	0.058	-0.043	0.209	0.084	0.158
Pb	-0.049	0.268	0.108	0.485***	0.409**	0.464***
As	0.112	0.347	0.194	0.011	0.027	0.077
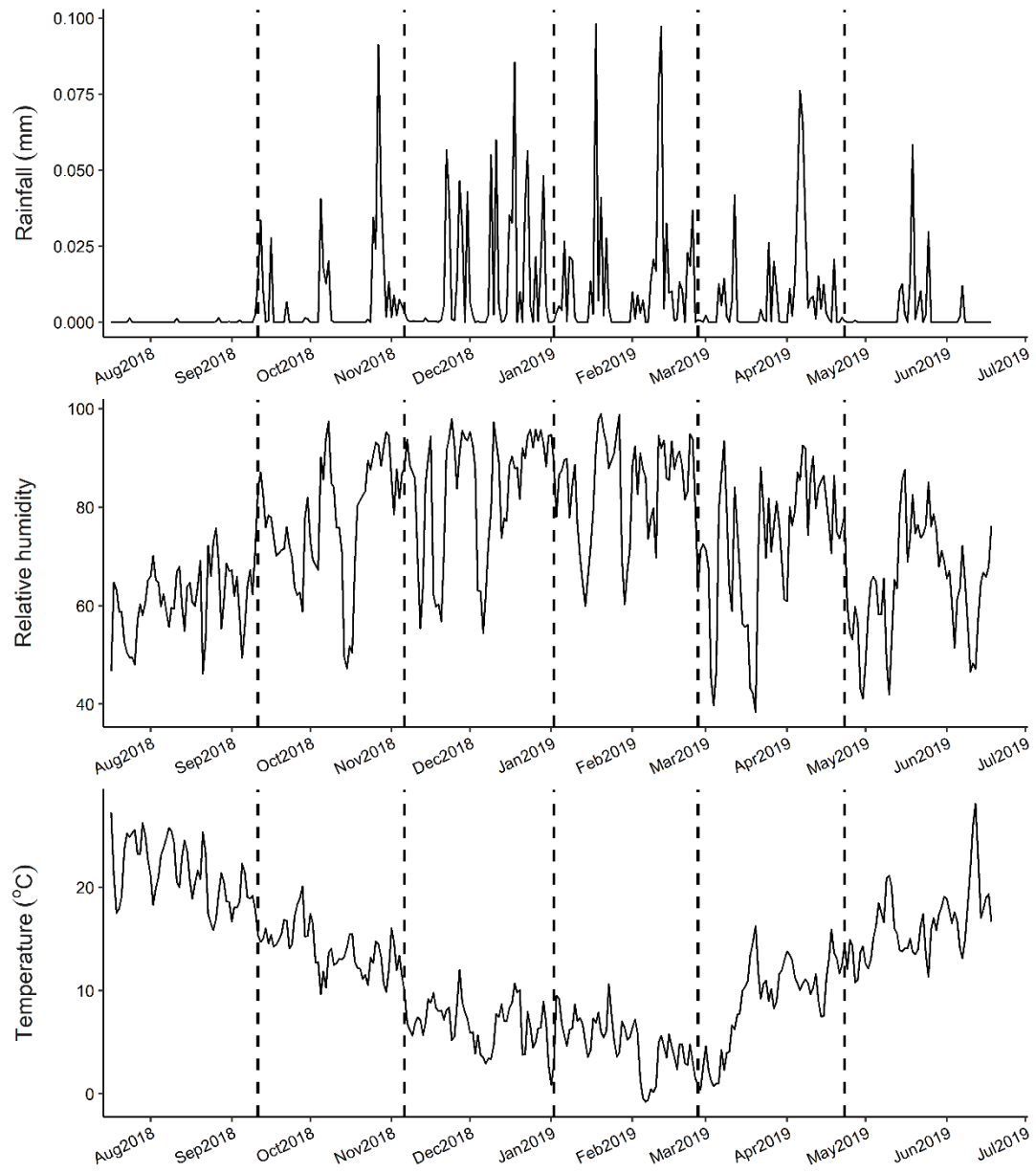
Figure 18. Time series showing rainfall (mm), relative humidity and temperature (°C) across all sites for the duration of the experiment. Dashed line indicates the duration moss exposure for each sampling period.
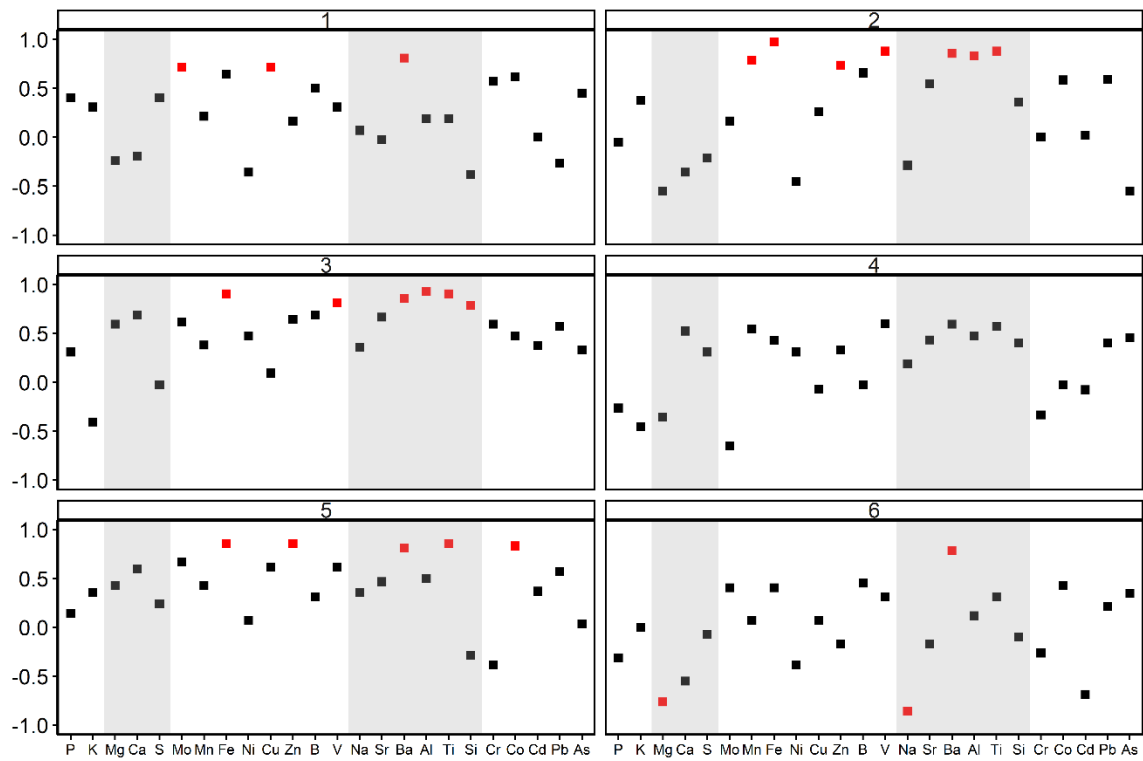
Figure 19. Spearman correlation coefficients comparing PM_{10} (ng.m^3) to *S. palustre* tissue concentration (mg/kg) for each element separated by sampling period. Grey boxes depict grouping of elements by class and red boxes represent significant correlations (p≤0.05), n=8.

Figure 20. Spearman correlation coefficients comparing bulk deposition (mg/kg) to *S. palustre* tissue concentration (mg/kg) for each element separated by sampling period. Grey boxes depict grouping of elements by class and red boxes represent significant correlations (p≤0.05), n=8.
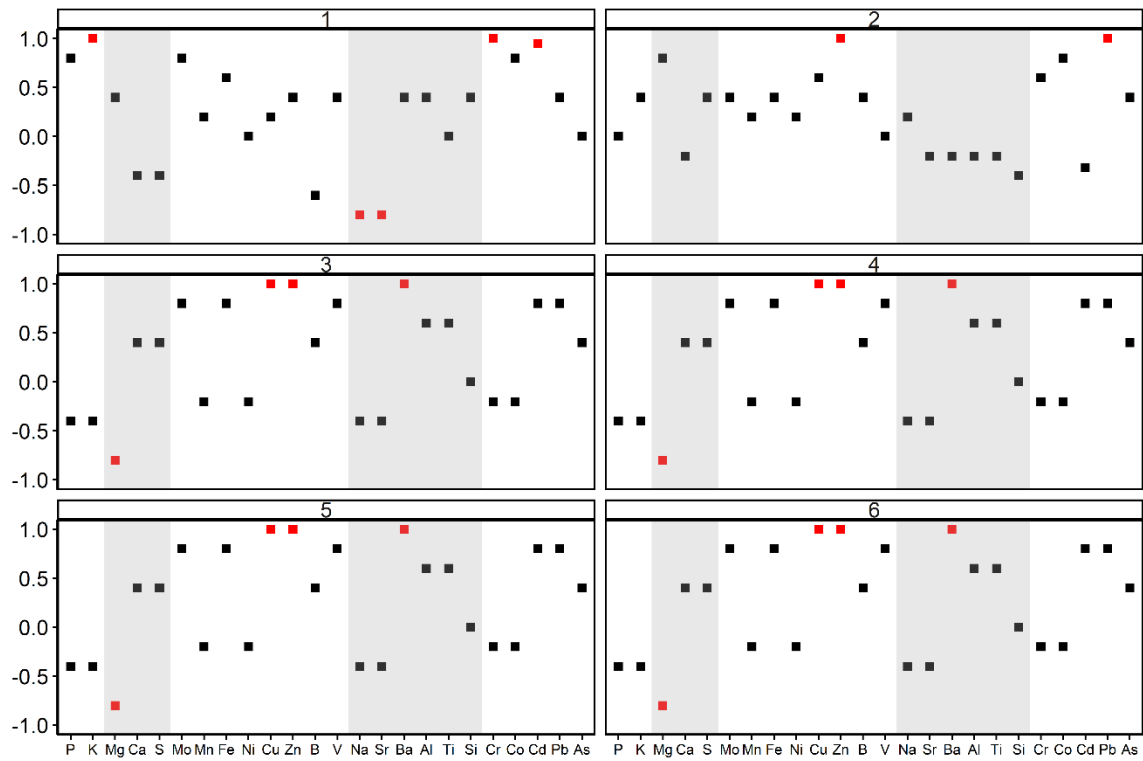
Figure 21. Spearman correlation coefficients comparing PM_{10} (ng.m^3) to *O. lyellii* tissue concentration (mg/kg) for each element separated by sampling period. Grey boxes depict grouping of elements by class and red boxes represent significant correlations (p≤0.05), n=4.
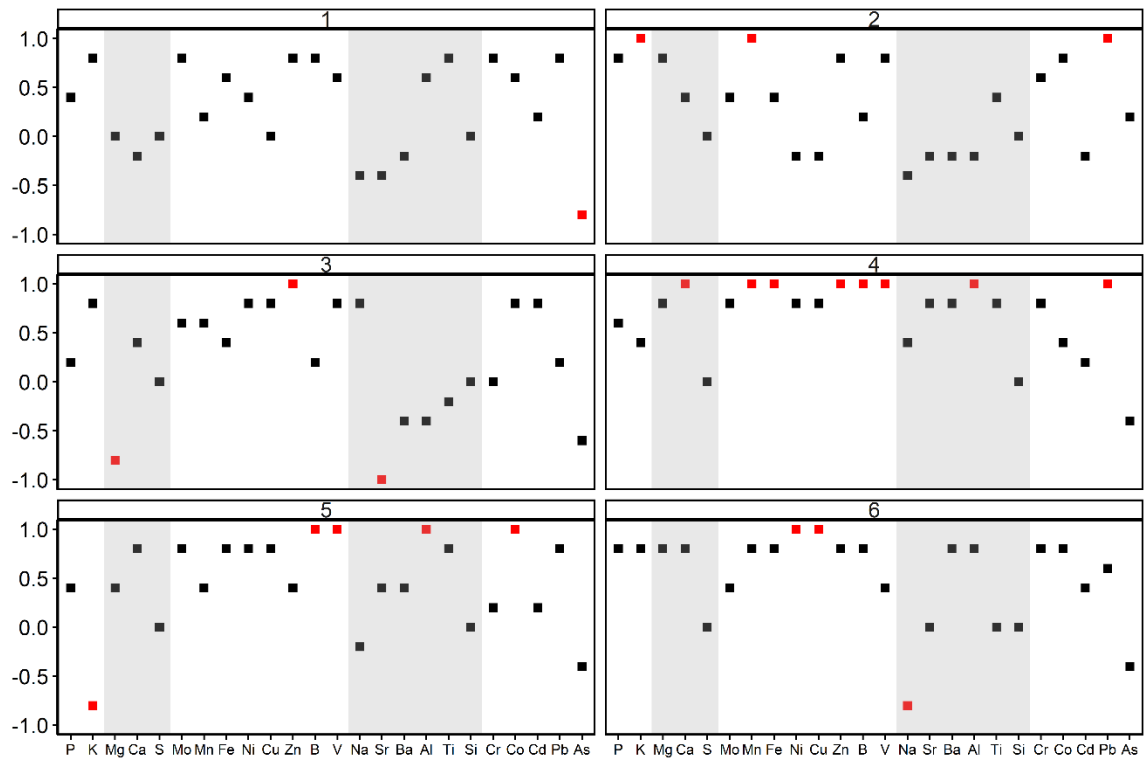
Figure 22. Spearman correlation coefficients comparing bulk deposition (mg/kg) to *O. lyellii* tissue concentration (mg/kg) for each element separated by sampling period. Grey boxes depict grouping of elements by class and red boxes represent significant correlations (p≤0.05), n=4.
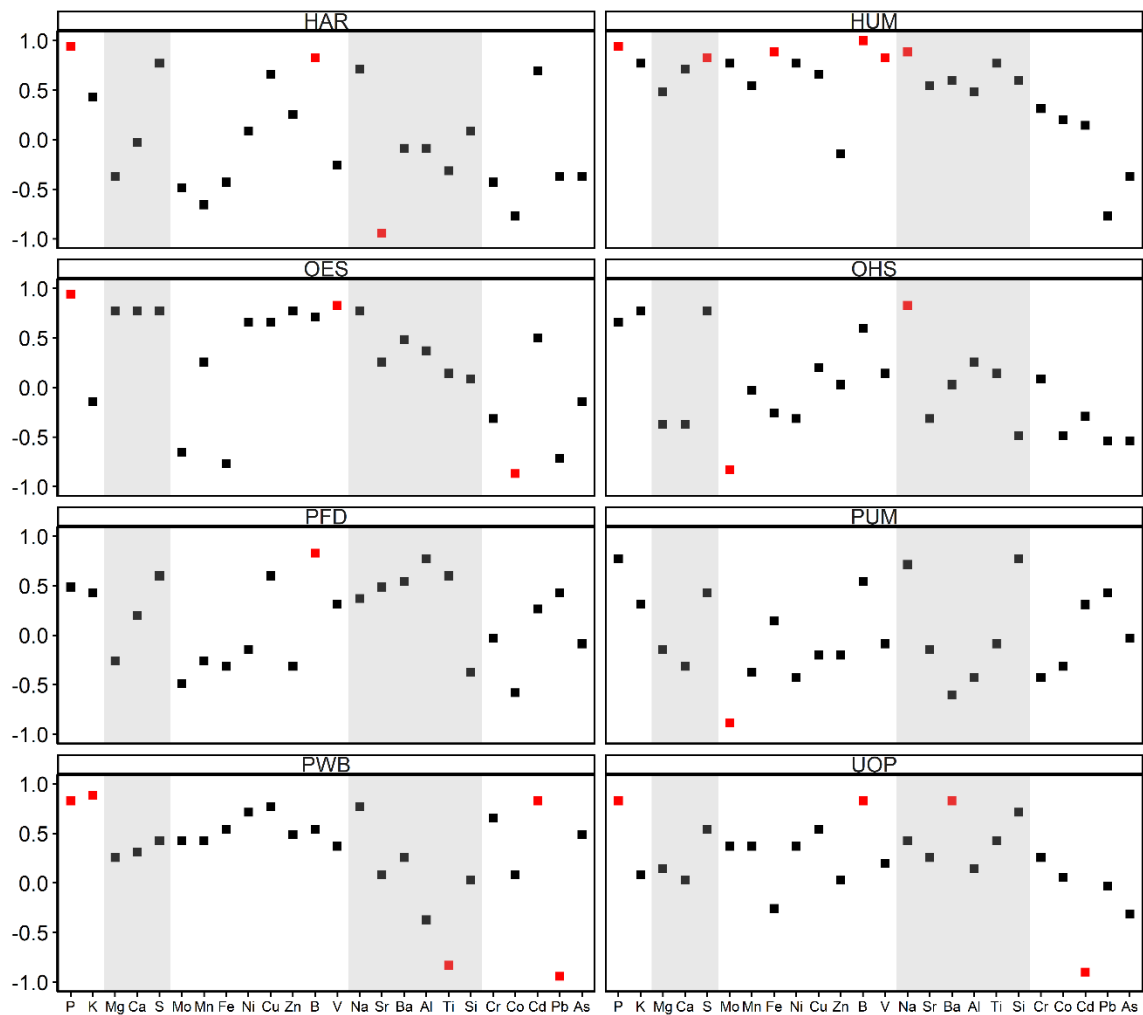
Figure 23. Spearman correlation coefficients comparing PM_{10} (ng.m^3) to *S. palustre* tissue concentration (mg/kg) for each element separated by location. Grey boxes depict grouping of elements by class and red boxes represent significant correlations ($p \leq 0.05$), n=6.
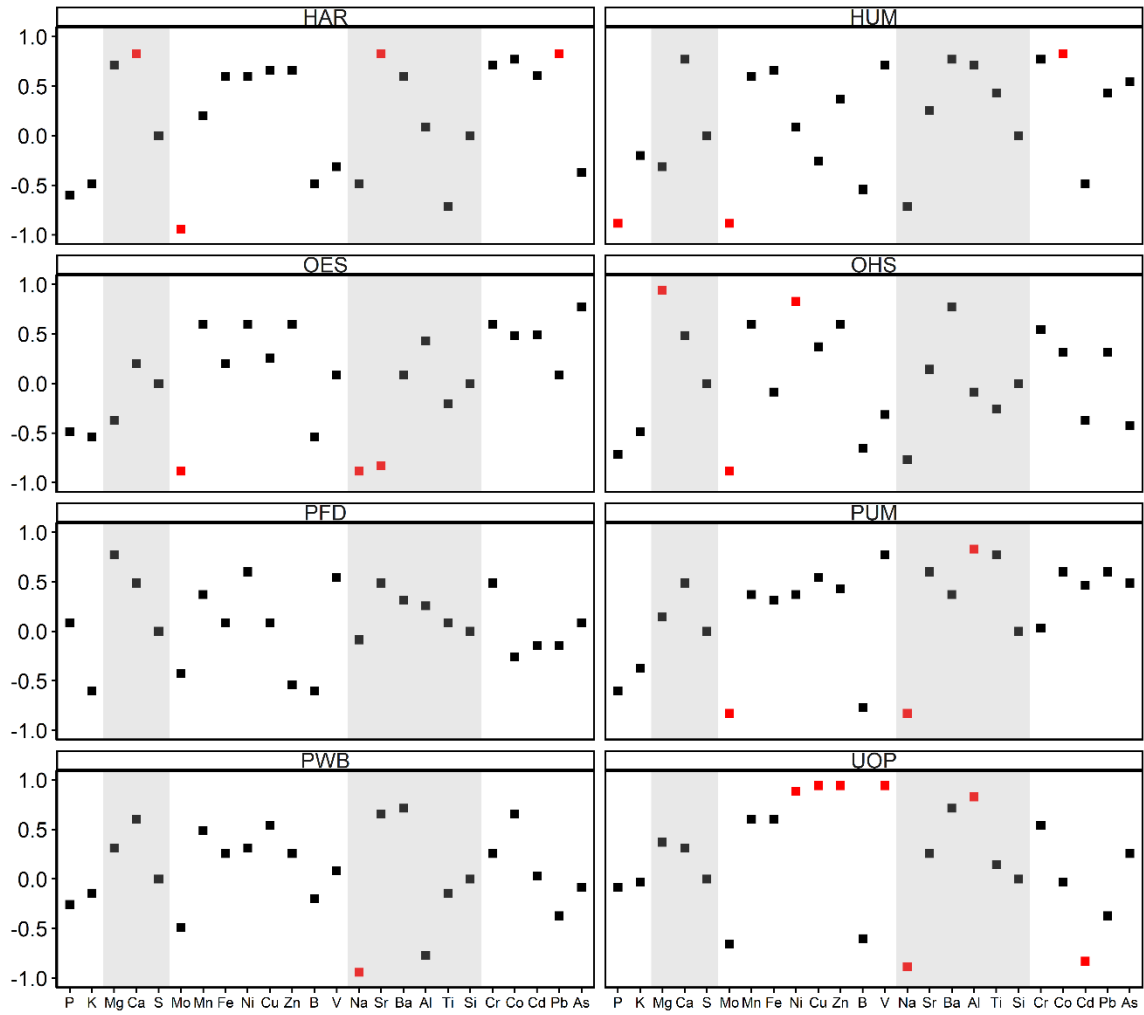
Figure 24. Spearman correlation coefficients comparing bulk deposition (mg/kg) to *S. palustre* tissue concentration (mg/kg) for each element separated by location. Grey boxes depict grouping of elements by class and red boxes represent significant correlations (p≤0.05), n=6.
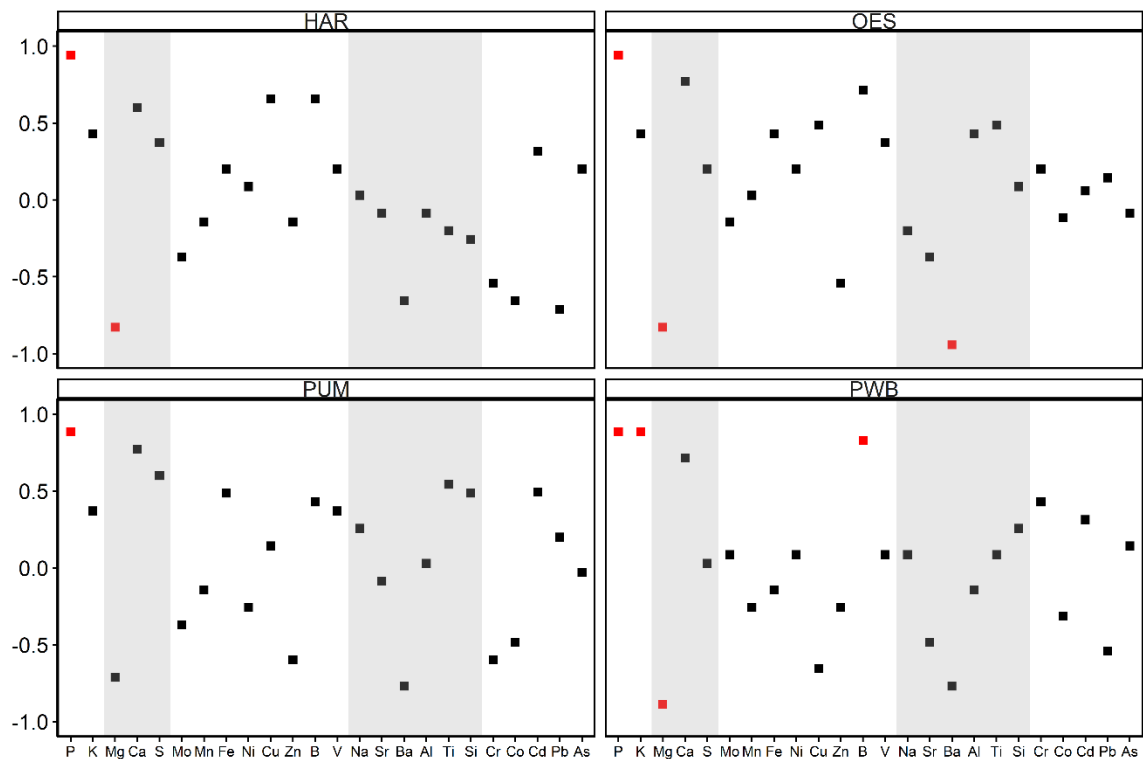
Figure 25. Spearman correlation coefficients comparing PM_{10} (ng.m^3) to *O. lyellii* tissue concentration (mg/kg) for each element separated by location. Grey boxes depict grouping of elements by class and red boxes represent significant correlations (p≤0.05), n=6.
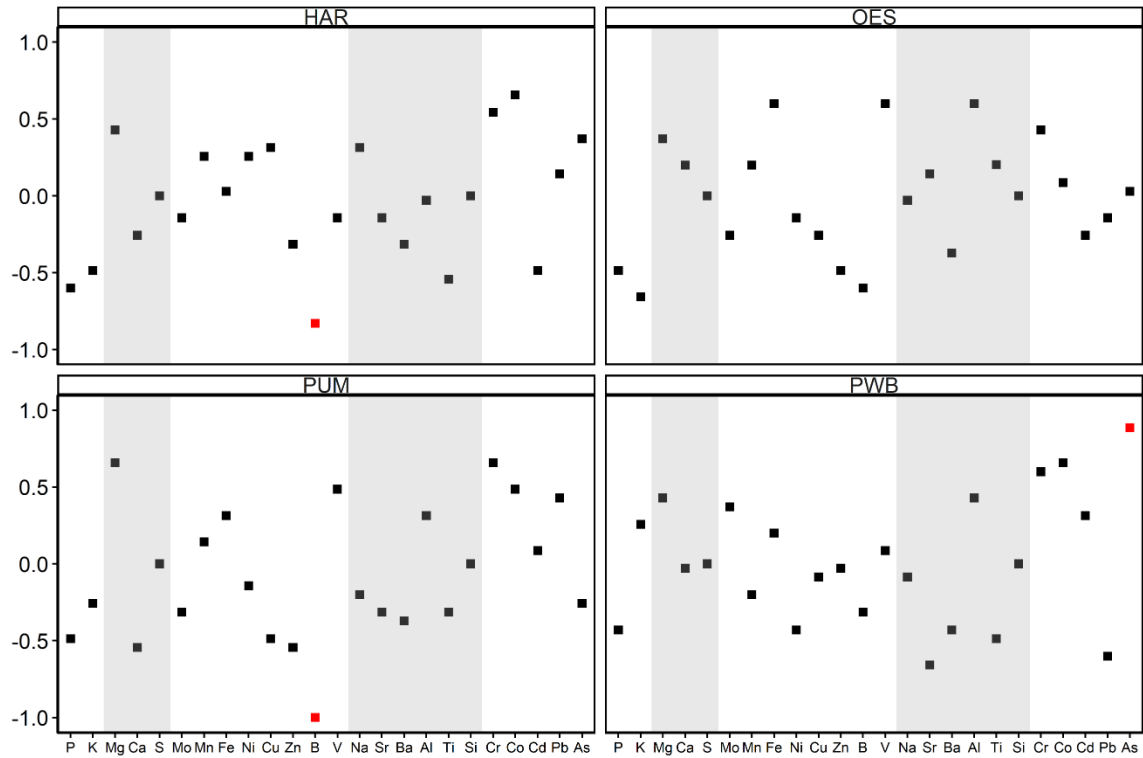
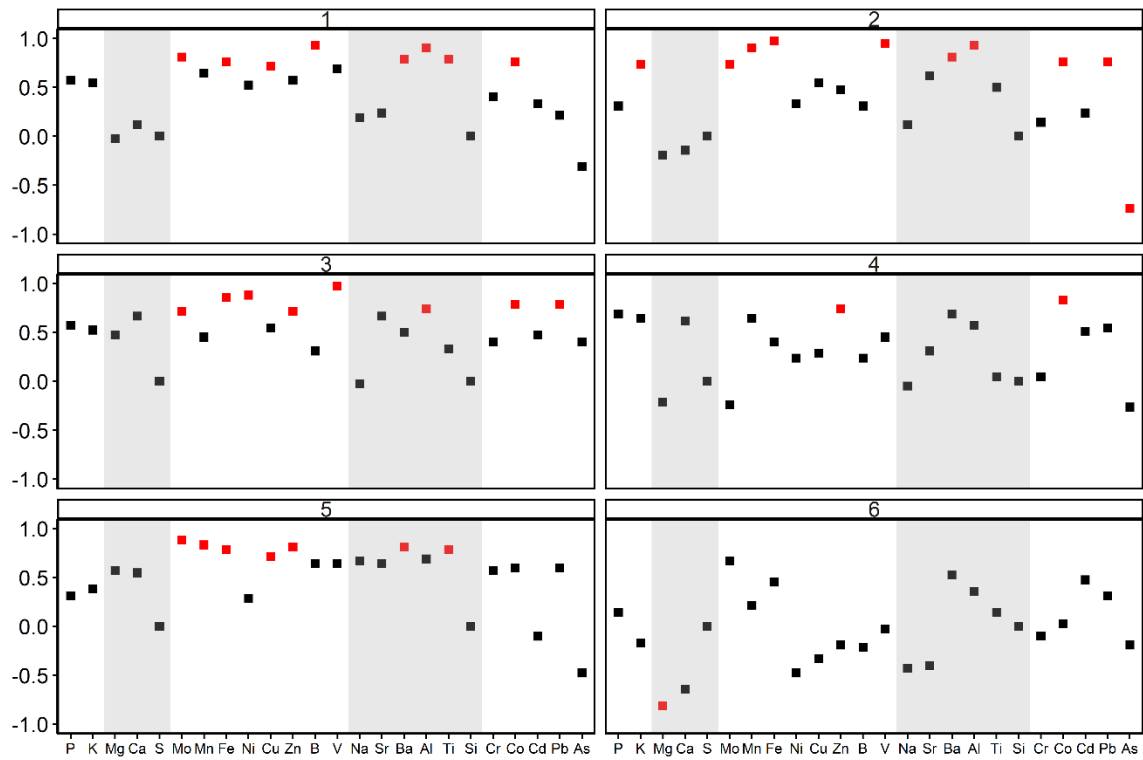Figure 26. Spearman correlation coefficients comparing bulk deposition (mg/kg) to *O. lyellii* tissue concentration (mg/kg) for each element separated by location. Grey boxes depict grouping of elements by class and red boxes represent significant correlations (p≤0.05), n=6.

106

References

Aboal, J. R., J. A. Fernández, T. Boquete, and A. Carballeira. 2010. "Is It Possible to Estimate Atmospheric Deposition of Heavy Metals by Analysis of Terrestrial Mosses?" *The Science of the Total Environment* 408 (24): 6291–97.

Ares, A., J. Aboal, A. Carballeira, and J. A. Fernández. 2015. "Do Moss Bags Containing Devitalized Sphagnum Denticulatum Reflect Heavy Metal Concentrations in Bulk Deposition?" *Ecological Indicators* 50 (March): 90–98.

Ares, A., J. R. Aboal, A. Carballeira, S. Giordano, P. Adamo, and J. A. Fernández. 2012. "Moss Bag Biomonitoring: A Methodological Review." *The Science of the Total Environment* 432 (August): 143–58.

Aydogan, Serap, Bengi Erdag, and Lale Yildiz Aktas. 2017. "Bioaccumulation and Oxidative Stress Impact of Pb, Ni, Cu, and Cr Heavy Metals in Two Bryophyte Species, Pleurochaete Squarrosa and Timmiella Barbuloides." *Turkish Journal of Botany* 41: 464–75.

Bates, J. W. 1992. "Mineral Nutrient Acquisition and Retention by Bryophytes." *Journal of Bryology* 17: 223–40.

Beike, Anna K., Valeria Spagnuolo, Volker Lüth, Feray Steinhart, Julia Ramos-Gómez, Matthias Krebs, Paola Adamo, et al. 2015. "Clonal in Vitro Propagation of Peat Mosses (Sphagnum L.) as Novel Green Resources for Basic and Applied Research." *Plant Cell, Tissue and Organ Culture* 120 (3): 1037–49.

Betsou, Chrysoula, Evangelia Diapouli, Evdoxia Tsakiri, Lambrini Papadopoulou, Marina Frontasyeva, Konstantinos Eleftheriadis, and Alexandra Ioannidou. 2021. "First-Time Source Apportionment Analysis of Deposited Particulate Matter from a Moss Biomonitoring Study in Northern Greece." *Atmosphere* 12 (2): 208.

Blagnytė, Rūta, and Dainius Paliulis. 2010. "Research into Heavy Metals Pollution of Atmosphere Applying Moss as Bioindicator: A Literature Review." *Environmental Research, Engineering and Management* 54 (4): 26–33.

Boquete, M. T., J. R. Aboal, A. Carballeira, and J. A. Fernández. 2017. "Do Mosses Exist Outside of Europe? A Biomonitoring Reflection." *The Science of the Total Environment* 593–594 (September): 567–70.

Boquete, M. T., A. Ares, J. A. Fernández, and J. R. Aboal. 2020. "Matching Times: Trying to Improve the Correlation between Heavy Metal Levels in Mosses and Bulk Deposition." *The Science of the Total Environment* 715 (May): 136955.

Burghard, C. J., D. B. Atkinson, and X. Zhu. 2016. "Electrochemical Analysis of Heavy Metal Contaminants in Plant Matter." In , 2016:B33H-0726. ui.adsabs.harvard.edu.

Capozzi, F., P. Adamo, A. Di Palma, J. R. Aboal, R. Bargagli, J. A. Fernandez, P. Lopez Mahia, et al. 2017. "Sphagnum Palustre Clone vs Native Pseudoscleropodium Purum: A First Trial in the Field to Validate the Future of the Moss Bag Technique." *Environmental Pollution* 225: 323–28.

Capozzi, F., S. Giordano, J. R. Aboal, P. Adamo, R. Bargagli, T. Boquete, A. Di Palma, et al. 2016. "Best Options for the Exposure of Traditional and Innovative Moss

Bags: A Systematic Evaluation in Three European Countries." *Environmental Pollution* 214: 362–73.

Clymo, R. S. 1963. "Ion Exchange in Sphagnum and Its Relation to Bog Ecology." *Annals of Botany* 27 (106): 309–24.

Clymo, R. S., and P. M. Hayward. 1982. "The Ecology of Sphagnum. Á In: Smith, AJE (Ed.), Bryophyte Ecology." Chapman and Hall, pp. 229Á290.

Couto, J. A., J. R. Aboal, J. A. Fernández, and A. Carballeira. 2004. "A New Method for Testing the Sensitivity of Active Biomonitoring: An Example of Its Application to a Terrestrial Moss." *Chemosphere* 57 (4): 303–8.

Di Palma, A., D. Crespo Pardo, V. Spagnuolo, P. Adamo, R. Bargagli, D. Cafasso, F. Capozzi, et al. 2016. "Molecular and Chemical Characterization of a Sphagnum Palustre Clone: Key Steps towards a Standardized and Sustainable Moss Bag Technique." *Ecological Indicators* 71 (December 2013): 388–97.

Di Palma, Anna, Fiore Capozzi, Valeria Spagnuolo, Simonetta Giordano, and Paola Adamo. 2017. "Atmospheric Particulate Matter Intercepted by Moss-Bags: Relations to Moss Trace Element Uptake and Land Use." *Chemosphere* 176: 361–68.

Di Palma, Anna, Aridane G. González, Paola Adamo, Simonetta Giordano, Ralf Reski, and Oleg S. Pokrovsky. 2019. "Biosurface Properties and Lead Adsorption in a Clone of Sphagnum Palustre (Mosses): Towards a Unified Protocol of Biomonitoring of Airborne Heavy Metal Pollution." *Chemosphere* 236 (December): 124375.

Dietz, Annette. 2013. "Development of Oregon Background Metals Concentrations in Soil." Department of Environmental Quality.

Donovan, Geoffrey H., Sarah E. Jovan, Demetrios Gatziolis, Igor Burstyn, Yvonne L. Michael, Michael C. Amacher, and Vicente J. Monleon. 2016. "Using an Epiphytic Moss to Identify Previously Unknown Sources of Atmospheric Cadmium Pollution." *The Science of the Total Environment* 559 (July): 84–93.

Environment Agency. 2007. *Review and Implementation Study of Biomonitoring for Assessment of Air Qualityoutcomes*. Bristol, England: Environment Agency.

European Parliament, Council of the European Union. 2008. "Directive 2008/50/EC of the European Parliament and of the Council." *EUR-Lex*. https://eur-lex.europa.eu/legal-content/EN/TXT/PDF/?uri=CELEX:32008L0050&from=en.

Fernández, J. A., M. T. Boquete, A. Carballeira, and J. R. Aboal. 2015. "A Critical Review of Protocols for Moss Biomonitoring of Atmospheric Deposition: Sampling and Sample Preparation." *The Science of the Total Environment* 517 (June): 132–50.

Foan, Louise, Maria Domercq, Raúl Bermejo, Jesús Miguel Santamaría, and Valérie Simon. 2015. "Mosses as an Integrating Tool for Monitoring PAH Atmospheric Deposition: Comparison with Total Deposition and Evaluation of Bioconcentration Factors. A Year-Long Case-Study." *Chemosphere* 119 (January): 452–58.

Galsomiès, Laurence, S. Ayrault, F. Carrot, C. Deschamps, and M. A. Letrouit-Galinou. 2003. "Interspecies Calibration in Mosses at Regional Scale - Heavy Metal and

Trace Elements Results from Ile-de-France." *Atmospheric Environment* 37 (2): 241–51.

Gatziolis, Demetrios, Sarah Jovan, Geoffrey Donovan, and Michael Amacher. 2016. "Elemental Atmospheric Pollution Assessment Via Moss-Based Measurements in Portland, Oregon. General Technical Report PNW-GTR-938," no. June: 55.

Gatziolis, Demetrios, Sarah Jovan, Geoffrey Donovan, Michael Amacher, and Vicente Monleon. 2016. "Elemental Atmospheric Pollution Assessment via Moss-Based Measurements in Portland, Oregon." 2016. https://www.fs.fed.us/pnw/pubs/pnw_gtr938.pdf.

Gerdol, Renato, Roberta Marchesini, Paola Iacumin, and Lisa Brancaleoni. 2014. "Monitoring Temporal Trends of Air Pollution in an Urban Area Using Mosses and Lichens as Biomonitors." *Chemosphere* 108: 388–95.

Harmens, H., D. A. Norris, D. M. Cooper, G. Mills, E. Steinnes, E. Kubin, L. Thöni, et al. 2011. "Nitrogen Concentrations in Mosses Indicate the Spatial Distribution of Atmospheric Nitrogen Deposition in Europe." *Environmental Pollution* 159 (10): 2852–60.

Harmens, H., D. A. Norris, E. Steinnes, E. Kubin, J. Piispanen, R. Alber, Y. Aleksiayenak, et al. 2010. "Mosses as Biomonitors of Atmospheric Heavy Metal Deposition: Spatial Patterns and Temporal Trends in Europe." *Environmental Pollution* 158 (10): 3144–56.

Jaishankar, Monisha, Tenzin Tseten, Naresh Anbalagan, Blessy B. Mathew, and Krishnamurthy N. Beeregowda. 2014. "Toxicity, Mechanism and Health Effects of Some Heavy Metals." *Interdisciplinary Toxicology* 7 (2): 60–72.

Jovan, Sarah E., Vicente J. Monleon, Geoffrey H. Donovan, Demetrios Gatziolis, and Michael C. Amacher. 2021. "Small-Scale Distributions of Polycyclic Aromatic Hydrocarbons in Urban Areas Using Geospatial Modeling: A Case Study Using the Moss Orthotrichum Lyellii in Portland, Oregon, U.S.A." *Atmospheric Environment* 256 (July): 118433.

Jozef M. Pacyna, and Elisabeth G. Pacyna. 2001. "An Assessment of Global and Regional Emissions of Trace Metals to the Atmosphere from Anthropogenic Sources Worldwide." *Environmental Reviews* 9 (4): 269–98.

Krug, Jonathan, Russell Long, Maribel Colón, Andrew Habel, Shawn Urbanski, and Matthew S. Landis. 2021. "Evaluation of Small Form Factor, Filter-Based PM2.5 Samplers for Temporary Non-Regulatory Monitoring during Wildland Fire Smoke Events." *Atmospheric Environment* 265 (November): 118718.

Limo, Jukka, Petriina Paturi, and Joni Mäkinen. 2018. "Magnetic Biomonitoring with Moss Bags to Assess Stop-and-Go Traffic Induced Particulate Matter and Heavy Metal Concentrations." *Atmospheric Environment* 195 (December): 187–95.

Lindgren, Å. 1998. "Road Construction Materials as a Source of Pollutants." *Doctoral Thesis*, no. 1998: 05. https://trid.trb.org/view/694966.

Liu, Hongxiao, Yinhong Hu, Feng Li, and Lingxiong Yuan. 2018. "Associations of Multiple Ecosystem Services and Disservices of Urban Park Ecological Infrastructure and the Linkages with Socioeconomic Factors." *Journal of Cleaner Production* 174: 868–79.

Lombi, Linda. 2018. "The Contribution of Digital Sociology to the Investigation of Air Pollution." In *Clinical Handbook of Air Pollution-Related Diseases*, edited by Fabio Capello and Antonio Vittorino Gaddi, 621–36. Cham: Springer International Publishing.

Markert, B., O. Wappelhorst, V. Weckert, U. Herpin, U. Siewers, K. Friese, and G. Breulmann. 1999. "The Use of Bioindicators for Monitoring the Heavy-Metal Status of the Environment." *Journal of Radioanalytical and Nuclear Chemistry* 240 (2): 425–29.

Nagajyoti, P., K. Lee, and T. Sreekanth. 2010. "Heavy Metals, Occurrence and Toxicity for Plants: A Review." *Environmental Chemistry Letters* 8 (3): 199–216.

Natali, Marco, Augusto Zanella, Aleksandar Rankovic, Damien Banas, Chiara Cantaluppi, Luc Abbadie, and Jean Christophe Lata. 2016. "Assessment of Trace Metal Air Pollution in Paris Using Slurry-TXRF Analysis on Cemetery Mosses." *Environmental Science and Pollution Research* 23 (23): 23496–510.

Nickel, Stefan, Anne Hertel, Roland Pesch, Winfried Schröder, Eiliv Steinnes, and Hilde Thelle Uggerud. 2014. "Modelling and Mapping Spatio-Temporal Trends of Heavy Metal Accumulation in Moss and Natural Surface Soil Monitored 1990-2010 throughout Norway by Multivariate Generalized Linear Models and Geostatistics." *Atmospheric Environment* 99: 85–93.

Nickel, Stefan, and Winfried Schröder. 2017. "Reorganisation of a Long-Term Monitoring Network Using Moss as Biomonitor for Atmospheric Deposition in Germany." *Ecological Indicators* 76: 194–206.

Owczarek, M., M. Guidotti, G. Blasi, C. De Simone, A. De Marco, and M. Spadoni. 2001. "Traffic Pollution Monitoring Using Lichens as Bioaccumulators of Heavy Metals and Policyclic Aromatic Hydrocarbons." *Fresenius Environmental Bulletin* 10 (1): 42–45.

Pérez-Llamazares, Alicia, J. Ángel Fernández, Alejo Carballeira, and Jesús R. Aboal. 2011. "The Sequential Elution Technique Applied to Cryptogams: A Literature Review." *Journal of Bryology* 33 (4): 267–78.

Public Health Division, Oregon Health Authority, Public Health Division. 2020. "Public Health Assessment-Precision Castparts Corporation (PCC) Structurals, Inc." https://sharedsystems.dhsoha.state.or.us/DHSForms/Served/le8299.pdf.

Reski, R., E. Decker, A. Beike, S. Giordano, and P. Adamo. 2016. "Passive Contaminant Sensor Device Used to Sense Air Pollutants Comprising Polycyclic Aromatic Hydrocarbons or Heavy Metals or Their Compounds, Comprises Axenic Devitalized Moss Clone." accedacris.ulpgc.es. 2016.

Russell A. Brunekreef, B. 2009. "A Focus on Particule Matter and Health." *Environmental, Science and Technology* 43 (13): 4620–25.

Schraufnagel, D. E., J. R. Balmes, C. T. Cowl, S. De Matteis, S. H. Jung, K. Mortimer, R. Perez-Padilla, et al. 2019. "Air Pollution and Noncommunicable Diseases: A Review by the Forum of International Respiratory Societies' Environmental Committee, Part 1: The Damaging Effects of Air Pollution." *Chest* 155 (2): 409–16.

Schraufnagel, Dean E. 2020. "The Health Effects of Ultrafine Particles." *Experimental & Molecular Medicine* 52 (3): 311–17.

Schraufnagel, Dean E., John R. Balmes, Clayton T. Cowl, Sara De Matteis, Soon-Hee Jung, Kevin Mortimer, Rogelio Perez-Padilla, et al. 2019. "Air Pollution and Noncommunicable Diseases: A Review by the Forum of International Respiratory Societies' Environmental Committee, Part 2: Air Pollution and Organ Systems." *Chest* 155 (2): 417–26.

Shimada, Akinori, Natsuko Kawamura, Mina Okajima, Theerayuth Kaewamatawong, Hiromi Inoue, and Takehito Morita. 2006. "Translocation Pathway of the Intratracheally Instilled Ultrafine Particles from the Lung into the Blood Circulation in the Mouse." *Toxicologic Pathology* 34 (7): 949–57.

Spagnuolo, V., S. Giordano, A. Pérez-Llamazares, A. Ares, A. Carballeira, J. A. Fernández, and J. R. Aboal. 2013. "Distinguishing Metal Bioconcentration from Particulate Matter in Moss Tissue: Testing Methods of Removing Particles Attached to the Moss Surface." *The Science of the Total Environment* 463–464 (October): 727–33.

Svozilík, Vladislav, Aneta Svozilíková Krakovská, Jan Bitta, and Petr Janˇcík. 2021. "Comparison of the Air Pollution Mathematical Model of PM10 and Moss Biomonitoring Results in the Tritia Region." *Atmosphere* 12 (May): 656.

Tretiach, M., E. Pittao, P. Crisafulli, and P. Adamo. 2011. "Influence of Exposure Sites on Trace Element Enrichment in Moss-Bags and Characterization of Particles Deposited on the Biomonitor Surface." *The Science of the Total Environment* 409 (4): 822–30.

Tyler, Germund. 1990. "Bryophytes and Heavy Metals: A Literature Review." *Botanical Journal of the Linnean Society. Linnean Society of London* 104 (1–3): 231–53.

United Nations. 2016. "Paris Agreement." https://unfccc.int/sites/default/files/english_paris_agreement.pdf.

U.S. Environmental Protection Agency. 1963. "Clean Air Act." *National Oceanic and Atmospheric Administration*. https://sgp.fas.org/crs/misc/RL30853.pdf.

Valavanidis, Athanasios, Konstantinos Fiotakis, and Thomais Vlachogianni. 2008. "Airborne Particulate Matter and Human Health: Toxicological Assessment and Importance of Size and Composition of Particles for Oxidative Damage and Carcinogenic Mechanisms." *Journal of Environmental Science and Health - Part C Environmental Carcinogenesis and Ecotoxicology Reviews* 26 (4): 339–62.

Wolterbeek, Bert. 2002. "Biomonitoring of Trace Element Air Pollution: Principles, Possibilities and Perspectives." *Environmental Pollution* 120 (1): 11–21.

Zechmeister, H. G., D. Hohenwallner, A. Riss, and A. Hanus-Illnar. 2005. "Estimation of Element Deposition Derived from Road Traffic Sources by Using Mosses." *Environmental Pollution* 138 (2): 238–49.

111

Table S1. Percentage of accumulation (P, K, Mg, Ca, S, Mo, Mn & Fe) in matched post-exposure moss tissue (C_f-C_0/C_0) at Errol Heights City Park (HAR) for *O. lyellii* (O) and *S. palustre* (S). Minimum, median and maximum values were calculated across all sampling periods.

Matched Pair	Site	Sampling period	P O	P S	K O	K S	Mg O	Mg S	Ca O	Ca S	S O	S S	Mo O	Mo S	Mn O	Mn S	Fe O	Fe S
1	HAR	1	-2%	14%	20%	19%	11%	29%	111%	35%	12%	24%	27%	18%	-1%	70%	18%	183%
2	HAR	1	-3%	17%	14%	21%	7%	33%	108%	46%	9%	26%	22%	23%	0%	87%	9%	254%
3	HAR	1	-3%	13%	16%	50%	7%	36%	110%	62%	8%	41%	25%	39%	-6%	103%	8%	286%
4	HAR	2	-32%	-11%	-41%	-17%	-4%	54%	92%	85%	-8%	12%	12%	-22%	-21%	98%	-12%	247%
5	HAR	2	-31%	-22%	-41%	-28%	2%	52%	100%	94%	-5%	10%	29%	-22%	-16%	102%	2%	249%
6	HAR	2	-30%	-26%	-38%	-29%	-5%	57%	87%	91%	-5%	5%	5%	-38%	-24%	106%	-19%	237%
7	HAR	3	-51%	-51%	-39%	-62%	9%	47%	5%	62%	-18%	-10%	3%	-59%	-20%	153%	-20%	234%
8	HAR	3	-48%	-53%	-36%	-62%	14%	50%	10%	66%	-12%	-13%	-27%	-69%	-16%	155%	-14%	221%
9	HAR	3	-49%	-51%	-37%	-60%	9%	44%	4%	65%	-18%	-12%	-12%	-63%	-22%	162%	-20%	230%
10	HAR	4	-67%	-59%	-52%	-62%	18%	32%	7%	30%	-17%	-23%	9%	-63%	-4%	103%	11%	321%
11	HAR	4	-67%	-55%	-51%	-61%	26%	38%	16%	34%	-13%	-18%	10%	-62%	11%	88%	13%	279%
12	HAR	4	-66%	-58%	-51%	-65%	15%	38%	2%	38%	-19%	-22%	-2%	-62%	-11%	93%	-6%	316%
13	HAR	5	-41%	-51%	-38%	-59%	22%	45%	5%	51%	2%	-11%	63%	-52%	53%	116%	53%	277%
14	HAR	5	-45%	-48%	-35%	-56%	17%	36%	1%	41%	0%	-12%	46%	-43%	27%	112%	45%	299%
15	HAR	5	-46%	-50%	-33%	-59%	8%	48%	-2%	60%	-10%	-11%	40%	-43%	28%	134%	35%	354%
16	HAR	6	-50%	-28%	-47%	-22%	-37%	24%	-22%	43%	-31%	-4%	-37%	-11%	-4%	74%	-37%	182%
17	HAR	6	-32%	-25%	-26%	-20%	-9%	28%	14%	40%	-13%	-1%	-9%	4%	55%	70%	21%	143%
18	HAR	6	-32%	-28%	-26%	-27%	-5%	33%	21%	47%	-2%	3%	-6%	12%	58%	86%	11%	205%
		Min	-67%	-59%	-52%	-65%	-37%	24%	-22%	30%	-31%	-23%	-37%	-69%	-24%	70%	-37%	143%
		Median	-43%	-38%	-37%	-43%	9%	38%	12%	49%	-9%	-7%	10%	-40%	-4%	103%	9%	248%
		Max	-2%	17%	20%	50%	26%	57%	111%	94%	12%	41%	63%	39%	58%	162%	53%	354%

112

Table S2. Percentage of accumulation (Ni, Cu, Zn, B, Na, Sr, Ba & Ti) in matched post-exposure moss tissue (C_f-C_0/C_0) at Errol Heights City Park (HAR) for *O. lyellii* (O) and *S. palustre* (S). Minimum, median and maximum values were calculated across all sampling periods.

Matched Pair	Site	Sampling period	Ni O	Ni S	Cu O	Cu S	Zn O	Zn S	B O	B S	Na O	Na S	Sr O	Sr S	Ba O	Ba S	Ti O	Ti S
1	HAR	1	122%	174%	104%	305%	78%	102%	189%	576%	-87%	29%	19%	83%	4%	634%	29%	11113%
2	HAR	1	120%	256%	99%	230%	82%	94%	170%	631%	-88%	31%	16%	102%	8%	742%	18%	16143%
3	HAR	1	135%	385%	101%	357%	70%	135%	168%	766%	-89%	64%	18%	132%	6%	917%	22%	19192%
4	HAR	2	193%	474%	24%	801%	37%	186%	-38%	445%	-92%	-4%	-2%	146%	-8%	1092%	-21%	15139%
5	HAR	2	121%	766%	25%	822%	37%	146%	-21%	258%	-90%	-23%	2%	155%	-5%	1097%	10%	11511%
6	HAR	2	102%	384%	114%	850%	46%	162%	-26%	239%	-91%	-18%	-3%	157%	-11%	1176%	-38%	16342%
7	HAR	3	49%	611%	59%	483%	15%	131%	-17%	105%	-38%	-51%	6%	138%	-10%	987%	-11%	15374%
8	HAR	3	37%	354%	189%	648%	29%	129%	-3%	70%	-33%	-51%	11%	136%	-5%	952%	-23%	14286%
9	HAR	3	28%	344%	56%	569%	19%	146%	-8%	156%	-35%	-50%	7%	143%	-9%	1158%	-12%	15134%
10	HAR	4	69%	692%	324%	997%	46%	97%	-17%	10%	-52%	-58%	18%	200%	16%	1282%	25%	24516%
11	HAR	4	72%	574%	128%	689%	45%	86%	-9%	18%	-51%	-59%	25%	189%	24%	1242%	21%	20833%
12	HAR	4	91%	832%	265%	860%	45%	105%	-19%	11%	-51%	-60%	15%	200%	9%	1288%	-23%	22263%
13	HAR	5	142%	354%	46%	245%	62%	99%	-14%	167%	-26%	-54%	5%	155%	19%	995%	75%	14907%
14	HAR	5	81%	474%	49%	226%	47%	96%	-22%	160%	-28%	-49%	4%	156%	15%	1004%	31%	22376%
15	HAR	5	70%	834%	32%	256%	43%	97%	-18%	183%	-34%	-51%	0%	174%	13%	1152%	53%	28298%
16	HAR	6	-1%	238%	-22%	180%	-8%	65%	40%	416%	-49%	-24%	-30%	108%	-13%	695%	-73%	14724%
17	HAR	6	45%	230%	12%	180%	26%	68%	23%	495%	-26%	-19%	0%	94%	24%	591%	18%	11197%
18	HAR	6	50%	308%	35%	207%	38%	78%	43%	379%	-28%	-23%	10%	117%	33%	727%	-14%	16956%
Min			-1%	174%	-22%	180%	-8%	65%	-38%	10%	-92%	-60%	-30%	83%	-13%	591%	-73%	11113%
Median			77%	384%	57%	420%	44%	100%	-12%	211%	-50%	-37%	6%	144%	7%	999%	14%	15758%
Max			193%	834%	324%	997%	82%	186%	189%	766%	-26%	64%	25%	200%	33%	1288%	75%	28298%

113

Table S3. Percentage of accumulation (Al, Si, V, Cr, Co, Cd, Pb & As) in matched post-exposure moss tissue (C$_f$–C$_0$/C$_0$) at Errol Heights City Park (HAR) for *O. lyellii* (O) and *S. palustre* (S). Minimum, median and maximum values were calculated across all sampling periods.

Matched Pair	Site	Sampling period	Al		Si		V		Cr		Co		Cd		Pb		As	
			O	S	O	S	O	S	O	S	O	S	O	S	O	S	O	S
1	HAR	1	26%	4997%	24%	3879%	16%	10338%	23%	934%	28%	2053%	1%	1013%	73%	208%	-62%	81%
2	HAR	1	16%	5803%	8%	4600%	11%	12456%	11%	1317%	14%	2477%	24%	835%	58%	258%	-5%	-47%
3	HAR	1	11%	6979%	2%	5692%	11%	14526%	16%	1835%	17%	4005%	-6%	1343%	57%	296%	-47%	-23%
4	HAR	2	-2%	5905%	-7%	4731%	-11%	12127%	91%	3891%	29%	4896%	4%	5206%	19%	336%	90%	-22%
5	HAR	2	8%	5438%	3%	4282%	2%	12266%	70%	4370%	41%	4966%	11%	6278%	26%	333%	54%	-100%
6	HAR	2	-37%	5893%	-61%	5004%	-23%	12370%	36%	3675%	14%	4668%	-1%	4196%	14%	403%	31%	-64%
7	HAR	3	-17%	4965%	11%	37888%	-15%	11994%	-10%	2247%	12%	3527%	-33%	1473%	1%	210%	-29%	220%
8	HAR	3	-8%	4535%	19%	3721%	-14%	10447%	-9%	1859%	12%	2290%	-24%	2193%	-14%	250%	-29%	-100%
9	HAR	3	-15%	5077%	9%	3994%	-15%	11894%	-15%	1553%	-1%	4342%	-16%	1955%	-12%	213%	-63%	-88%
10	HAR	4	14%	9218%	27%	7457%	12%	18138%	20%	2975%	42%	5179%	116%	-100%	35%	263%	-1%	-18%
11	HAR	4	17%	7913%	41%	6652%	13%	16035%	19%	2641%	43%	6248%	94%	-100%	45%	240%	11%	-1%
12	HAR	4	-13%	8001%	-24%	5904%	-3%	17178%	1%	2896%	25%	5603%	150%	-100%	9%	262%	67%	21%
13	HAR	5	41%	6542%	14%	4726%	50%	137715%	90%	1975%	81%	4870%	-83%	-100%	66%	208%	31%	-35%
14	HAR	5	47%	7704%	25%	5843%	39%	16950%	43%	2466%	63%	4950%	-92%	-100%	51%	285%	14%	-48%
15	HAR	5	26%	8301%	1%	6027%	33%	20545%	39%	3670%	59%	10359%	-80%	-100%	50%	335%	-3%	-5%
16	HAR	6	-56%	5107%	-96%	3948%	-42%	12457%	-49%	1389%	-33%	2059%	-64%	1625%	-64%	160%	-1%	7%
17	HAR	6	17%	4155%	-3%	3450%	6%	9437%	16%	1207%	8%	2262%	-24%	1932%	14%	188%	-4%	40%
18	HAR	6	10%	6054%	-24%	5314%	7%	13029%	1%	1460%	-5%	2731%	-28%	1831%	3%	191%	39%	-75%
		Min	-56%	4155%	-96%	3450%	-42%	9437%	-49%	934%	-33%	2053%	-92%	-100%	-64%	160%	-63%	-100%
		Median	10%	5899%	5%	4729%	6%	12457%	17%	2111%	21%	4505%	-11%	1408%	23%	254%	-1%	-22%
		Max	47%	9218%	41%	7457%	50%	20545%	91%	4370%	81%	10359%	150%	6278%	73%	403%	90%	220%

114

Table S 4. Percentage of accumulation (P, K, Mg, Ca, S, Mo, Mn & Fe) in matched post-exposure moss tissue (C_f-C_0/C_0) Oregon Episcopal School (OES) for *O. lyellii* (O) and *S. palustre* (S). Minimum, median and maximum values were calculated across all sampling periods.

Matched Pair	Site	Sampling period	P		K		Mg		Ca		S		Mo		Mn		Fe	
			O	S	O	S	O	S	O	S	O	S	O	S	O	S	O	S
19	OES	1	-12%	-24%	4%	-26%	3%	97%	88%	100%	-1%	7%	4%	-7%	-15%	90%	-7%	95%
20	OES	1	-2%	-2%	14%	-7%	10%	80%	104%	87%	8%	17%	12%	5%	-4%	92%	10%	116%
21	OES	1	-12%	-4%	3%	-5%	4%	75%	90%	83%	0%	16%	12%	6%	-21%	85%	2%	117%
22	OES	2	-29%	-30%	-39%	-37%	4%	59%	106%	103%	-5%	1%	8%	-43%	-17%	137%	2%	193%
23	OES	2	-27%	-34%	-34%	-37%	7%	65%	113%	99%	-4%	-1%	69%	-48%	10%	103%	45%	156%
24	OES	2	-28%	-31%	-38%	-37%	2%	62%	99%	103%	-2%	2%	10%	-52%	-19%	92%	-7%	156%
25	OES	3	-48%	-50%	-32%	-61%	11%	50%	5%	62%	-14%	-8%	-14%	-65%	-19%	145%	-19%	146%
26	OES	3	-50%	-53%	-36%	-63%	5%	47%	2%	62%	-18%	-13%	-18%	-65%	-9%	159%	-27%	160%
27	OES	3	-42%	-54%	-27%	-64%	18%	43%	12%	56%	-9%	-12%	-8%	-72%	-11%	137%	-18%	112%
28	OES	4	-69%	-53%	-54%	-52%	10%	35%	-4%	37%	-21%	-17%	-17%	-57%	-16%	70%	-6%	211%
29	OES	4	-65%	-53%	-49%	-54%	24%	32%	9%	35%	-7%	-20%	-5%	-59%	-6%	55%	-4%	103%
30	OES	4	-68%	-53%	-51%	-55%	19%	32%	2%	30%	-16%	-19%	-3%	-58%	-8%	58%	-9%	141%
31	OES	5	-42%	-44%	-42%	-53%	15%	26%	-4%	29%	2%	-14%	47%	-46%	32%	71%	53%	138%
32	OES	5	-34%	-45%	-36%	-51%	12%	31%	-10%	37%	0%	-13%	29%	-48%	14%	67%	18%	112%
33	OES	5	-38%	-48%	-38%	-54%	19%	31%	-3%	32%	4%	-14%	37%	-53%	28%	72%	43%	130%
34	OES	6	-29%	-39%	-22%	-35%	-8%	48%	14%	65%	-13%	2%	-10%	-15%	67%	82%	6%	120%
35	OES	6	-28%	-29%	-23%	-23%	-6%	37%	15%	48%	-10%	0%	-15%	-11%	45%	63%	5%	94%
36	OES	6	-29%	-36%	-20%	-33%	-5%	49%	14%	70%	-7%	-3%	-12%	-8%	53%	77%	11%	95%
		Min	-69%	-54%	-54%	-64%	-8%	26%	-10%	29%	-21%	-20%	-18%	-72%	-21%	55%	-27%	94%
		Median	-32%	-42%	-35%	-44%	8%	48%	13%	62%	-6%	-6%	0%	-48%	-7%	83%	2%	125%
		Max	-2%	-2%	14%	-5%	24%	97%	113%	103%	8%	17%	69%	6%	67%	159%	53%	211%

Table S 5. Percentage of accumulation (Ni, Cu, Zn, B, Na, Sr, Ba & Ti) in matched post-exposure moss tissue (C_f-C_0/C_0) Oregon Episcopal School (OES) for *O. lyellii* (O) and *S. palustre* (S). Minimum, median and maximum values were calculated across all sampling periods.

Matched Pair	Site	Sampling period	Ni O	Ni S	Cu O	Cu S	Zn O	Zn S	B O	B S	Na O	Na S	Sr O	Sr S	Ba O	Ba S	Ti O	Ti S
19	OES	1	97%	-6%	77%	89%	38%	46%	136%	252%	-89%	15%	6%	461%	-7%	479%	-27%	5696%
20	OES	1	102%	-32%	87%	90%	48%	56%	148%	336%	-87%	29%	16%	364%	3%	520%	28%	8658%
21	OES	1	85%	-44%	77%	82%	28%	43%	99%	438%	-88%	31%	9%	328%	-6%	520%	27%	9013%
22	OES	2	21%	22%	1%	248%	20%	87%	-26%	215%	-92%	-33%	5%	153%	-1%	823%	20%	11542%
23	OES	2	72%	32%	11%	352%	15%	78%	-21%	193%	-90%	-30%	6%	148%	-3%	716%	46%	10300%
24	OES	2	10%	45%	9%	525%	17%	76%	-26%	326%	-92%	-33%	3%	147%	-6%	606%	5%	7570%
25	OES	3	-27%	-2%	53%	393%	-3%	80%	-6%	5%	-32%	-48%	7%	108%	-11%	677%	-35%	5786%
26	OES	3	-34%	-5%	9%	350%	2%	69%	-15%	43%	-36%	-55%	0%	114%	-14%	752%	-21%	8003%
27	OES	3	-9%	-4%	48%	499%	3%	65%	5%	11%	-27%	-54%	14%	100%	-6%	614%	-7%	4203%
28	OES	4	8%	-29%	255%	624%	18%	54%	-41%	115%	-56%	-54%	6%	120%	5%	822%	-22%	6901%
29	OES	4	42%	-4%	143%	483%	48%	44%	-13%	57%	-51%	-55%	18%	118%	13%	744%	-24%	4879%
30	OES	4	13%	-30%	126%	720%	26%	56%	-32%	14%	-52%	-56%	12%	113%	10%	847%	-24%	6536%
31	OES	5	24%	3%	38%	223%	41%	52%	-20%	52%	-25%	-49%	-3%	80%	6%	497%	79%	8432%
32	OES	5	12%	-51%	31%	149%	31%	40%	-15%	65%	-21%	-51%	-6%	81%	2%	442%	-8%	4475%
33	OES	5	8%	-8%	31%	96%	38%	52%	-28%	75%	-19%	-51%	0%	90%	9%	511%	64%	8400%
34	OES	6	2%	18%	-5%	387%	8%	75%	15%	501%	-24%	-24%	0%	180%	28%	466%	15%	4333%
35	OES	6	-3%	6%	8%	340%	4%	63%	14%	444%	-22%	-15%	3%	141%	26%	502%	17%	5827%
36	OES	6	18%	-26%	13%	398%	10%	51%	32%	379%	-22%	-13%	4%	266%	30%	452%	25%	3675%
Min			-34%	-51%	-5%	82%	-3%	40%	-41%	5%	-92%	-56%	-6%	80%	-14%	442%	-35%	3675%
Median			12%	-5%	34%	351%	19%	56%	-14%	154%	-43%	-41%	5%	130%	2%	563%	10%	6718%
Max			102%	45%	255%	720%	48%	87%	148%	501%	-19%	31%	18%	461%	30%	847%	79%	11542%

Table S 6. Percentage of accumulation (Al, Si, V, Cr, Co, Cd, Pb & As) in matched post-exposure moss tissue (C_f-C_0/C_0) at Oregon Episcopal School (OES) for *O. lyellii* (O) and *S. palustre* (S). Minimum, median and maximum values were calculated across all sampling periods.

Matched Pair	Site	Sampling period	Al		Si		V		Cr		Co		Cd		Pb		As	
			O	S	O	S	O	S	O	S	O	S	O	S	O	S	O	S
19	OES	1	-25%	1931%	-44%	6696%	-11%	6755%	-17%	82%	-12%	701%	-9%	70%	14%	162%	41%	-33%
20	OES	1	12%	2927%	10%	7003%	11%	7459%	10%	229%	16%	754%	0%	762%	52%	236%	4%	-14%
21	OES	1	2%	3089%	0%	6852%	5%	7515%	2%	202%	0%	690%	-14%	568%	40%	195%	-45%	-45%
22	OES	2	15%	4469%	13%	4444%	2%	7795%	12%	1444%	15%	1152%	49%	8618%	-11%	207%	-27%	62%
23	OES	2	24%	4293%	17%	3837%	21%	7244%	74%	1037%	52%	1094%	54%	9164%	6%	154%	7%	45%
24	OES	2	2%	3026%	0%	2391%	-8%	6416%	0%	1432%	8%	1418%	-3%	4563%	-17%	68%	-41%	18%
25	OES	3	-27%	2314%	-15%	1971%	-22%	4215%	-23%	565%	-14%	929%	-33%	1638%	-39%	107%	51%	-41%
26	OES	3	-28%	2786%	-4%	2423%	-24%	5909%	-29%	600%	-23%	841%	-20%	1656%	-21%	127%	11%	1%
27	OES	3	-8%	1977%	48%	1614%	-14%	3851%	-10%	545%	-3%	1003%	-32%	1452%	-5%	52%	-18%	24%
28	OES	4	-33%	2520%	-50%	2209%	-13%	4599%	-16%	808%	-2%	1207%	77%	-100%	-12%	116%	61%	62%
29	OES	4	-21%	2081%	-57%	1800%	-6%	3774%	-15%	621%	1%	796%	110%	-100%	-12%	99%	10%	16%
30	OES	4	-18%	2499%	-36%	2141%	-9%	4104%	-14%	579%	-6%	859%	89%	-100%	-12%	105%	3%	-7%
31	OES	5	41%	3034%	22%	2600%	52%	5555%	58%	563%	70%	819%	-99%	-100%	57%	157%	-25%	-37%
32	OES	5	1%	2169%	-19%	1793%	13%	4220%	9%	398%	15%	842%	-93%	-100%	11%	100%	50%	52%
33	OES	5	34%	3128%	28%	2710%	41%	5930%	40%	587%	45%	1176%	-96%	-100%	48%	100%	-23%	-38%
34	OES	6	15%	1714%	-1%	2636%	3%	4979%	-9%	273%	-5%	863%	-27%	-3%	12%	72%	50%	49%
35	OES	6	14%	2395%	-4%	3453%	3%	5543%	-8%	186%	-5%	663%	-31%	-100%	9%	58%	-53%	-23%
36	OES	6	23%	1486%	5%	3715%	9%	4626%	7%	86%	-5%	566%	-29%	35%	15%	96%	-24%	9%
		Min	-33%	1486%	-57%	1614%	-24%	3774%	-29%	82%	-23%	566%	-99%	-100%	-39%	52%	-53%	-45%
		Median	2%	2510%	-1%	2618%	2%	5549%	-4%	564%	-1%	851%	-17%	53%	8%	106%	3%	5%
		Max	41%	4469%	48%	7003%	52%	7795%	74%	1444%	70%	1418%	110%	9164%	57%	236%	61%	62%

117

Table S7. Percentage of accumulation (P, K, Mg, Ca, S, Mo, Mn & Fe) in matched post-exposure moss tissue (C_f-C_0/C_0) Bryant St. Pumphouse (PUM) for *O. lyellii* (O) and *S. palustre* (S). Minimum, median and maximum values were calculated across all sampling periods.

Matched Pair	Site	Sampling period	P		K		Mg		Ca		S		Mo		Mn		Fe	
			O	S	O	S	O	S	O	S	O	S	O	S	O	S	O	S
37	PUM	1	-4%	-3%	6%	-5%	-1%	4%	98%	13%	2%	2%	17%	-7%	22%	24%	1%	89%
38	PUM	1	-3%	-9%	10%	-6%	1%	1%	95%	6%	5%	-1%	16%	-1%	-6%	26%	3%	107%
39	PUM	1	-4%	-6%	5%	-2%	0%	5%	97%	9%	2%	3%	9%	-7%	-4%	21%	-10%	67%
40	PUM	2	-37%	-32%	-54%	-40%	-10%	45%	83%	72%	-16%	10%	18%	-37%	-27%	155%	-12%	232%
41	PUM	2	-31%	-45%	-52%	-57%	-14%	44%	82%	76%	-20%	-8%	10%	-57%	-31%	80%	-29%	175%
42	PUM	2	-35%	-41%	-54%	-54%	-10%	49%	73%	71%	-16%	-11%	6%	-52%	-32%	98%	-29%	237%
43	PUM	3	-43%	-50%	-33%	-62%	9%	46%	6%	66%	-8%	-11%	-6%	-71%	-17%	108%	-15%	235%
44	PUM	3	-47%	-54%	-36%	-62%	12%	44%	5%	61%	-10%	-15%	-20%	-74%	-28%	79%	-32%	131%
45	PUM	3	-46%	-52%	-37%	-61%	4%	42%	-1%	62%	-14%	-11%	-17%	-70%	-25%	96%	-34%	212%
46	PUM	4	-67%	-52%	-54%	-55%	19%	27%	7%	21%	-11%	-15%	-2%	-63%	-5%	59%	4%	193%
47	PUM	4	-64%	-43%	-55%	-46%	20%	38%	9%	34%	-8%	-3%	2%	-53%	-1%	70%	21%	239%
48	PUM	4	-64%	-53%	-54%	-60%	24%	29%	11%	24%	-5%	-15%	2%	-66%	4%	53%	27%	173%
49	PUM	5	-41%	-46%	-33%	-52%	10%	41%	0%	54%	-1%	-5%	40%	-48%	26%	137%	48%	398%
50	PUM	5	-37%	-40%	-27%	-46%	12%	33%	2%	37%	2%	-4%	41%	-41%	47%	118%	57%	351%
51	PUM	5	-38%	-48%	-28%	-55%	12%	20%	0%	27%	-2%	-16%	42%	-53%	25%	103%	41%	333%
52	PUM	6	-30%	-10%	-25%	-16%	-4%	41%	15%	55%	1%	22%	-5%	8%	68%	166%	23%	438%
53	PUM	6	-26%	-32%	-20%	-32%	-3%	35%	17%	50%	2%	0%	-3%	-4%	61%	138%	22%	354%
54	PUM	6	-30%	-27%	-23%	-28%	-3%	37%	18%	49%	2%	0%	-7%	-4%	62%	144%	28%	384%
		Min	-67%	-54%	-55%	-62%	-14%	1%	-1%	6%	-20%	-16%	-20%	-74%	-32%	21%	-34%	67%
		Median	-37%	-42%	-33%	-49%	3%	37%	13%	50%	-4%	-4%	4%	-50%	-2%	97%	4%	233%
		Max	-3%	-3%	10%	-2%	24%	49%	98%	76%	5%	22%	42%	8%	68%	166%	57%	438%

118

Table S8. Percentage of accumulation (Ni, Cu, Zn, B, Na, Sr, Ba & Ti) in matched post-exposure moss tissue (C_r-C_0/C_0) Bryant St. Pumphouse (PUM) for *O. lyellii* (O) and *S. palustre* (S). Minimum, median and maximum values were calculated across all sampling periods.

Matched Pair	Site	Sampling period	Ni O	Ni S	Cu O	Cu S	Zn O	Zn S	B O	B S	Na O	Na S	Sr O	Sr S	Ba O	Ba S	Ti O	Ti S
37	PUM	1	96%	-23%	76%	103%	48%	29%	185%	280%	-90%	2%	7%	32%	4%	269%	13%	8594%
38	PUM	1	109%	-31%	81%	125%	51%	21%	161%	289%	-89%	1%	10%	37%	0%	314%	12%	9148%
39	PUM	1	92%	-54%	77%	129%	55%	22%	190%	321%	-92%	4%	8%	32%	0%	242%	-33%	5571%
40	PUM	2	19%	28%	-7%	548%	7%	98%	-28%	127%	-93%	-37%	-8%	107%	-11%	765%	-3%	6114%
41	PUM	2	19%	19%	-9%	391%	37%	78%	-53%	103%	-94%	-56%	-7%	112%	-6%	734%	-25%	8790%
42	PUM	2	25%	117%	-2%	324%	20%	93%	-52%	178%	-94%	-50%	-7%	122%	-11%	1255%	-38%	12454%
43	PUM	3	-27%	45%	54%	291%	38%	90%	-8%	267%	-32%	-51%	5%	158%	-10%	891%	-4%	15477%
44	PUM	3	-34%	-15%	65%	428%	10%	72%	-19%	84%	-39%	-51%	10%	129%	-8%	770%	-47%	7353%
45	PUM	3	-28%	-4%	49%	475%	2%	95%	-15%	96%	-36%	-47%	4%	145%	-11%	739%	-43%	15330%
46	PUM	4	-1%	300%	69%	615%	31%	50%	-26%	33%	-54%	-58%	20%	135%	17%	741%	7%	8555%
47	PUM	4	17%	-11%	130%	288%	31%	49%	-2%	94%	-53%	-44%	22%	164%	17%	871%	35%	14036%
48	PUM	4	20%	-31%	104%	1033%	31%	47%	-7%	60%	-53%	-60%	23%	142%	18%	772%	42%	8414%
49	PUM	5	25%	40%	39%	207%	44%	86%	-5%	121%	-31%	-44%	3%	244%	12%	1029%	71%	24422%
50	PUM	5	42%	41%	44%	185%	82%	97%	-4%	175%	-27%	-36%	7%	211%	16%	918%	60%	22937%
51	PUM	5	31%	10%	40%	141%	46%	64%	-12%	155%	-24%	-48%	4%	179%	13%	908%	52%	27471%
52	PUM	6	18%	33%	26%	295%	24%	169%	18%	460%	-28%	-11%	13%	149%	40%	968%	-12%	22544%
53	PUM	6	15%	39%	14%	218%	25%	116%	27%	293%	-22%	-25%	14%	164%	39%	1019%	-3%	25738%
54	PUM	6	23%	24%	29%	223%	24%	120%	37%	274%	-25%	-25%	14%	156%	39%	1035%	7%	25719%
		Min	-34%	-54%	-9%	103%	2%	21%	-53%	33%	-94%	-60%	-8%	32%	-11%	242%	-47%	5571%
		Median	20%	22%	46%	289%	31%	82%	-6%	165%	-46%	-44%	8%	143%	8%	822%	2%	13245%
		Max	109%	300%	130%	1033%	82%	169%	190%	460%	-22%	4%	23%	244%	40%	1255%	71%	27471%

119

Table S 9. Percentage of accumulation (Al, Si, V, Cr, Co, Cd, Pb & As) in matched post-exposure moss tissue (C_t-C_0/C_0) at Bryant St. Pumphouse (PUM) for *O. lyellii* (O) and *S. palustre* (S). Minimum, median and maximum values were calculated across all sampling periods.

Matched Pair	Site	Sampling period	Al		Si		V		Cr		Co		Cd		Pb		As	
			O	S	O	S	O	S	O	S	O	S	O	S	O	S	O	S
37	PUM	1	-1%	2812%	-5%	2428%	0%	5798%	1%	133%	-1%	875%	28%	176%	53%	128%	-48%	-53%
38	PUM	1	8%	34888%	9%	2983%	3%	6861%	4%	208%	8%	859%	-8%	412%	50%	105%	-22%	-78%
39	PUM	1	-25%	25770%	-42%	2095%	-14%	4669%	-5%	0%	-14%	735%	7%	278%	31%	62%	58%	-25%
40	PUM	2	-10%	2124%	-7%	901%	-16%	5531%	24%	1390%	-5%	1359%	-10%	1543%	5%	193%	152%	49%
41	PUM	2	-25%	3509%	-29%	2111%	-28%	7897%	11%	896%	-16%	1743%	-21%	1317%	2%	244%	-98%	15%
42	PUM	2	-26%	45066%	-27%	3878%	-31%	8626%	16%	1772%	-9%	1476%	-23%	3102%	-7%	270%	72%	202%
43	PUM	3	13%	59344%	23%	4429%	-11%	11406%	-20%	1041%	-9%	2043%	-18%	2166%	14%	328%	68%	-38%
44	PUM	3	-48%	35671%	-60%	3236%	-33%	6342%	-47%	575%	-28%	1219%	-28%	1878%	-27%	215%	128%	-9%
45	PUM	3	-28%	55556%	-13%	3968%	-29%	11485%	-38%	768%	-23%	1723%	-34%	2356%	-20%	312%	14%	-98%
46	PUM	4	15%	49905%	30%	3712%	3%	8402%	-5%	3681%	18%	1957%	102%	-100%	40%	196%	-12%	64%
47	PUM	4	27%	6024%	36%	4975%	16%	101115%	12%	938%	34%	1704%	187%	-100%	65%	319%	11%	41%
48	PUM	4	35%	45188%	58%	3348%	25%	7499%	18%	671%	40%	1204%	183%	-100%	78%	275%	22%	55%
49	PUM	5	46%	119987%	18%	8723%	44%	21695%	42%	1452%	60%	3271%	-84%	-100%	117%	730%	-11%	16%
50	PUM	5	44%	11097%	12%	8231%	48%	186685%	80%	1158%	129%	3105%	-85%	-100%	108%	629%	-31%	-37%
51	PUM	5	40%	9860%	19%	6997%	35%	18771%	38%	1080%	55%	2985%	-82%	-100%	100%	677%	-9%	-14%
52	PUM	6	2%	65225%	-49%	1593%	14%	22642%	0%	2166%	0%	3217%	-48%	-100%	-7%	337%	60%	95%
53	PUM	6	31%	84266%	4%	7347%	15%	196760%	2%	1510%	-1%	2036%	-42%	986%	27%	298%	18%	-20%
54	PUM	6	32%	87366%	4%	7083%	20%	21600%	14%	1671%	45%	2386%	-44%	719%	22%	290%	-37%	57%
		Min	-48%	2124%	-60%	901%	-33%	4669%	-47%	0%	-28%	735%	-85%	-100%	-27%	62%	-98%	-98%
		Median	5%	5230%	4%	3795%	3%	9370%	8%	1060%	0%	1733%	-22%	345%	29%	282%	12%	3%
		Max	46%	119987%	58%	8723%	48%	22642%	80%	3681%	129%	3271%	187%	3102%	117%	730%	152%	202%

120

Table S10. Percentage of accumulation (P, K, Mg, Ca, S, Mo, Mn & Fe) in matched post-exposure moss tissue (C_f-C_0/C_0) Portland Water Bureau (PWB) for *O. lyellii* (O) and *S. palustre* (S). Minimum, median and maximum values were calculated across all sampling periods.

Matched Pair	Site	Sampling period	P O	P S	K O	K S	Mg O	Mg S	Ca O	Ca S	S O	S S	Mo O	Mo S	Mn O	Mn S	Fe O	Fe S
55	PWB	1	-17%	22%	-2%	26%	-11%	41%	71%	54%	-8%	37%	7%	21%	-14%	134%	0%	361%
56	PWB	1	-6%	42%	14%	45%	3%	62%	98%	73%	4%	67%	18%	45%	-6%	236%	9%	674%
57	PWB	1	0%	36%	21%	33%	9%	44%	112%	59%	9%	52%	28%	31%	5%	147%	16%	406%
58	PWB	2	-27%	-8%	-20%	60%	1%	92%	91%	89%	0%	18%	26%	-41%	-13%	315%	6%	565%
59	PWB	2	-28%	-34%	70%	-37%	10%	62%	98%	102%	-6%	0%	27%	-35%	-1%	195%	19%	544%
60	PWB	2	-26%	-20%	18%	18%	4%	56%	101%	68%	-2%	17%	43%	-17%	-2%	248%	18%	518%
61	PWB	3	-47%	-47%	8%	-35%	5%	50%	11%	80%	-16%	-10%	-2%	-68%	-21%	176%	-24%	416%
62	PWB	3	-51%	-48%	-25%	-39%	8%	50%	12%	77%	-16%	-7%	5%	-64%	-8%	200%	-4%	369%
63	PWB	3	-50%	-51%	-8%	-56%	11%	43%	11%	69%	-13%	-13%	-6%	-69%	-15%	149%	-15%	330%
64	PWB	4	-69%	-50%	-49%	-51%	15%	48%	9%	45%	-21%	-14%	10%	-64%	1%	132%	24%	381%
65	PWB	4	-65%	-49%	-49%	-48%	27%	49%	20%	51%	-8%	-13%	10%	-61%	19%	151%	27%	443%
66	PWB	4	-64%	-50%	-40%	-53%	29%	34%	16%	35%	-6%	-18%	5%	-61%	14%	125%	25%	381%
67	PWB	5	-42%	-50%	-42%	-59%	9%	41%	-1%	59%	-5%	-9%	40%	-52%	25%	165%	42%	414%
68	PWB	5	-32%	-28%	-33%	-38%	27%	54%	10%	64%	13%	21%	62%	-42%	46%	160%	85%	367%
69	PWB	5	-40%	-44%	-33%	-50%	16%	40%	11%	45%	1%	-3%	41%	-50%	29%	183%	41%	561%
70	PWB	6	-26%	-44%	-15%	-34%	-1%	24%	19%	32%	6%	-11%	0%	-23%	58%	115%	37%	264%
71	PWB	6	-27%	-34%	-19%	-24%	-2%	23%	22%	34%	-3%	-7%	4%	-10%	60%	101%	28%	259%
72	PWB	6	-20%	-47%	-15%	-40%	-2%	27%	24%	43%	3%	-13%	12%	-20%	68%	110%	44%	256%
		Min	-69%	-51%	-49%	-59%	-11%	23%	-1%	32%	-21%	-18%	-6%	-69%	-21%	101%	-24%	256%
		Median	-30%	-44%	-17%	-38%	8%	46%	20%	59%	-4%	-7%	11%	-42%	3%	155%	22%	394%
		Max	0%	42%	70%	60%	29%	92%	112%	102%	13%	67%	62%	45%	68%	315%	85%	674%

121

Table S 11. Percentage of accumulation (Ni, Cu, Zn, B, Na, Sr, Ba & Ti) in matched post-exposure moss tissue (Cf-C0/C0) Portland Water Bureau (PWB) for *O. lyellii* (O) and *S. palustre* (S). Minimum, median and maximum values were calculated across all sampling periods.

Matched Pair	Site	Sampling period	Ni O	Ni S	Cu O	Cu S	Zn O	Zn S	B O	B S	Na O	Na S	Sr O	Sr S	Ba O	Ba S	Ti O	Ti S
55	PWB	1	83%	59%	62%	260%	49%	146%	138%	725%	-90%	34%	-6%	135%	-16%	1031%	14%	25426%
56	PWB	1	105%	167%	81%	531%	58%	248%	194%	1069%	-89%	60%	10%	201%	-4%	1534%	29%	29367%
57	PWB	1	109%	100%	96%	358%	77%	203%	247%	869%	-89%	44%	15%	120%	2%	1006%	35%	17990%
58	PWB	2	47%	141%	53%	768%	65%	280%	70%	1611%	-93%	-64%	0%	466%	-10%	27004%	-17%	24807%
59	PWB	2	45%	126%	18%	460%	62%	265%	174%	829%	-93%	-49%	-1%	311%	-7%	2043%	34%	22919%
60	PWB	2	49%	108%	27%	478%	62%	227%	92%	959%	-92%	-42%	0%	322%	-5%	1967%	35%	23419%
61	PWB	3	-16%	92%	98%	547%	27%	150%	80%	240%	-45%	-57%	4%	305%	-11%	1920%	-39%	30540%
62	PWB	3	10%	58%	36%	307%	19%	147%	21%	213%	-40%	-53%	7%	292%	-9%	1825%	11%	24064%
63	PWB	3	-18%	61%	73%	355%	22%	132%	62%	24%	-41%	-53%	7%	238%	-7%	1562%	-23%	22296%
64	PWB	4	15%	36%	108%	289%	38%	141%	8%	136%	-53%	-55%	15%	233%	16%	1891%	36%	19655%
65	PWB	4	26%	64%	111%	343%	57%	144%	-3%	144%	-50%	-53%	24%	253%	24%	2205%	46%	29464%
66	PWB	4	46%	44%	328%	445%	66%	101%	7%	57%	-49%	-56%	20%	206%	16%	1679%	10%	29672%
67	PWB	5	25%	46%	28%	270%	55%	179%	-1%	157%	-29%	-54%	-7%	193%	2%	1593%	66%	20093%
68	PWB	5	57%	85%	48%	279%	78%	198%	14%	265%	-17%	-35%	3%	155%	14%	1302%	109%	15763%
69	PWB	5	35%	65%	47%	329%	68%	174%	7%	244%	-25%	-42%	5%	211%	19%	1739%	34%	39120%
70	PWB	6	32%	54%	29%	380%	50%	99%	109%	544%	-21%	-39%	14%	137%	42%	1048%	22%	19073%
71	PWB	6	14%	25%	13%	313%	40%	82%	76%	591%	-22%	-27%	10%	117%	35%	962%	44%	19166%
72	PWB	6	24%	9%	29%	470%	46%	94%	72%	493%	-17%	-43%	14%	128%	42%	1027%	65%	19742%
		Min	-18%	9%	13%	260%	19%	82%	-3%	24%	-93%	-64%	-7%	117%	-16%	962%	-39%	15763%
		Median	33%	63%	51%	356%	56%	148%	71%	379%	-47%	-46%	7%	209%	2%	1636%	34%	23169%
		Max	109%	167%	328%	768%	78%	280%	247%	1611%	-17%	60%	24%	466%	42%	27004%	109%	39120%

Table S12. Percentage of accumulation (Al, Si, V, Cr, Co, Cd, Pb & As) in matched post-exposure moss tissue (C_f-C_0/C_0) at Portland Water Bureau (PWB) for *O. lyellii* (O) and *S. palustre* (S). Minimum, median and maximum values were calculated across all sampling periods.

Matched Pair	Site	Sampling period	Al		Si		V		Cr		Co		Cd		Pb		As	
			O	S	O	S	O	S	O	S	O	S	O	S	O	S	O	S
55	PWB	1	1%	6926%	-4%	5911%	0%	18714%	-5%	1158%	3%	2719%	-21%	1107%	34%	314%	-48%	-36%
56	PWB	1	6%	11142%	1%	9284%	11%	26937%	12%	2921%	18%	5872%	-3%	3196%	49%	457%	-35%	67%
57	PWB	1	12%	4279%	-1%	407%	17%	18595%	19%	1380%	21%	26888%	15%	613%	62%	223%	-54%	63%
58	PWB	2	-18%	7930%	-52%	3169%	-2%	22772%	24%	2241%	13%	45546%	8%	3316%	-5%	315%	0%	-9%
59	PWB	2	20%	5162%	21%	1672%	14%	20578%	33%	2421%	47%	42555%	14%	37448%	21%	300%	-14%	206%
60	PWB	2	19%	7970%	21%	5649%	15%	20746%	44%	1962%	45%	4110%	27%	2478%	25%	267%	118%	33%
61	PWB	3	-37%	8133%	-41%	7559%	-24%	19514%	-27%	1624%	-11%	3539%	-21%	2764%	-28%	327%	30%	9%
62	PWB	3	-8%	7403%	17%	7731%	-3%	16677%	2%	1335%	1%	3118%	-26%	1987%	11%	307%	30%	-21%
63	PWB	3	-13%	6757%	6%	5929%	-17%	15475%	-19%	1295%	2%	26800%	-32%	2859%	-39%	302%	-46%	-21%
64	PWB	4	19%	8090%	31%	7393%	12%	15808%	17%	1294%	32%	2937%	162%	1102%	38%	256%	-11%	-29%
65	PWB	4	32%	9768%	55%	8855%	27%	20782%	21%	1639%	42%	3729%	35%	-8%	58%	400%	22%	-47%
66	PWB	4	15%	8607%	20%	7707%	21%	17945%	17%	1426%	42%	33711%	114%	-100%	37%	331%	-3%	-52%
67	PWB	5	27%	6312%	6%	34044%	39%	18712%	38%	1288%	58%	35555%	-88%	-100%	52%	256%	-22%	7%
68	PWB	5	58%	3861%	39%	790%	73%	15510%	80%	1223%	102%	3300%	-86%	-100%	81%	299%	-20%	78%
69	PWB	5	38%	10953%	15%	9040%	36%	28219%	36%	1881%	59%	54465%	-88%	-100%	30%	420%	1%	-59%
70	PWB	6	33%	6497%	-3%	5962%	30%	14781%	21%	835%	32%	2009%	-42%	518%	9%	224%	-42%	-61%
71	PWB	6	36%	57750%	14%	5272%	25%	13828%	16%	805%	24%	1820%	-3%	1135%	36%	261%	-26%	17%
72	PWB	6	47%	5991%	17%	5553%	41%	14351%	32%	736%	26%	1801%	-3%	1158%	51%	256%	30%	15%
		Min	-37%	3861%	-52%	407%	-24%	13828%	-27%	736%	-11%	1801%	-88%	-100%	-39%	223%	-54%	-61%
		Median	19%	7164%	14%	5920%	16%	18654%	20%	13557%	29%	3335%	-3%	1121%	35%	301%	-13%	-1%
		Max	58%	11142%	55%	92284%	73%	28219%	80%	2921%	102%	5872%	162%	3748%	81%	457%	118%	206%

123
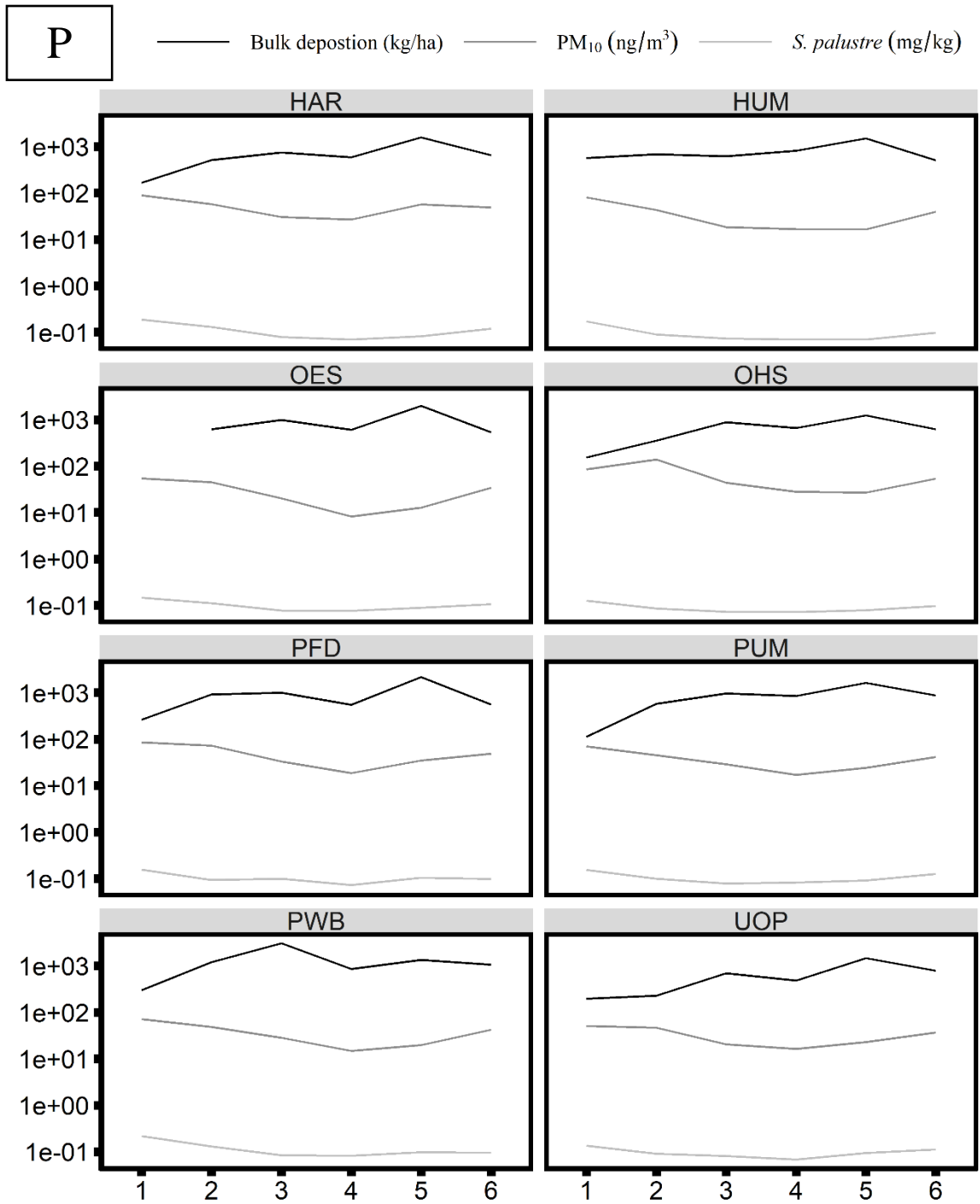
Figure S1. Timeseries showing Bulk deposition (mg/kg), ambient PM_{10} (ng/m^3) and *S. palustre* tissue concertation (mg/kg) for phosphorous separated by site over 6 sampling periods. The y-axis is log transformed for visual comparison and OES bulk deposition for sampling period 1 are omitted due to 0 values from no precipitation during that period.
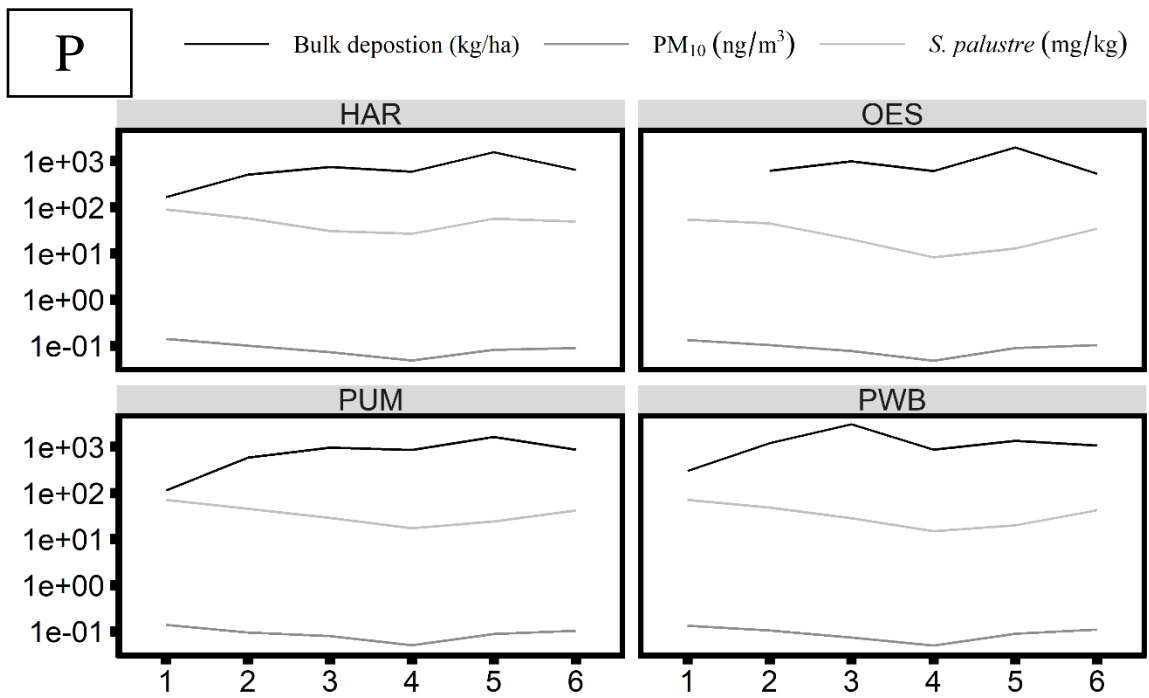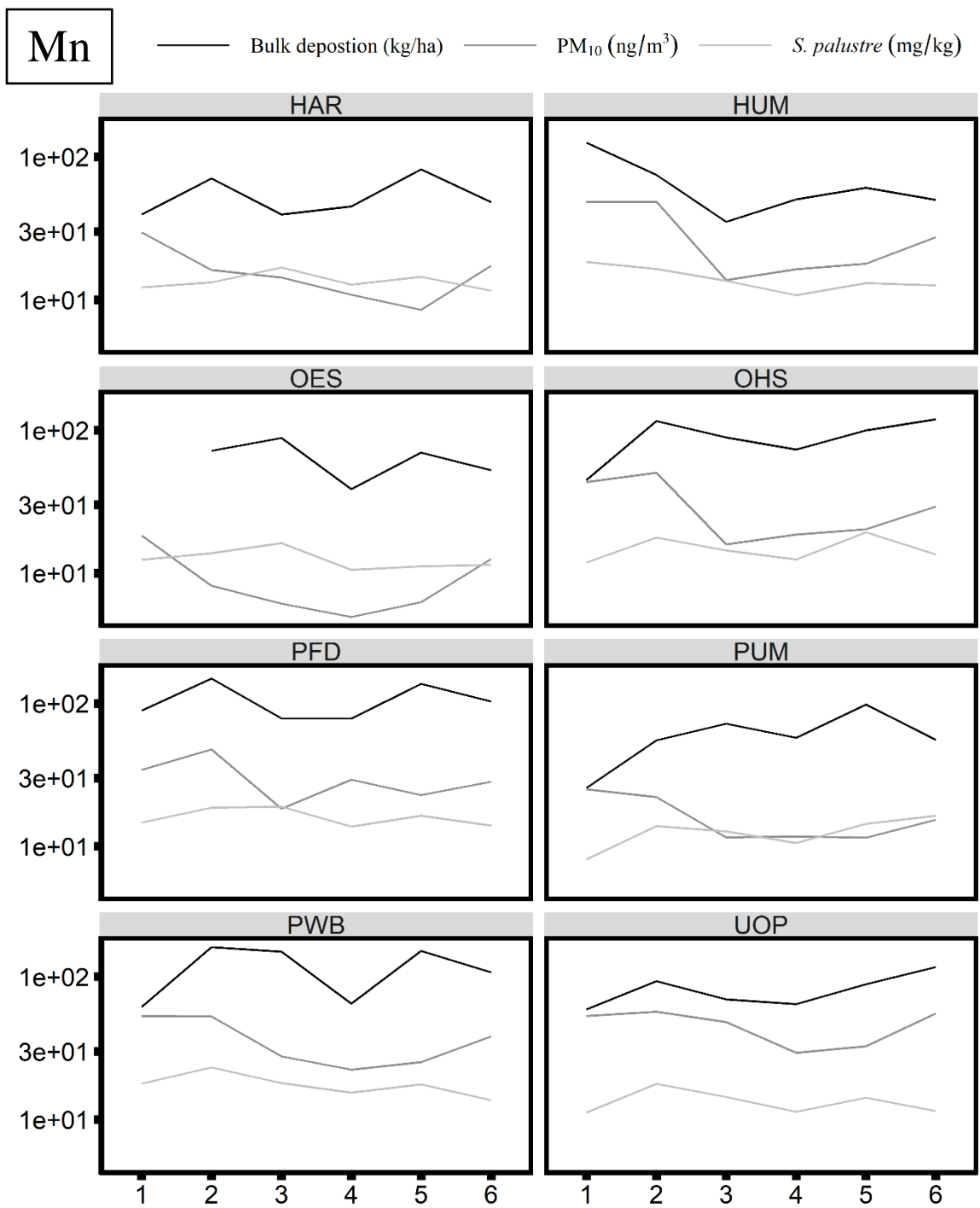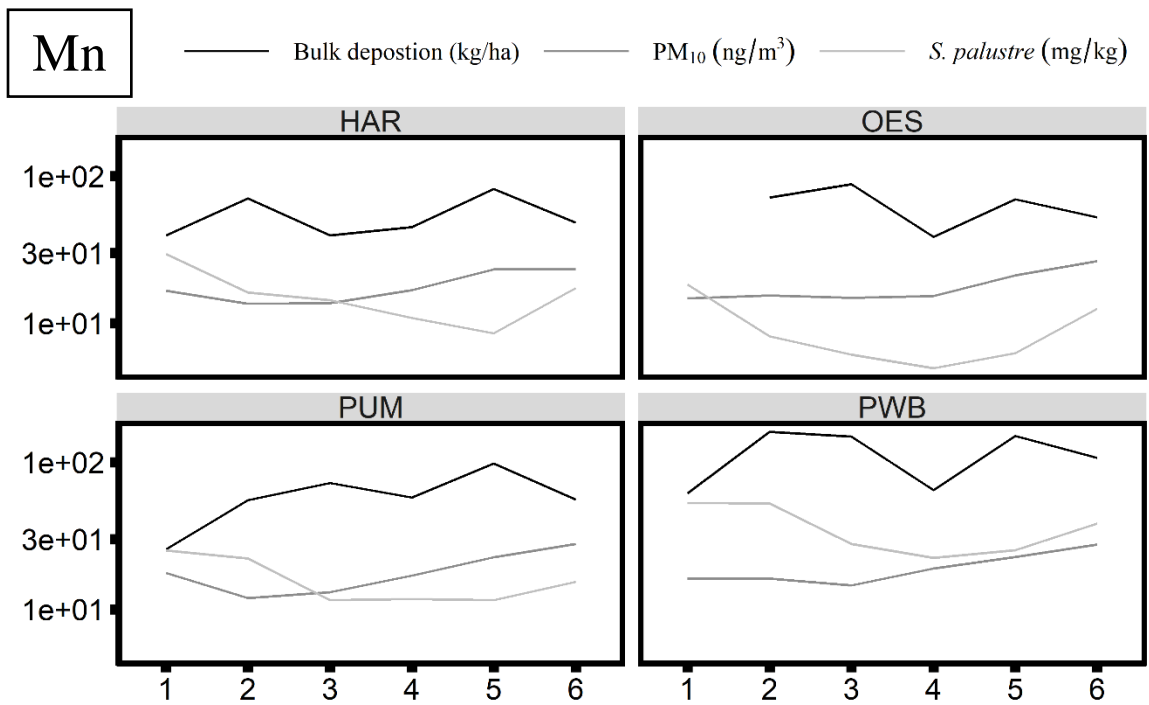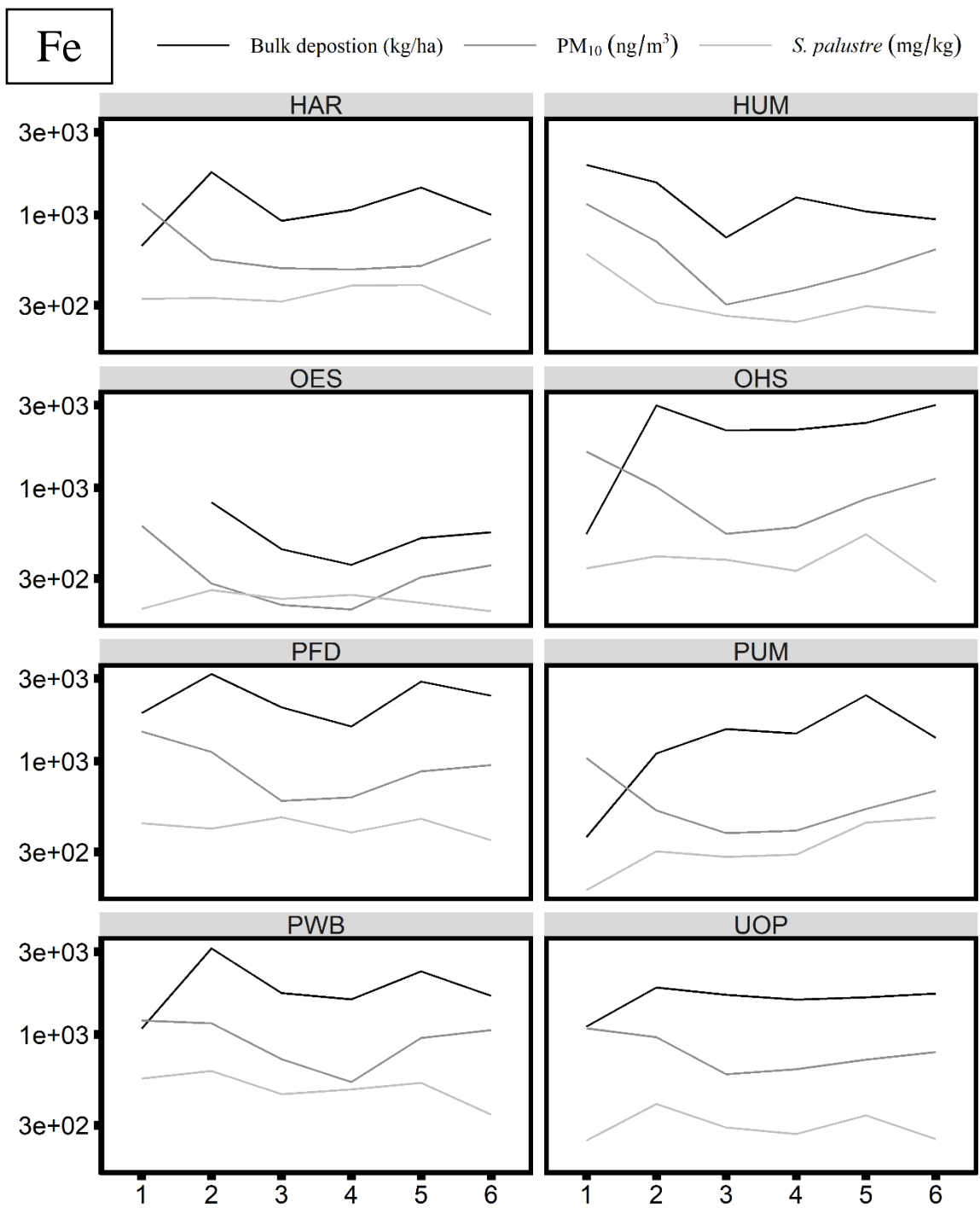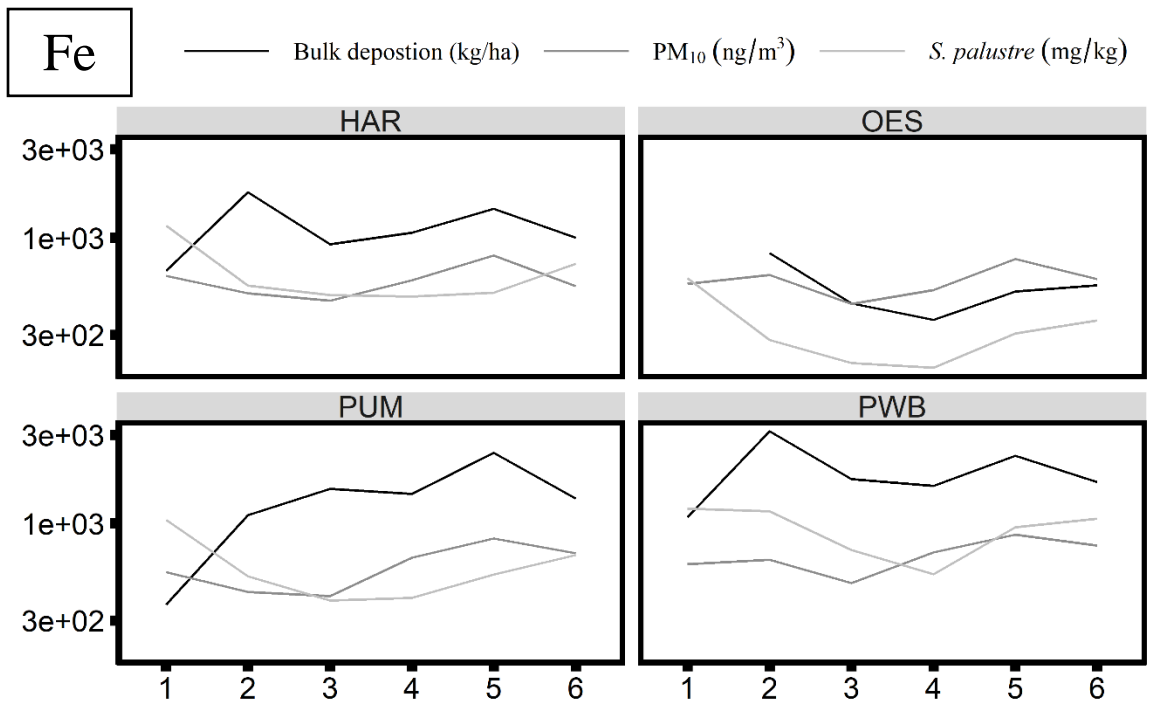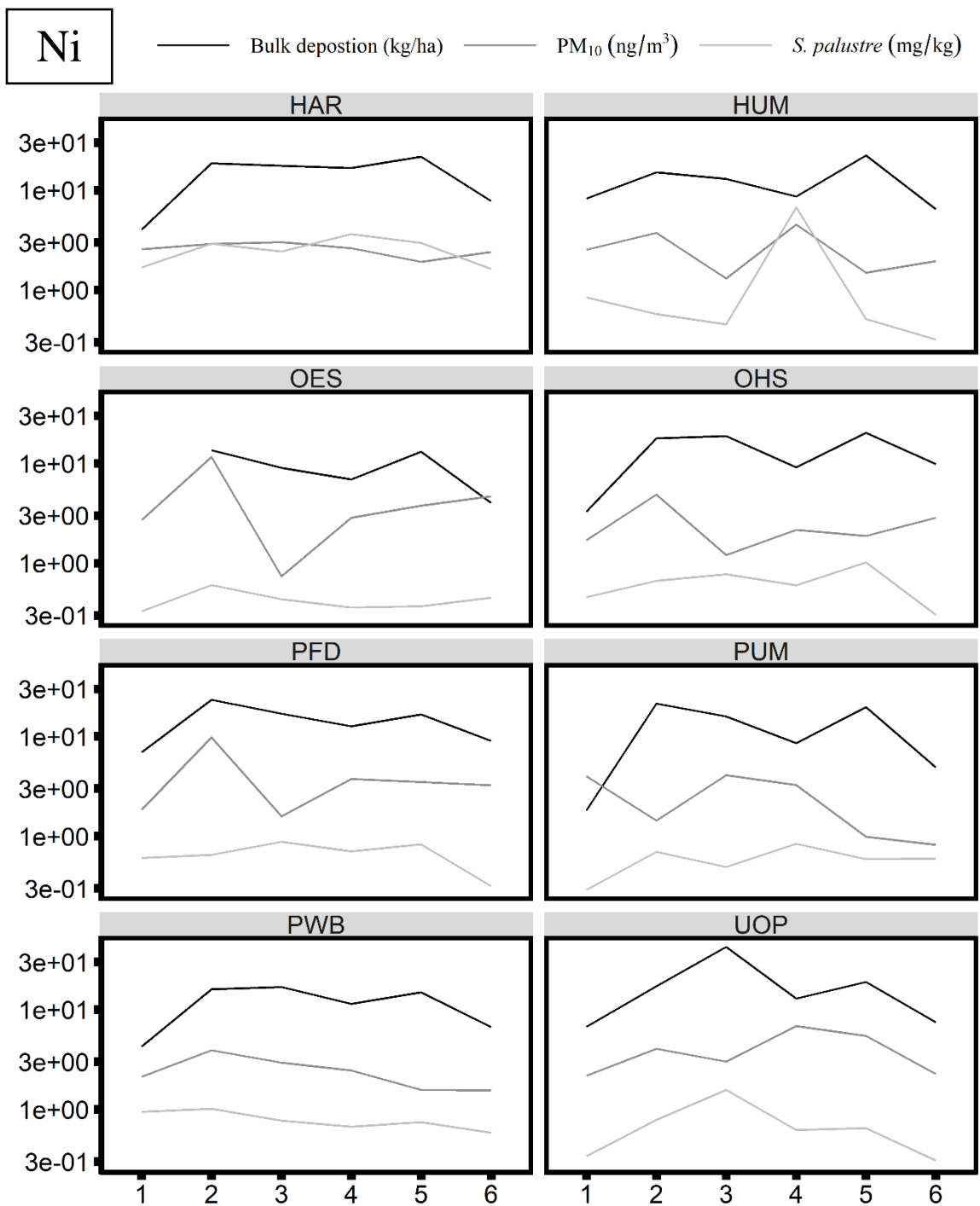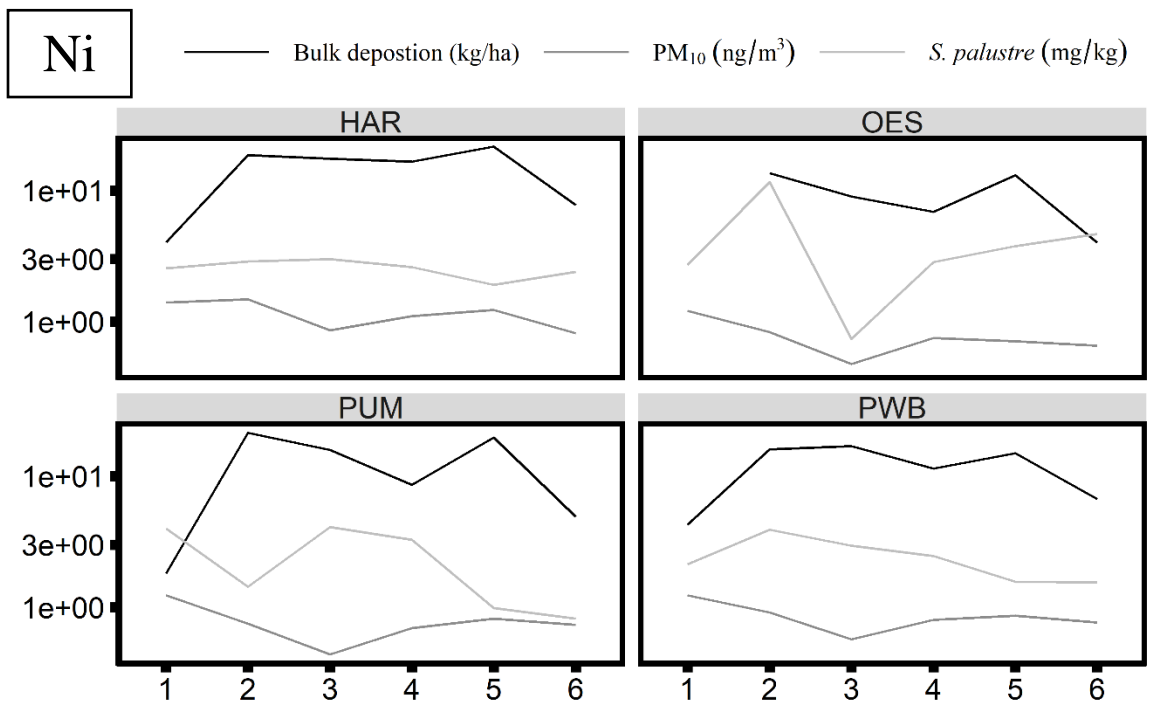
Figure S2. Timeseries showing Bulk deposition (mg/kg), ambient PM_{10} (ng/m^3) and *O. lyellii* tissue concertation (mg/kg) for phosphorous separated by site over 6 sampling periods. The y-axis is log transformed for visual comparison and OES bulk deposition for sampling period 1 are omitted due to 0 values from no precipitation during that period.
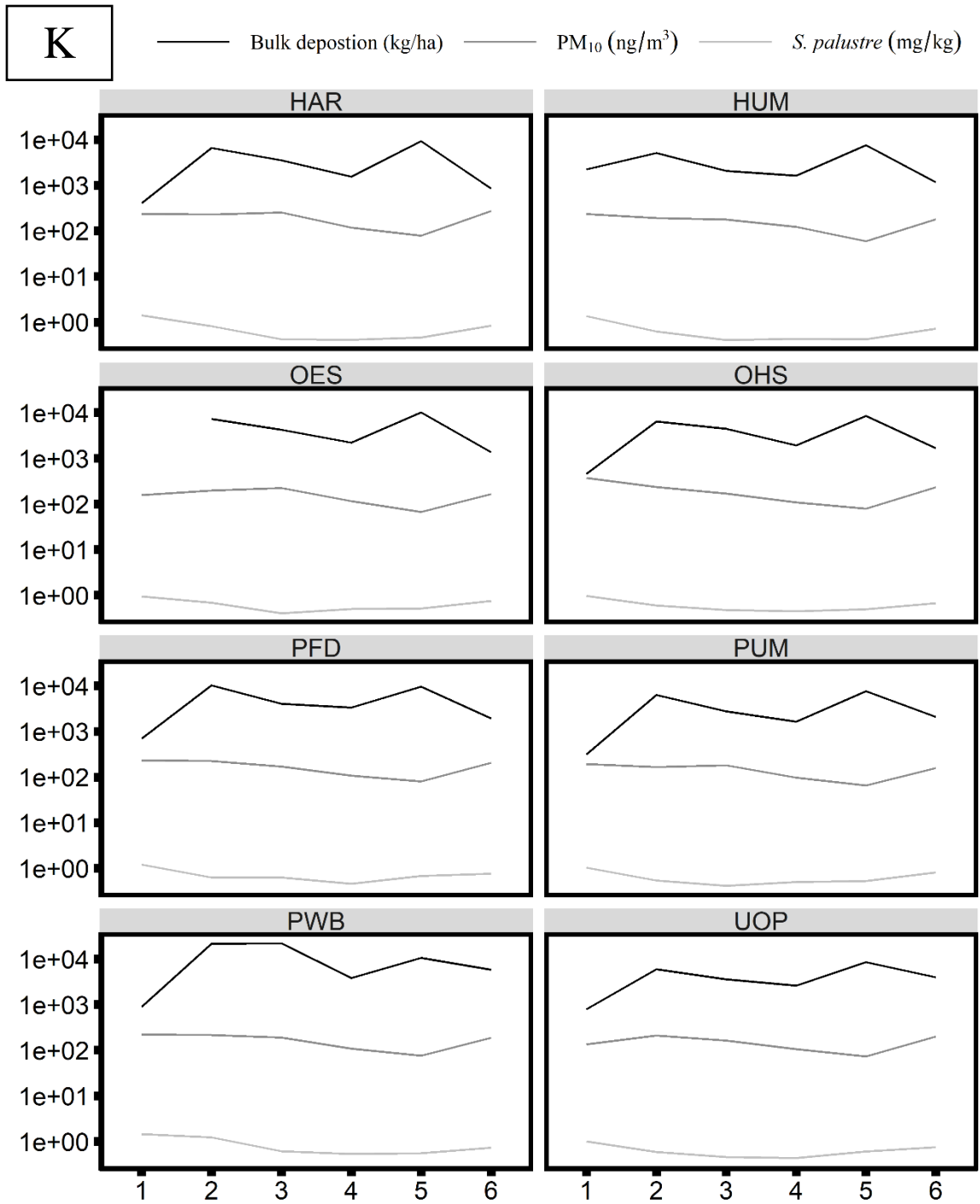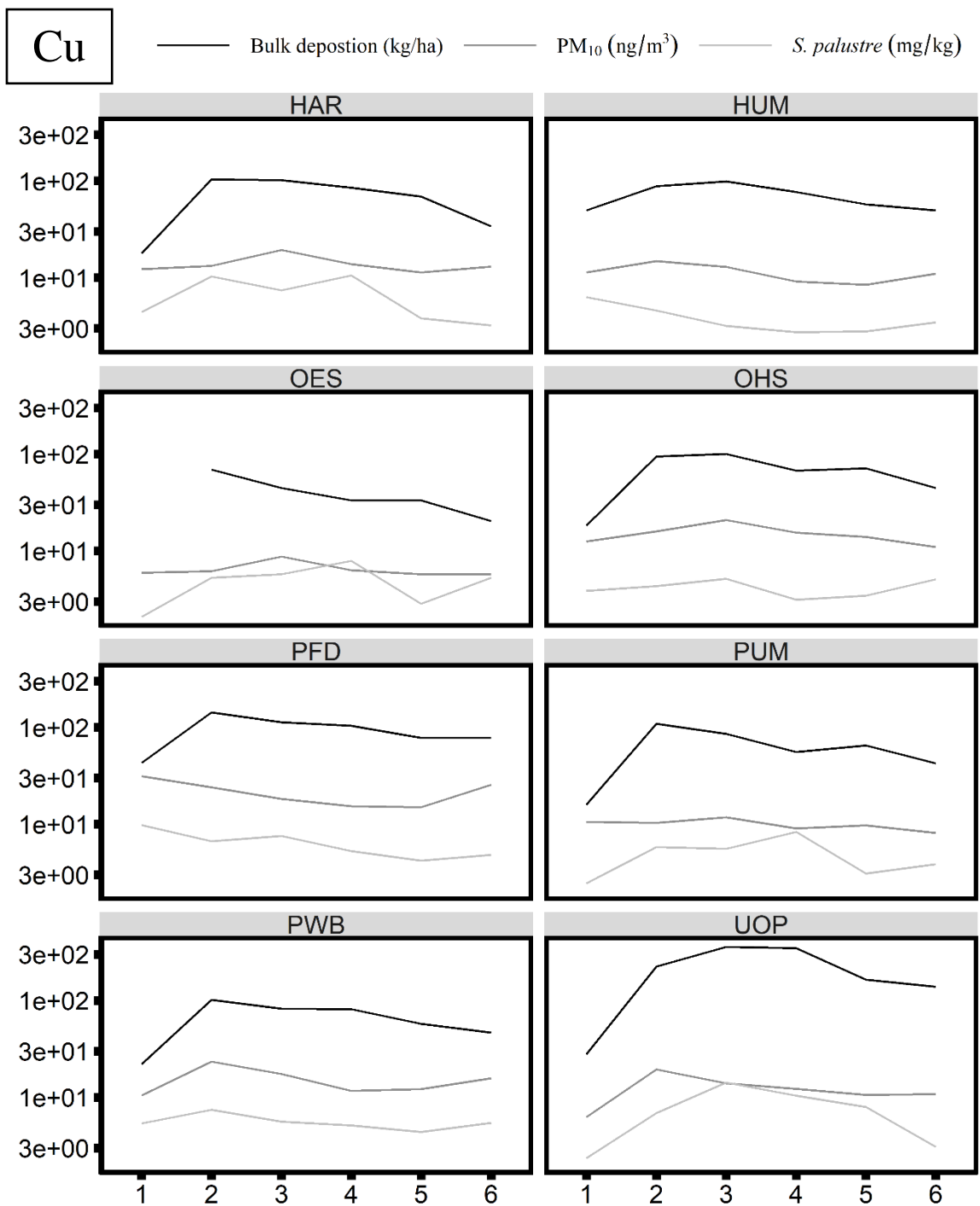
Figure S3. Timeseries showing Bulk deposition (mg/kg), ambient PM_{10} (ng/m³) and *S. palustre* tissue concertation (mg/kg) for potassium separated by site over 6 sampling periods. The y-axis is log transformed for visual comparison and OES bulk deposition for sampling period 1 are omitted due to 0 values from no precipitation during that period.
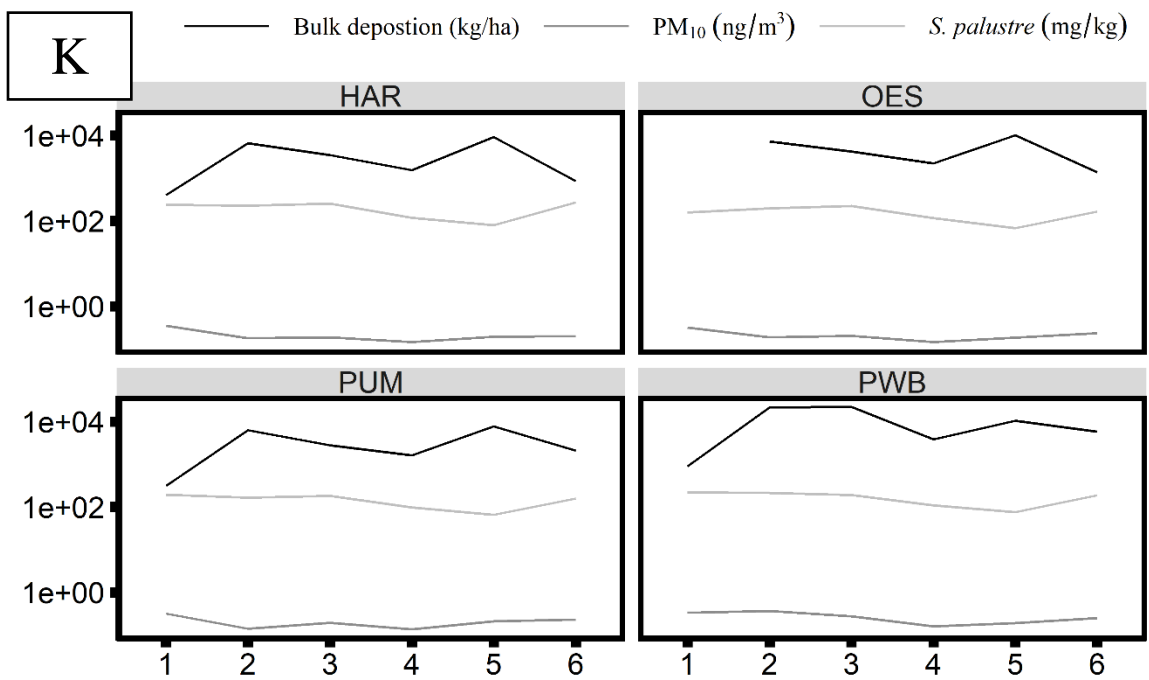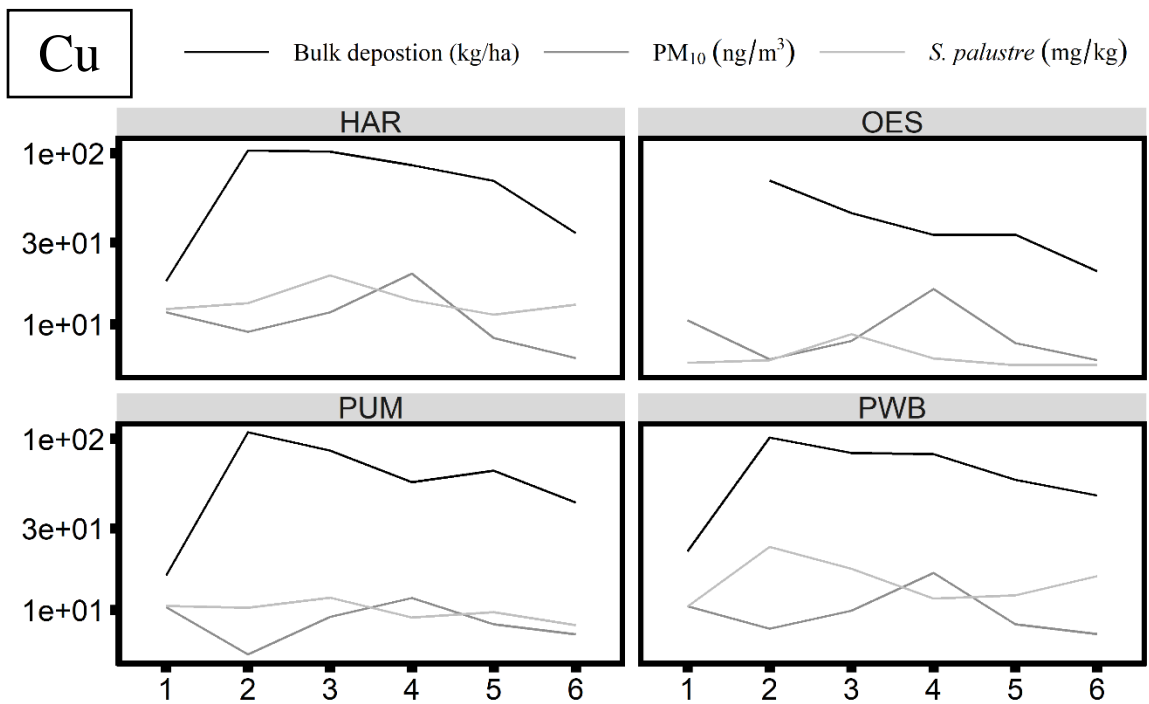
Figure S4. Timeseries showing Bulk deposition (mg/kg), ambient PM_{10} (ng/m^3) and *O. lyellii* tissue concertation (mg/kg) for potassium separated by site over 6 sampling periods. The y-axis is log transformed for visual comparison and OES bulk deposition for sampling period 1 are omitted due to 0 values from no precipitation during that period.
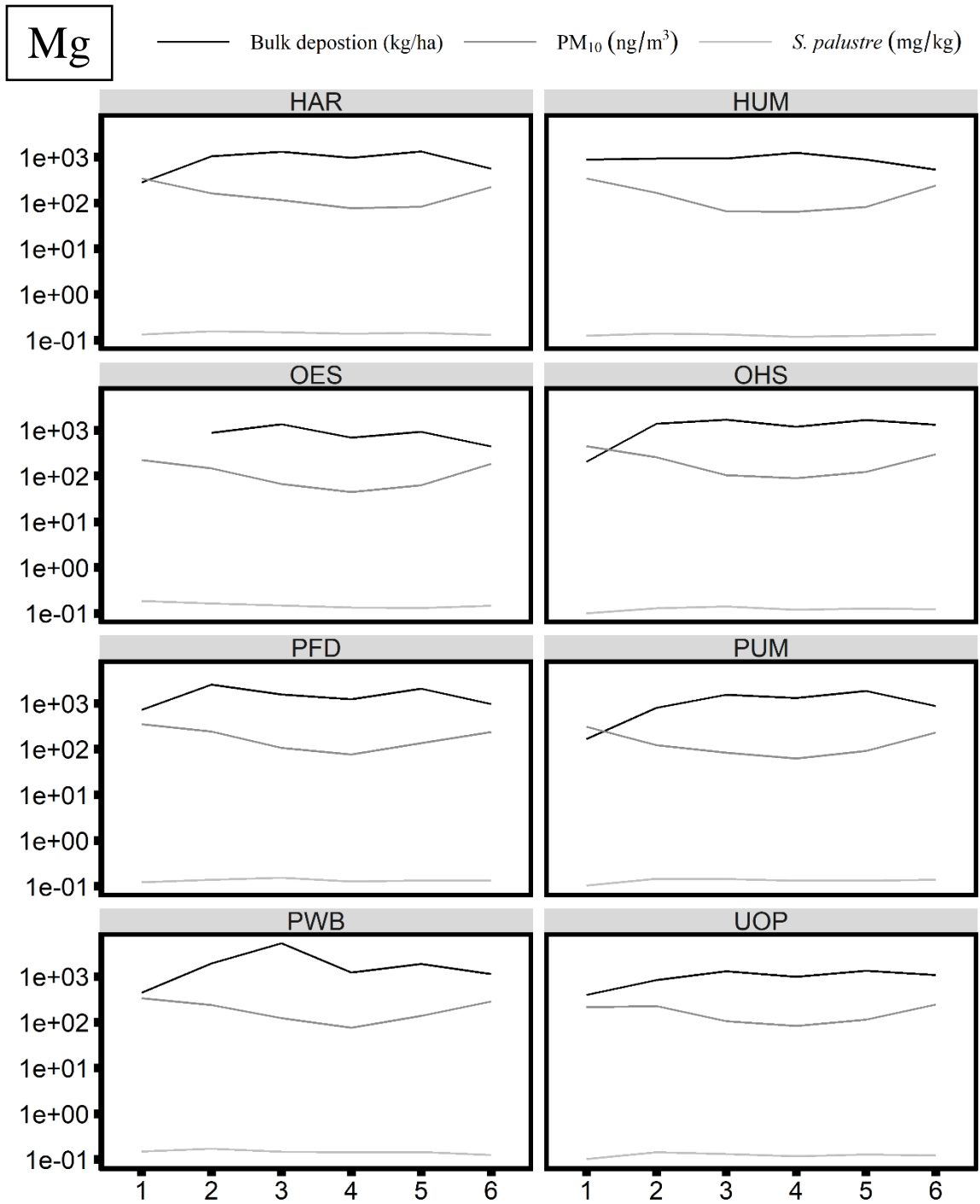
Figure S5. Timeseries showing Bulk deposition (mg/kg), ambient PM_{10} (ng/m^3) and *S. palustre* tissue concertation (mg/kg) for magnesium separated by site over 6 sampling periods. The y-axis is log transformed for visual comparison and OES bulk deposition for sampling period 1 are omitted due to 0 values from no precipitation during that period.
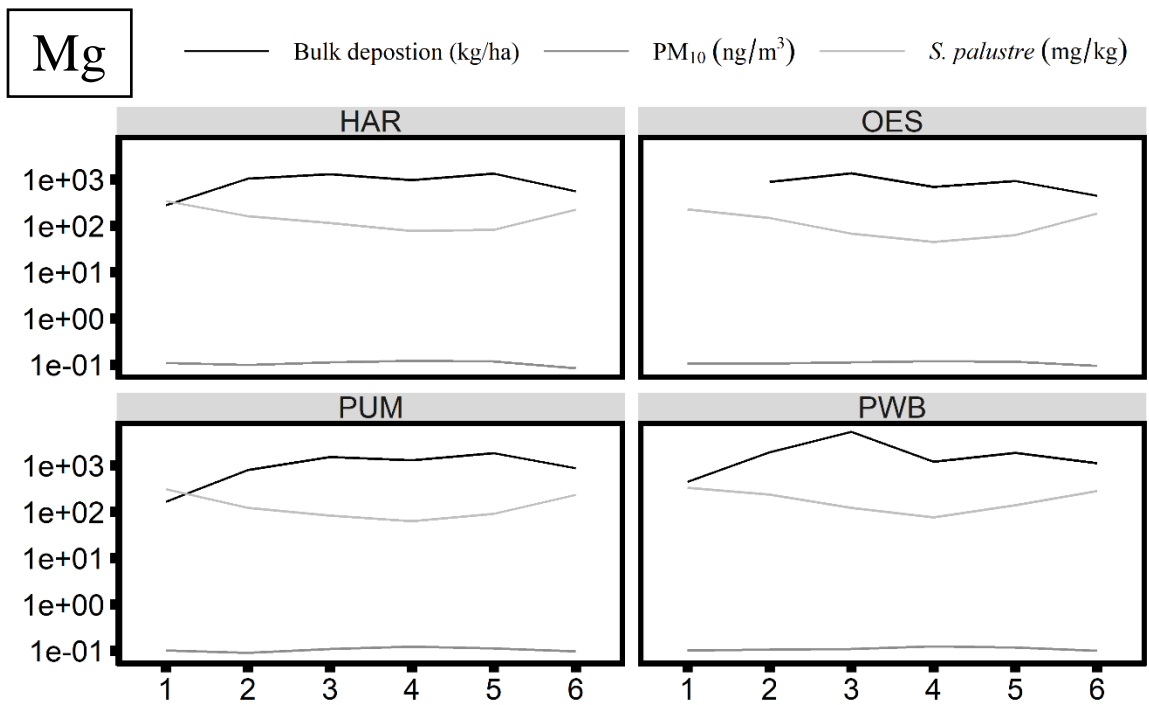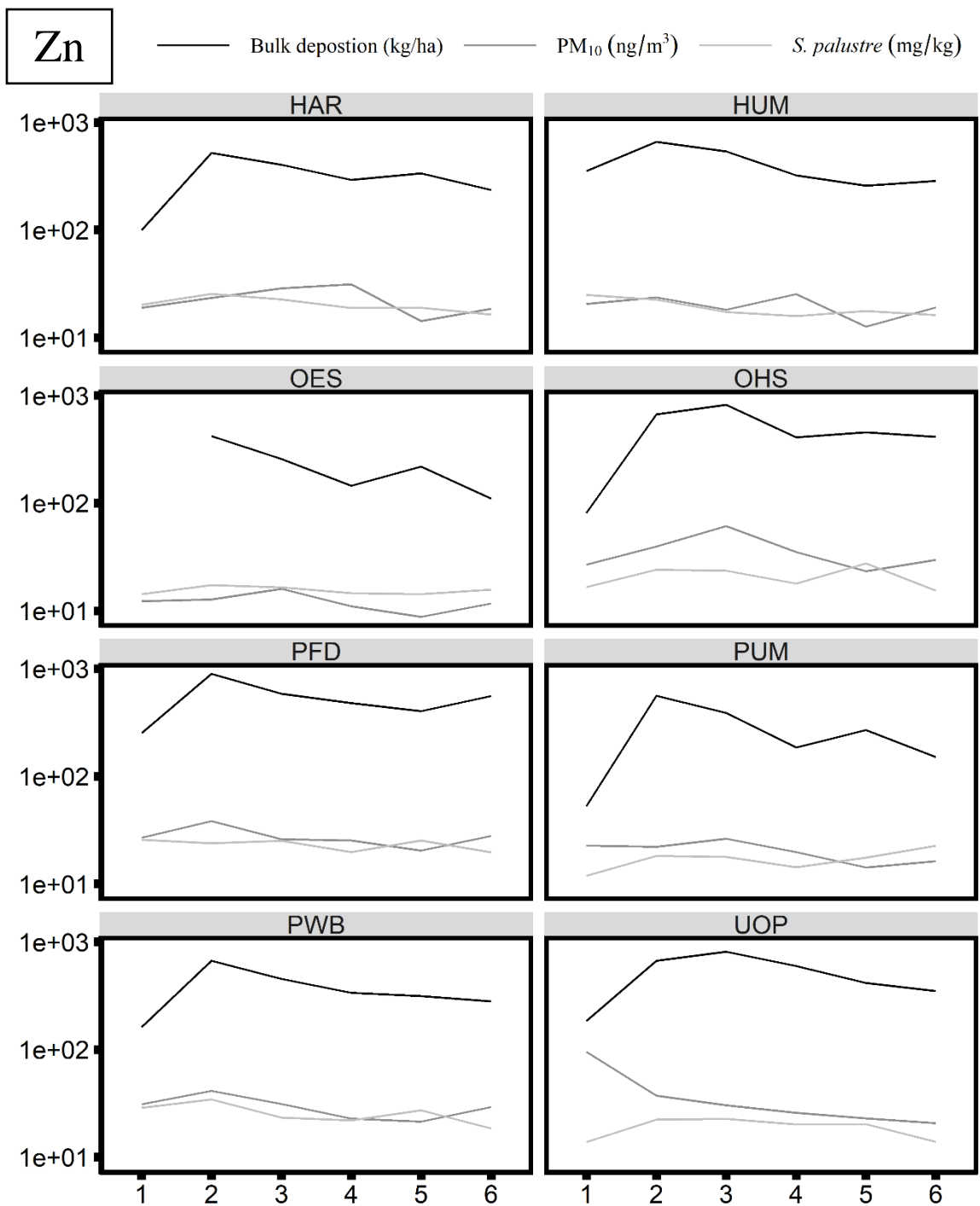
Figure S6. Timeseries showing Bulk deposition (mg/kg), ambient PM_{10} (ng/m^3) and *O. lyellii* tissue concertation (mg/kg) for magnesium separated by site over 6 sampling periods. The y-axis is log transformed for visual comparison and OES bulk deposition for sampling period 1 are omitted due to 0 values from no precipitation during that period.
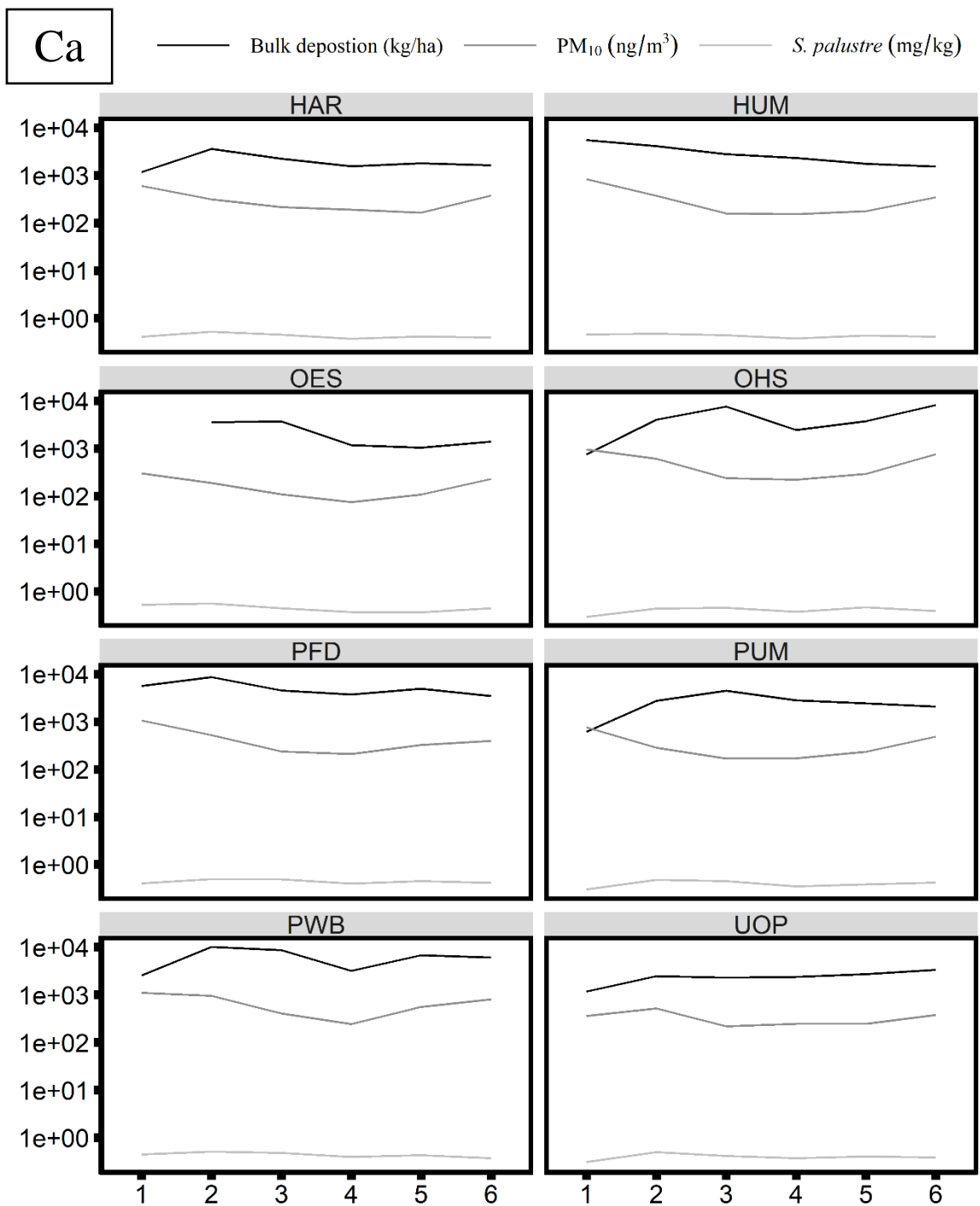
Figure S7. Timeseries showing Bulk deposition (mg/kg), ambient PM_{10} (ng/m^3) and *S. palustre* tissue concertation (mg/kg) for calcium separated by site over 6 sampling periods. The y-axis is log transformed for visual comparison and OES bulk deposition for sampling period 1 are omitted due to 0 values from no precipitation during that period.
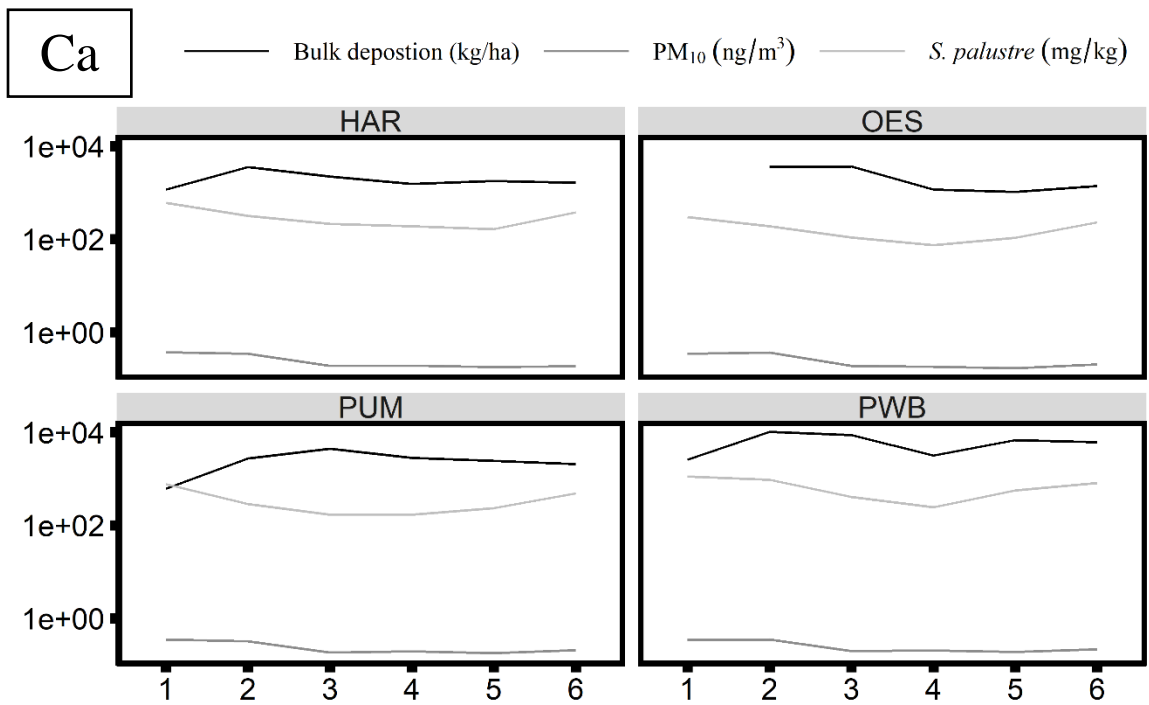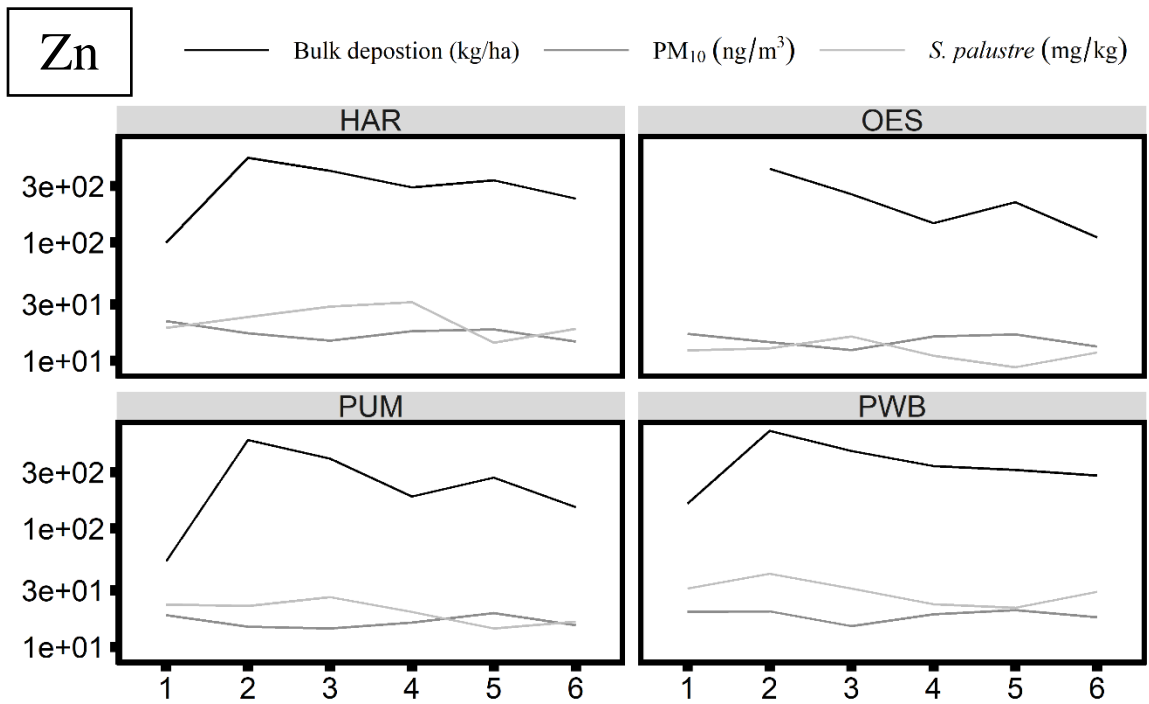
Figure S8. Timeseries showing Bulk deposition (mg/kg), ambient PM_{10} (ng/m^3) and *O. lyellii* tissue concertation (mg/kg) for calcium separated by site over 6 sampling periods. The y-axis is log transformed for visual comparison and OES bulk deposition for sampling period 1 are omitted due to 0 values from no precipitation during that period.
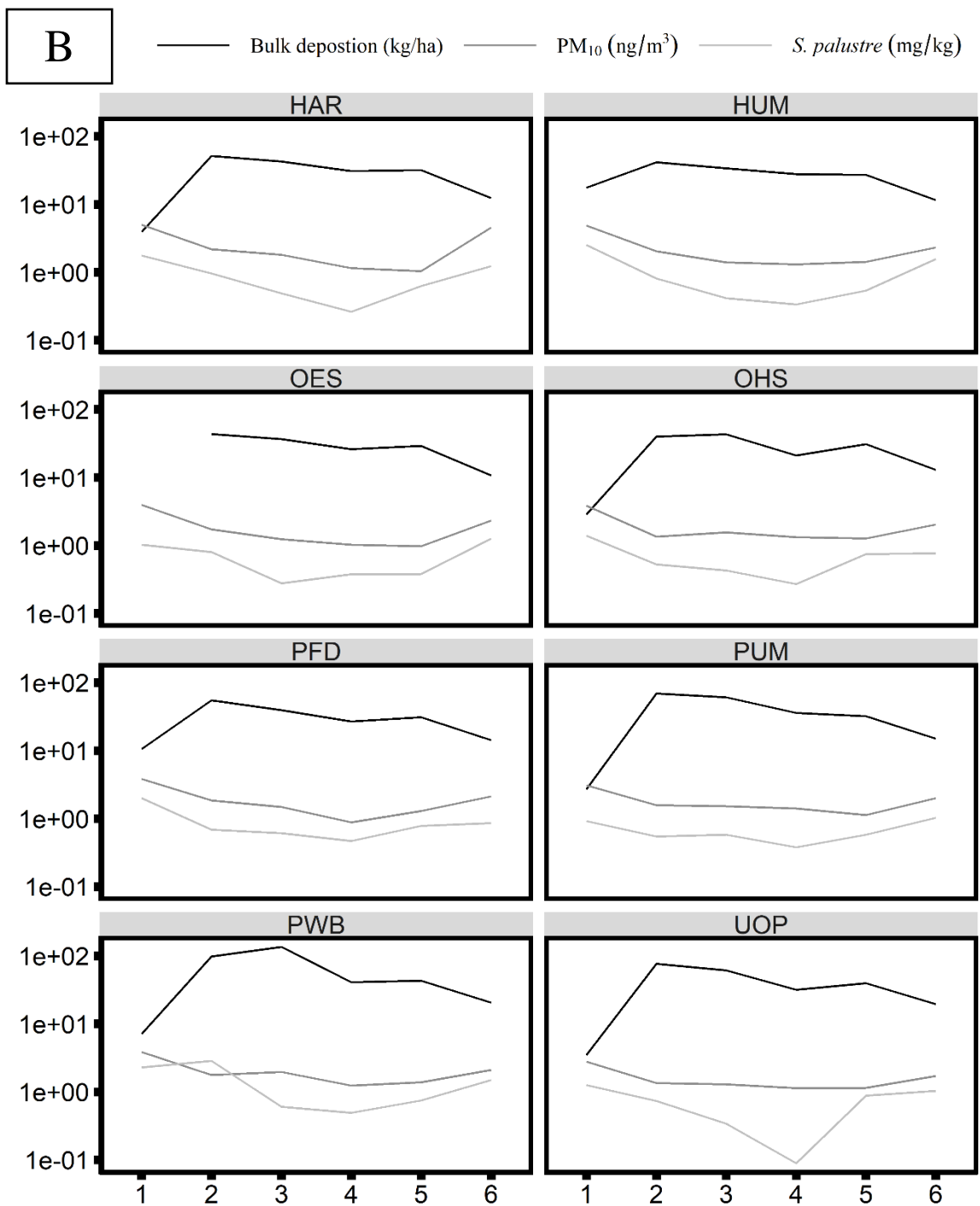
131
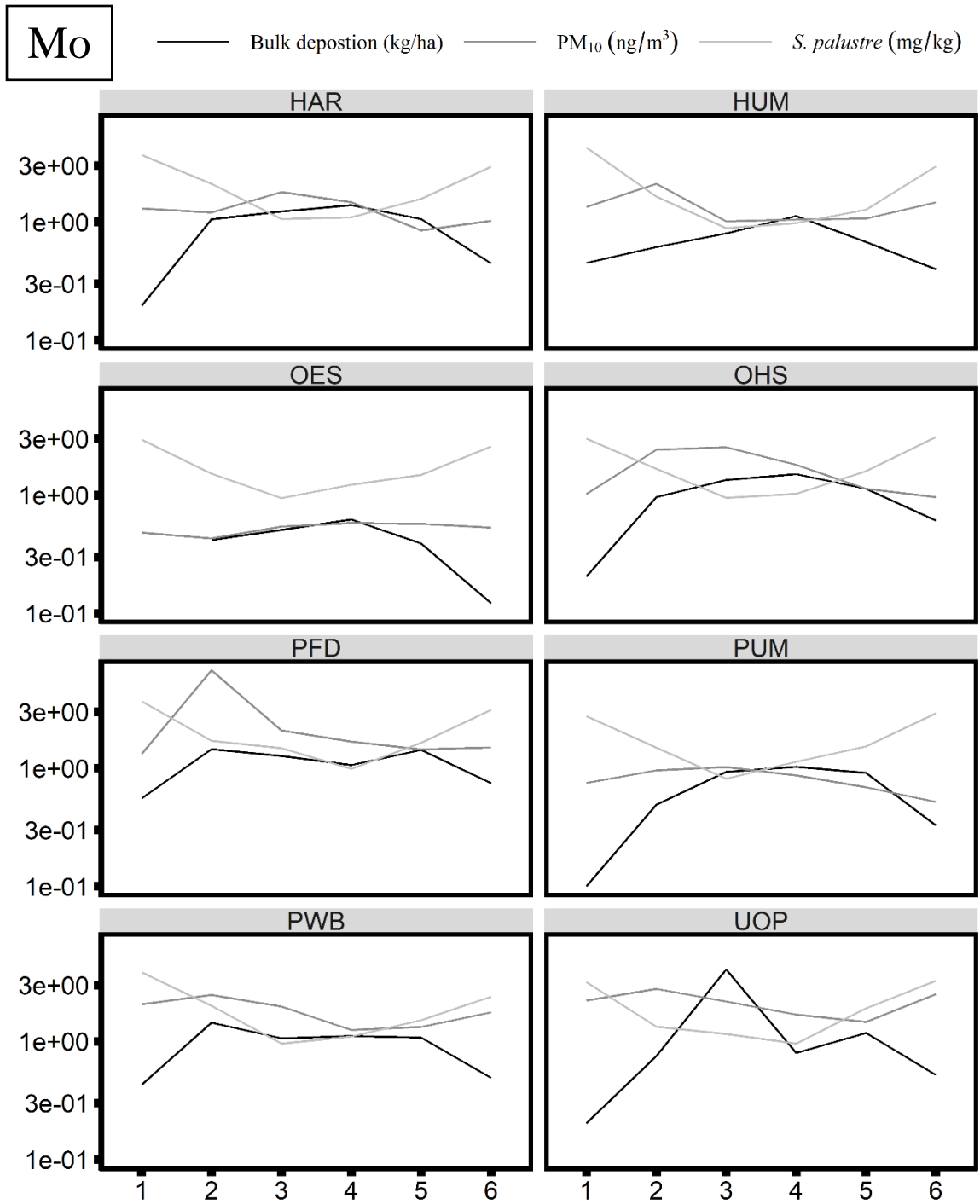
Figure S9. Timeseries showing Bulk deposition (mg/kg), ambient PM_{10} (ng/m^3) and *S. palustre* tissue concertation (mg/kg) for molybdenum separated by site over 6 sampling periods. The y-axis is log transformed for visual comparison and OES bulk deposition for sampling period 1 are omitted due to 0 values from no precipitation during that period.
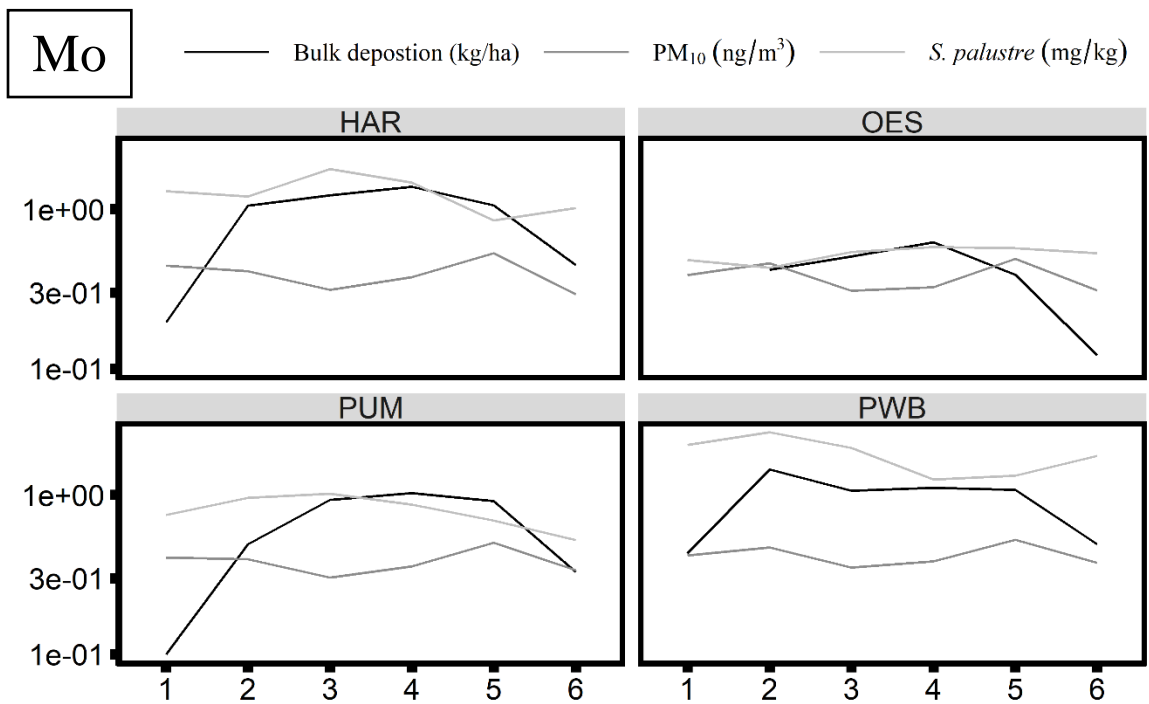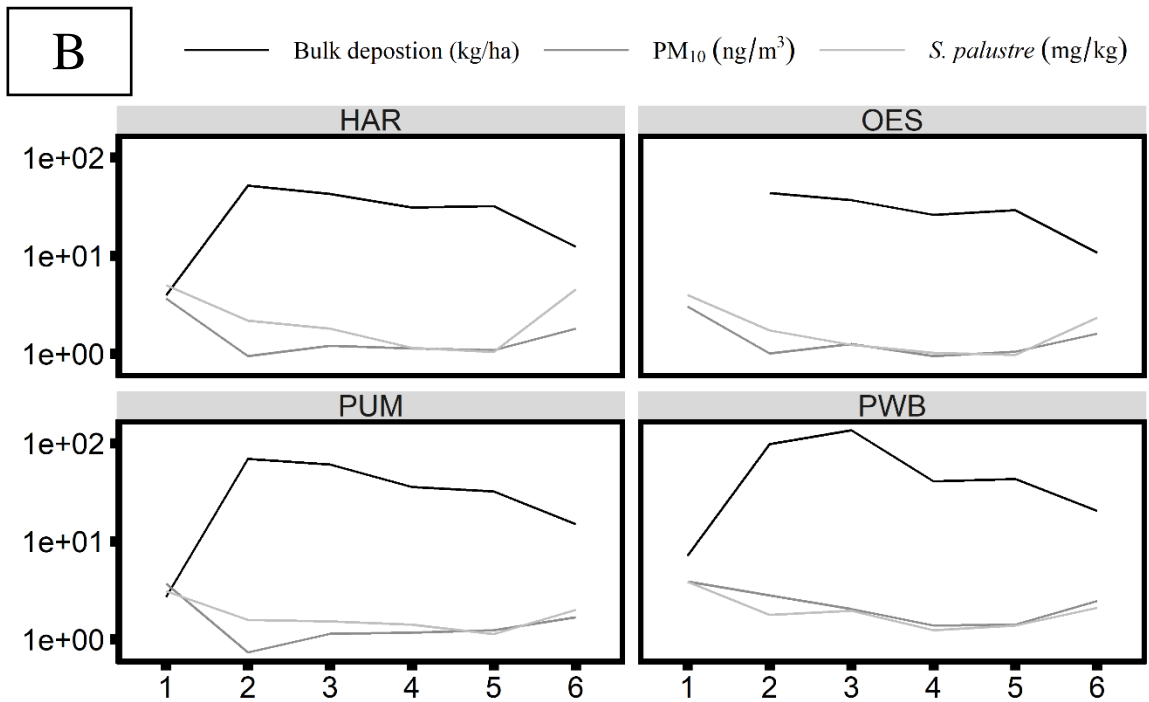
Figure S10. Timeseries showing Bulk deposition (mg/kg), ambient PM_{10} (ng/m^3) and *O. lyellii* tissue concertation (mg/kg) for molybdenum separated by site over 6 sampling periods. The y-axis is log transformed for visual comparison and OES bulk deposition for sampling period 1 are omitted due to 0 values from no precipitation during that period.

Figure S11. Timeseries showing Bulk deposition (mg/kg), ambient PM_{10} (ng/m³) and *S. palustre* tissue concertation (mg/kg) for manganese separated by site over 6 sampling periods. The y-axis is log transformed for visual comparison and OES bulk deposition for sampling period 1 are omitted due to 0 values from no precipitation during that period.
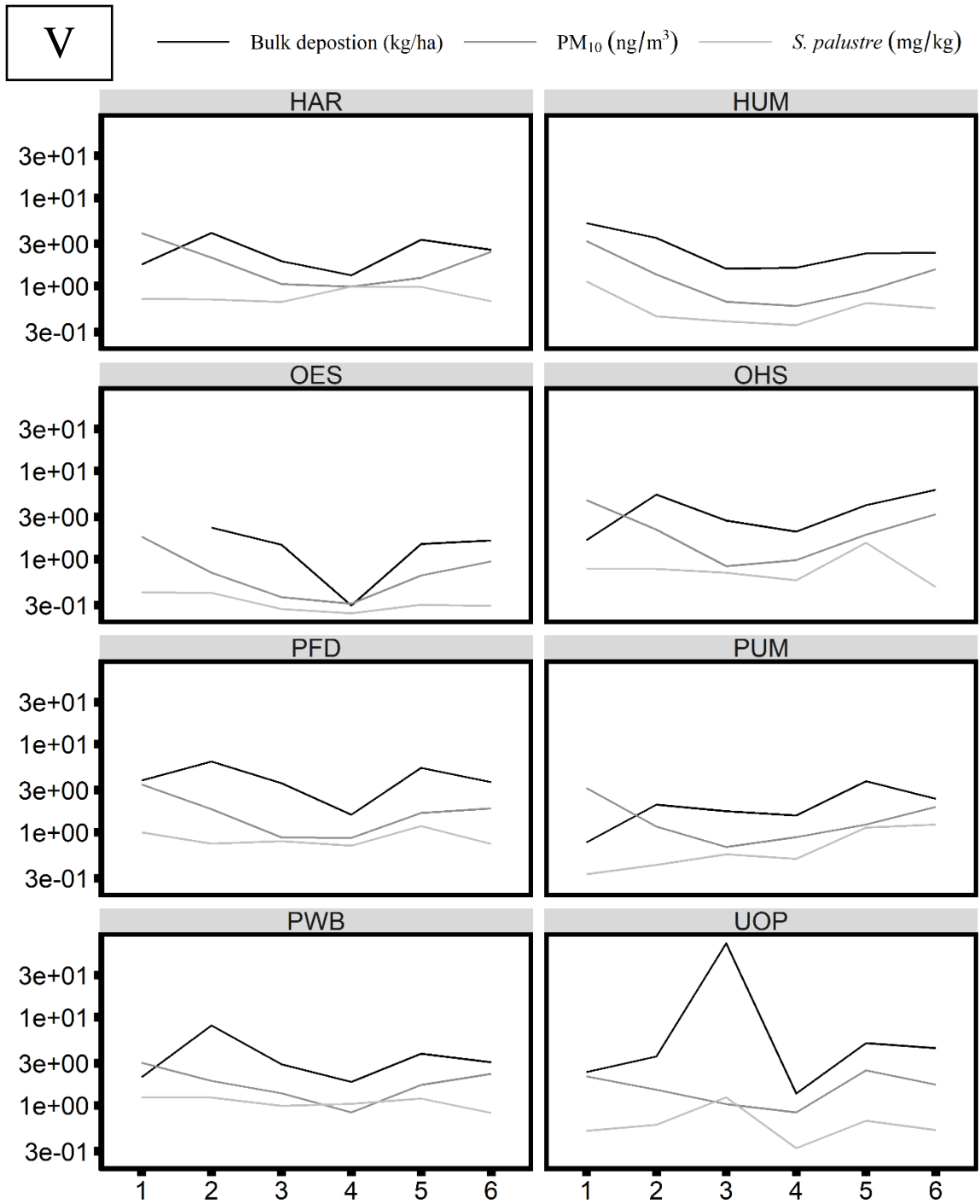
Figure S 12. Timeseries showing Bulk deposition (mg/kg), ambient PM_{10} (ng/m^3) and *O. lyellii* tissue concertation (mg/kg) for manganese separated by site over 6 sampling periods. The y-axis is log transformed for visual comparison and OES bulk deposition for sampling period 1 are omitted due to 0 values from no precipitation during that period.

Figure S13. Timeseries showing Bulk deposition (mg/kg), ambient PM_{10} (ng/m^3) and *S. palustre* tissue concertation (mg/kg) for iron separated by site over 6 sampling periods. The y-axis is log transformed for visual comparison and OES bulk deposition for sampling period 1 are omitted due to 0 values from no precipitation during that period.
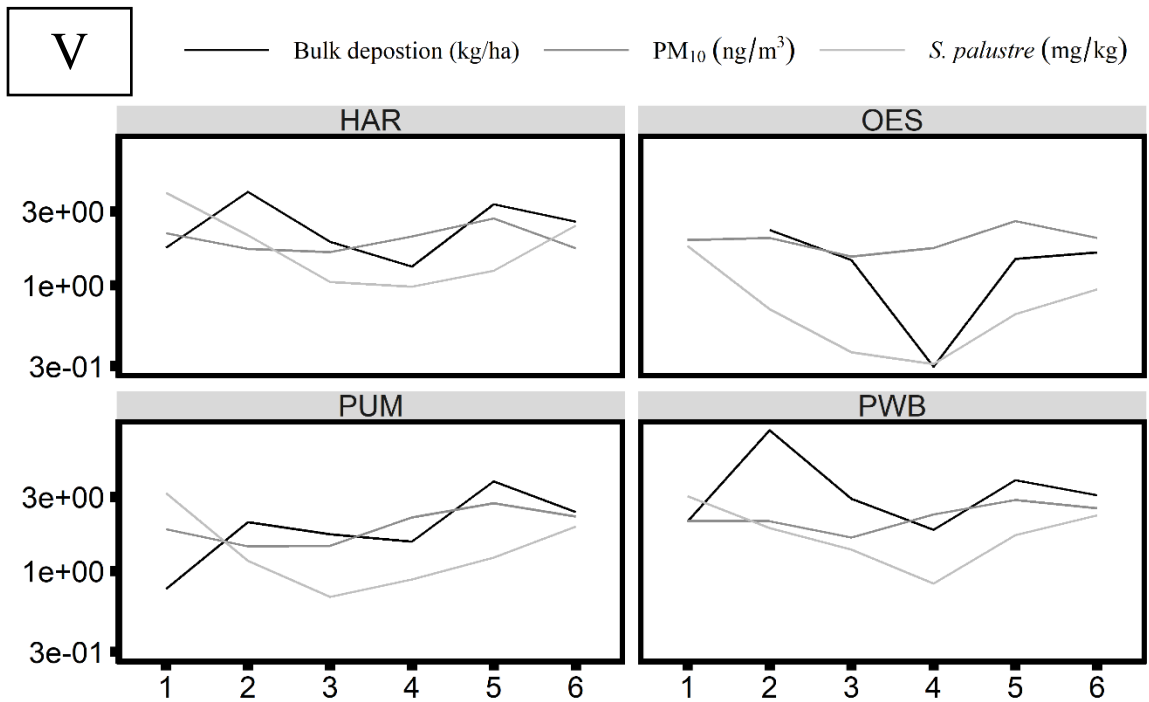
Figure S14. Timeseries showing Bulk deposition (mg/kg), ambient PM_{10} (ng/m^3) and *O. lyellii* tissue concertation (mg/kg) for iron separated by site over 6 sampling periods. The y-axis is log transformed for visual comparison and OES bulk deposition for sampling period 1 are omitted due to 0 values from no precipitation during that period.
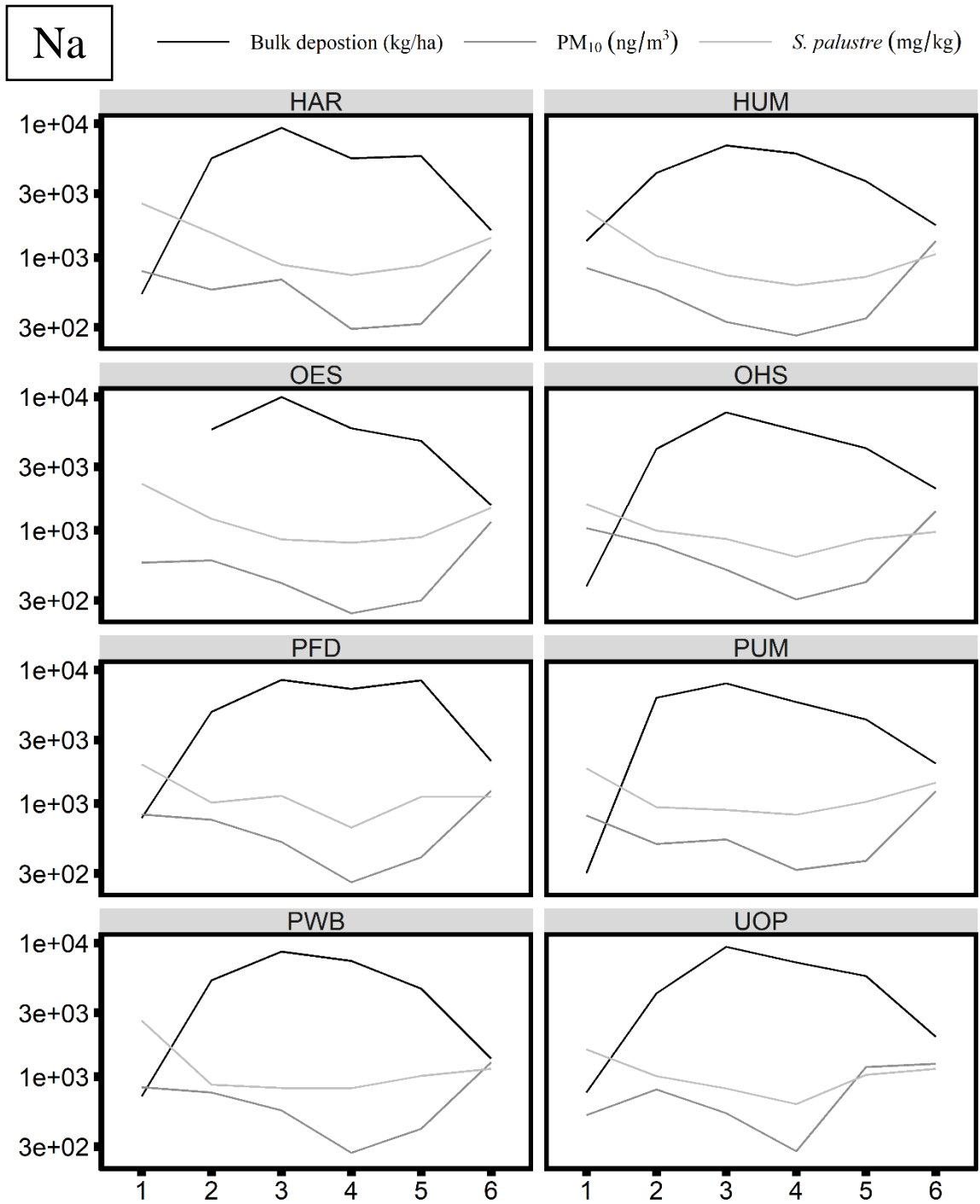
Figure S15. Timeseries showing Bulk deposition (mg/kg), ambient PM_{10} (ng/m^3) and *S. palustre* tissue concertation (mg/kg) for nickel separated by site over 6 sampling periods. The y-axis is log transformed for visual comparison and OES bulk deposition for sampling period 1 are omitted due to 0 values from no precipitation during that period.

Figure S16. Timeseries showing Bulk deposition (mg/kg), ambient PM_{10} (ng/m^3) and *O. lyellii* tissue concertation (mg/kg) for nickel separated by site over 6 sampling periods. The y-axis is log transformed for visual comparison and OES bulk deposition for sampling period 1 are omitted due to 0 values from no precipitation during that period.
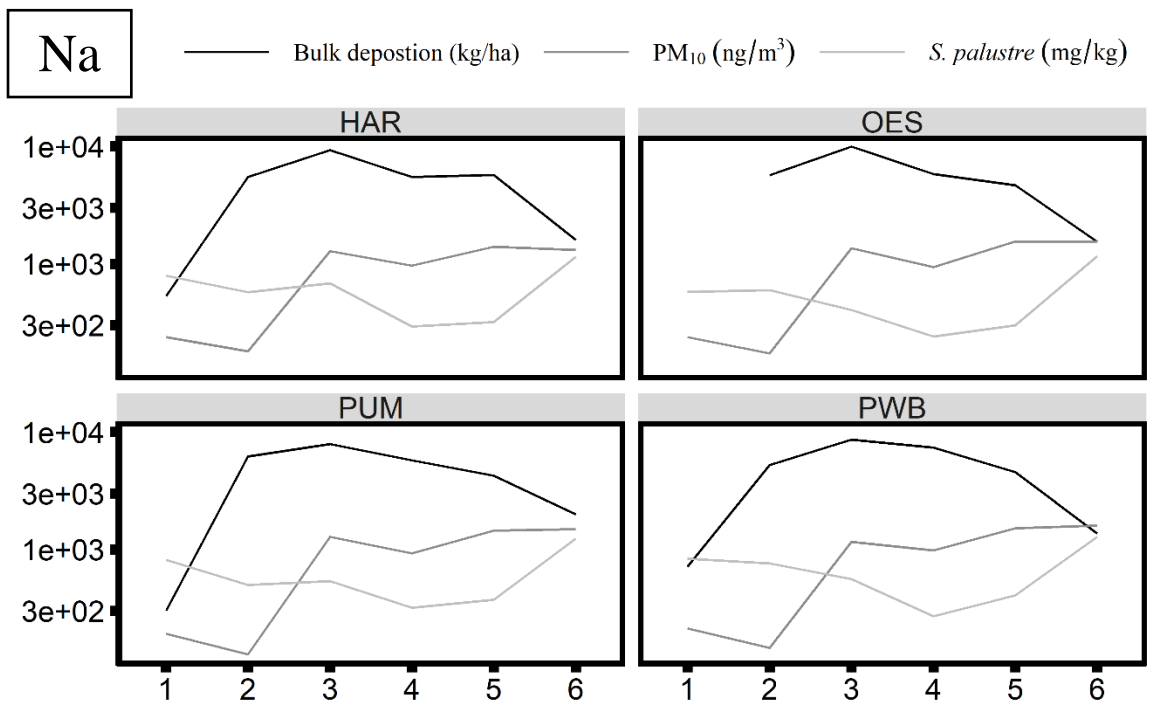
Figure S17. Timeseries showing Bulk deposition (mg/kg), ambient PM_{10} (ng/m³) and *S. palustre* tissue concertation (mg/kg) for copper separated by site over 6 sampling periods. The y-axis is log transformed for visual comparison and OES bulk deposition for sampling period 1 are omitted due to 0 values from no precipitation during that period.
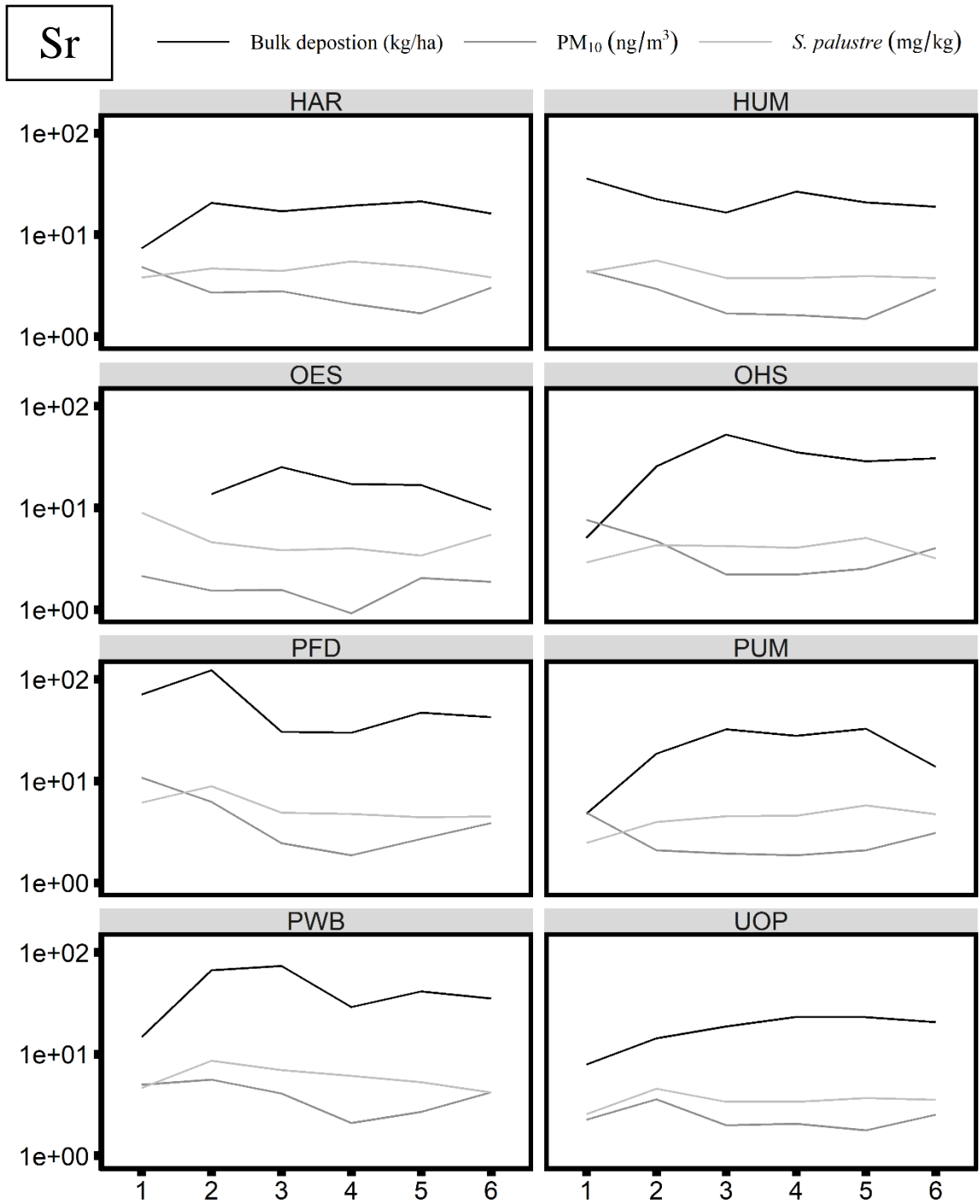
Figure S18. Timeseries showing Bulk deposition (mg/kg), ambient PM_{10} (ng/m³) and *O. lyellii* tissue concertation (mg/kg) for copper separated by site over 6 sampling periods. The y-axis is log transformed for visual comparison and OES bulk deposition for sampling period 1 are omitted due to 0 values from no precipitation during that period.

Figure S19. Timeseries showing Bulk deposition (mg/kg), ambient PM_{10} (ng/m³) and *S. palustre* tissue concertation (mg/kg) for zinc separated by site over 6 sampling periods. The y-axis is log transformed for visual comparison and OES bulk deposition for sampling period 1 are omitted due to 0 values from no precipitation during that period.
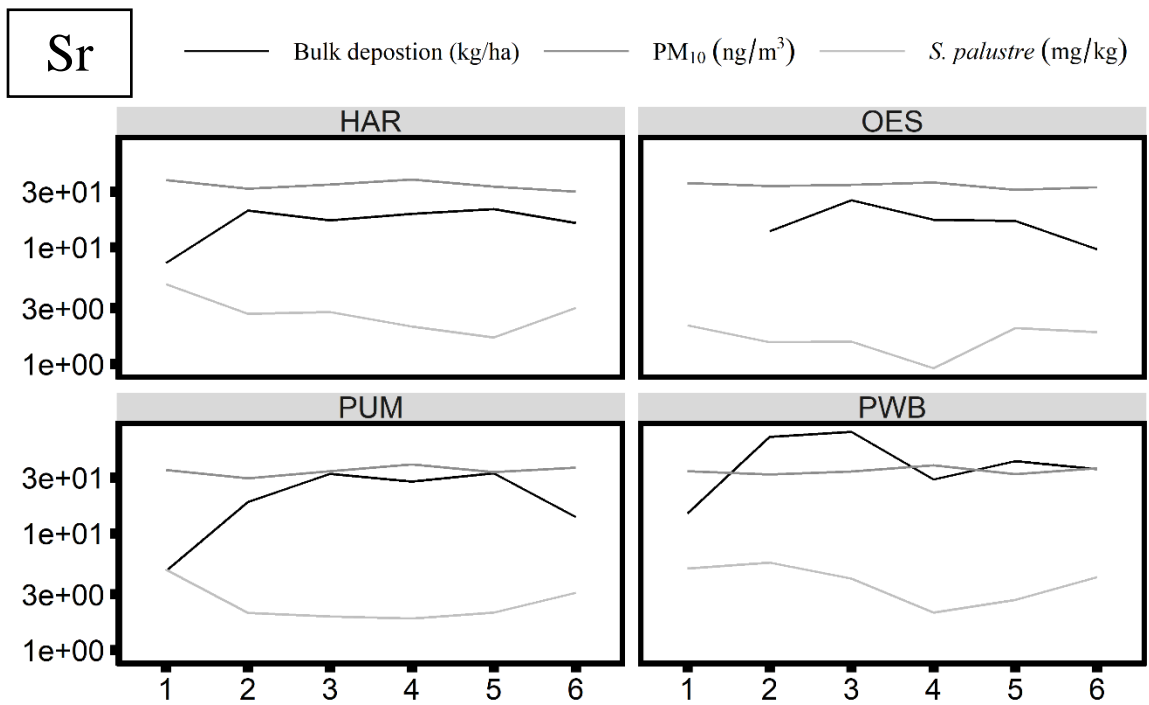
142

Figure S20. Timeseries showing Bulk deposition (mg/kg), ambient PM_{10} (ng/m^3) and *O. lyellii* tissue concertation (mg/kg) for zinc separated by site over 6 sampling periods. The y-axis is log transformed for visual comparison and OES bulk deposition for sampling period 1 are omitted due to 0 values from no precipitation during that period.
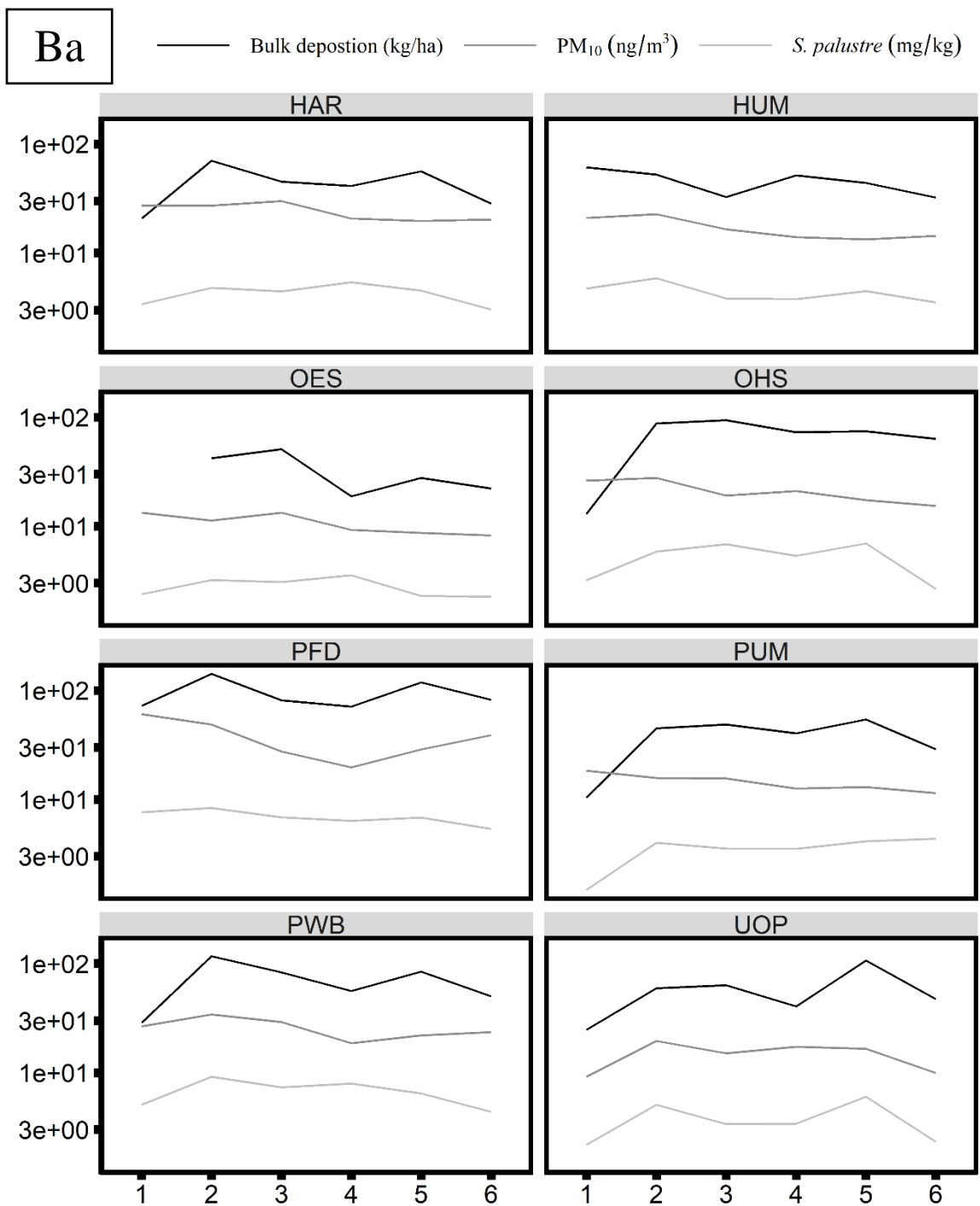
Figure S21. Timeseries showing Bulk deposition (mg/kg), ambient PM_{10} (ng/m³) and *S. palustre* tissue concertation (mg/kg) for boron separated by site over 6 sampling periods. The y-axis is log transformed for visual comparison and OES bulk deposition for sampling period 1 are omitted due to 0 values from no precipitation during that period.

Figure S22. Timeseries showing Bulk deposition (mg/kg), ambient PM$_{10}$ (ng/m^3) and *O. lyellii* tissue concertation (mg/kg) for boron separated by site over 6 sampling periods. The y-axis is log transformed for visual comparison and OES bulk deposition for sampling period 1 are omitted due to 0 values from no precipitation during that period.
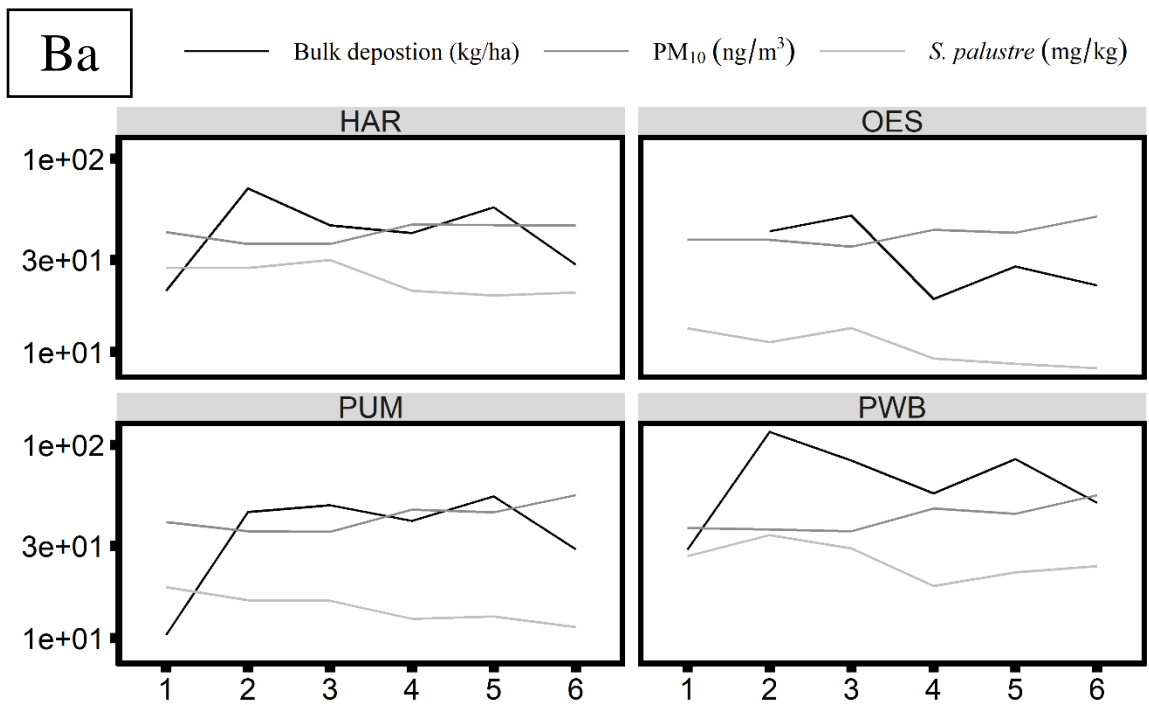
Figure S23. Timeseries showing Bulk deposition (mg/kg), ambient PM$_{10}$ (ng/m^3) and *S. palustre* tissue concertation (mg/kg) for vanadium separated by site over 6 sampling periods. The y-axis is log transformed for visual comparison and OES bulk deposition for sampling period 1 are omitted due to 0 values from no precipitation during that period.
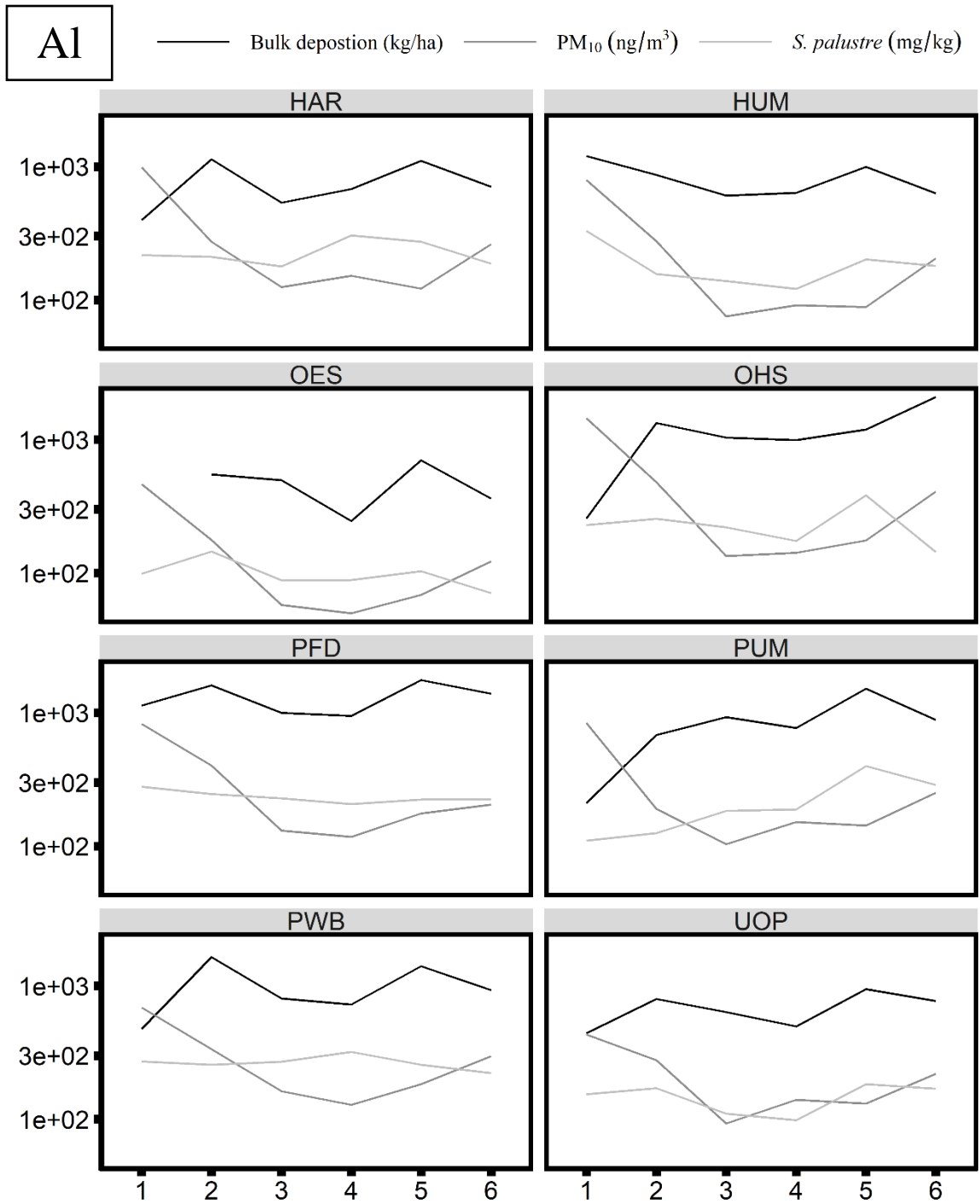
Figure S24. Timeseries showing Bulk deposition (mg/kg), ambient PM_{10} (ng/m^3) and *O. lyellii* tissue concertation (mg/kg) for vanadium separated by site over 6 sampling periods. The y-axis is log transformed for visual comparison and OES bulk deposition for sampling period 1 are omitted due to 0 values from no precipitation during that period.

Figure S25. Timeseries showing Bulk deposition (mg/kg), ambient PM_{10} (ng/m^3) and *S. palustre* tissue concertation (mg/kg) for sodium separated by site over 6 sampling periods. The y-axis is log transformed for visual comparison and OES bulk deposition for sampling period 1 are omitted due to 0 values from no precipitation during that period.
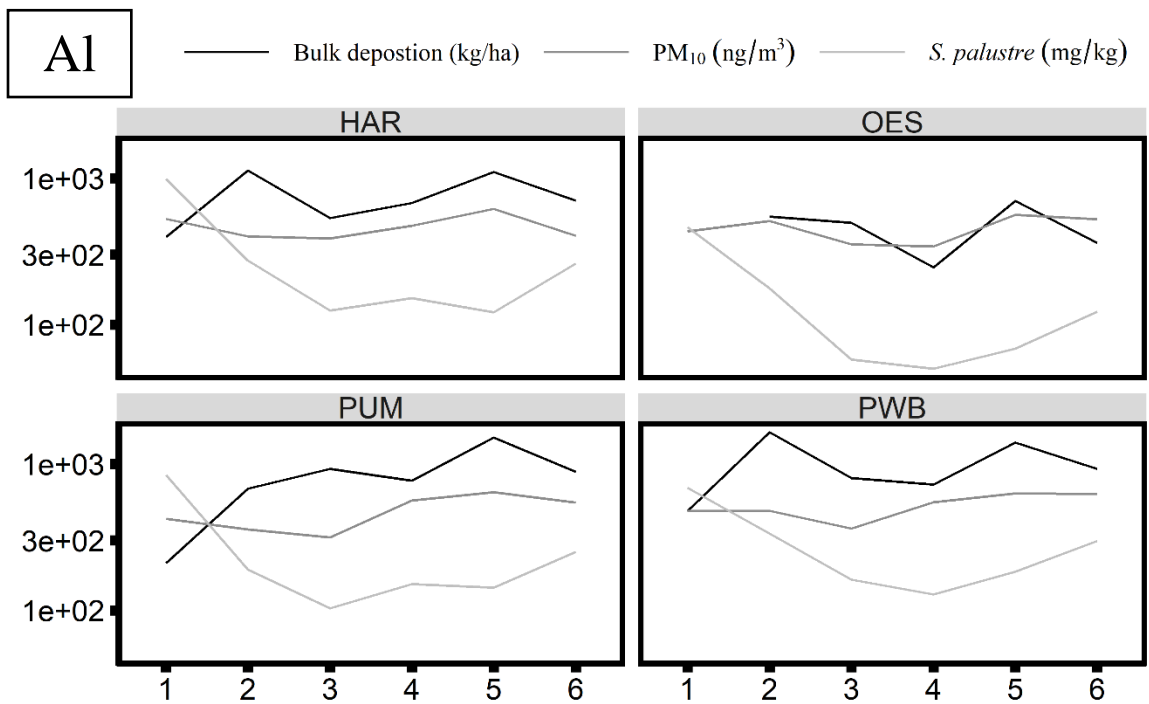
Figure S26. Timeseries showing Bulk deposition (mg/kg), ambient PM_{10} (ng/m³) and *O. lyellii* tissue concertation (mg/kg) for sodium separated by site over 6 sampling periods. The y-axis is log transformed for visual comparison and OES bulk deposition for sampling period 1 are omitted due to 0 values from no precipitation during that period.
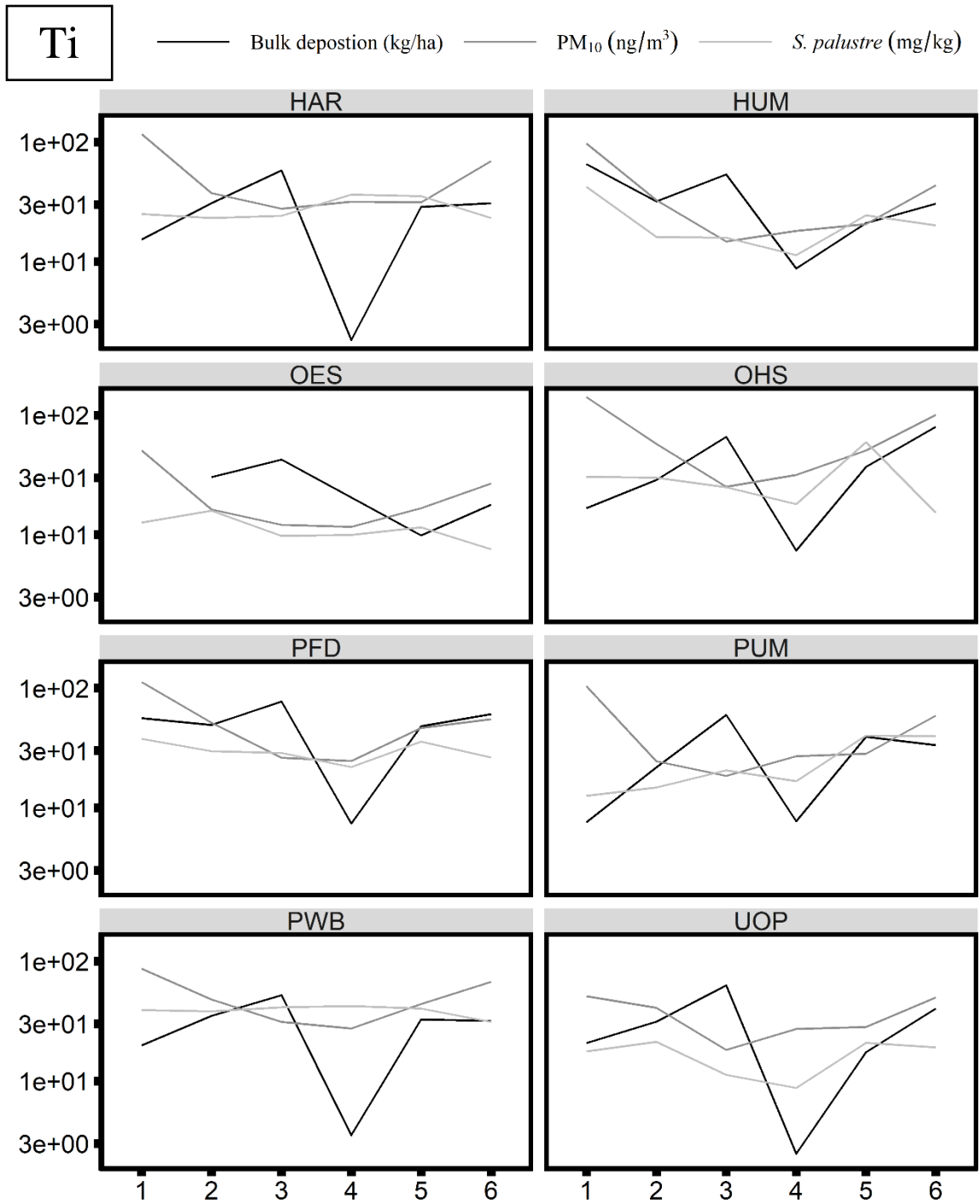
Figure S27. Timeseries showing Bulk deposition (mg/kg), ambient PM$_{10}$ (ng/m^3) and *S. palustre* tissue concertation (mg/kg) for strontium separated by site over 6 sampling periods. The y-axis is log transformed for visual comparison and OES bulk deposition for sampling period 1 are omitted due to 0 values from no precipitation during that period.

Figure S28. Timeseries showing Bulk deposition (mg/kg), ambient PM_{10} (ng/m^3) and *O. lyellii* tissue concertation (mg/kg) for strontium separated by site over 6 sampling periods. The y-axis is log transformed for visual comparison and OES bulk deposition for sampling period 1 are omitted due to 0 values from no precipitation during that period.
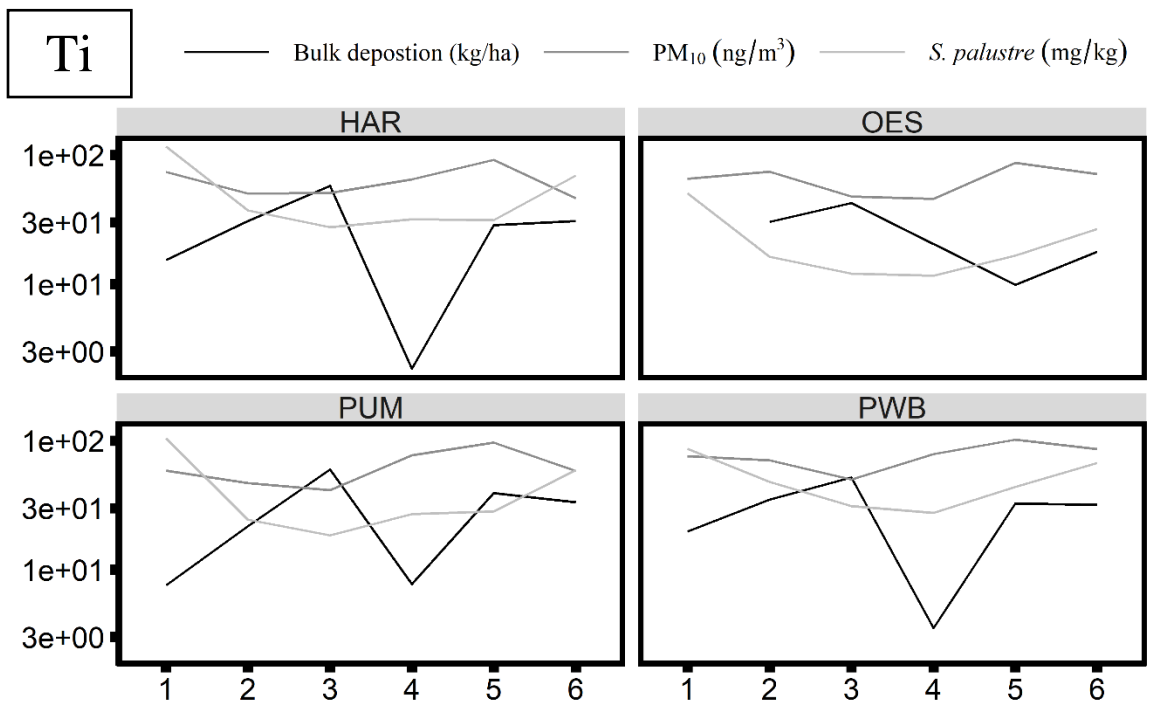
Figure S29. Timeseries showing Bulk deposition (mg/kg), ambient PM_{10} (ng/m³) and *S. palustre* tissue concertation (mg/kg) for barium separated by site over 6 sampling periods. The y-axis is log transformed for visual comparison and OES bulk deposition for sampling period 1 are omitted due to 0 values from no precipitation during that period.
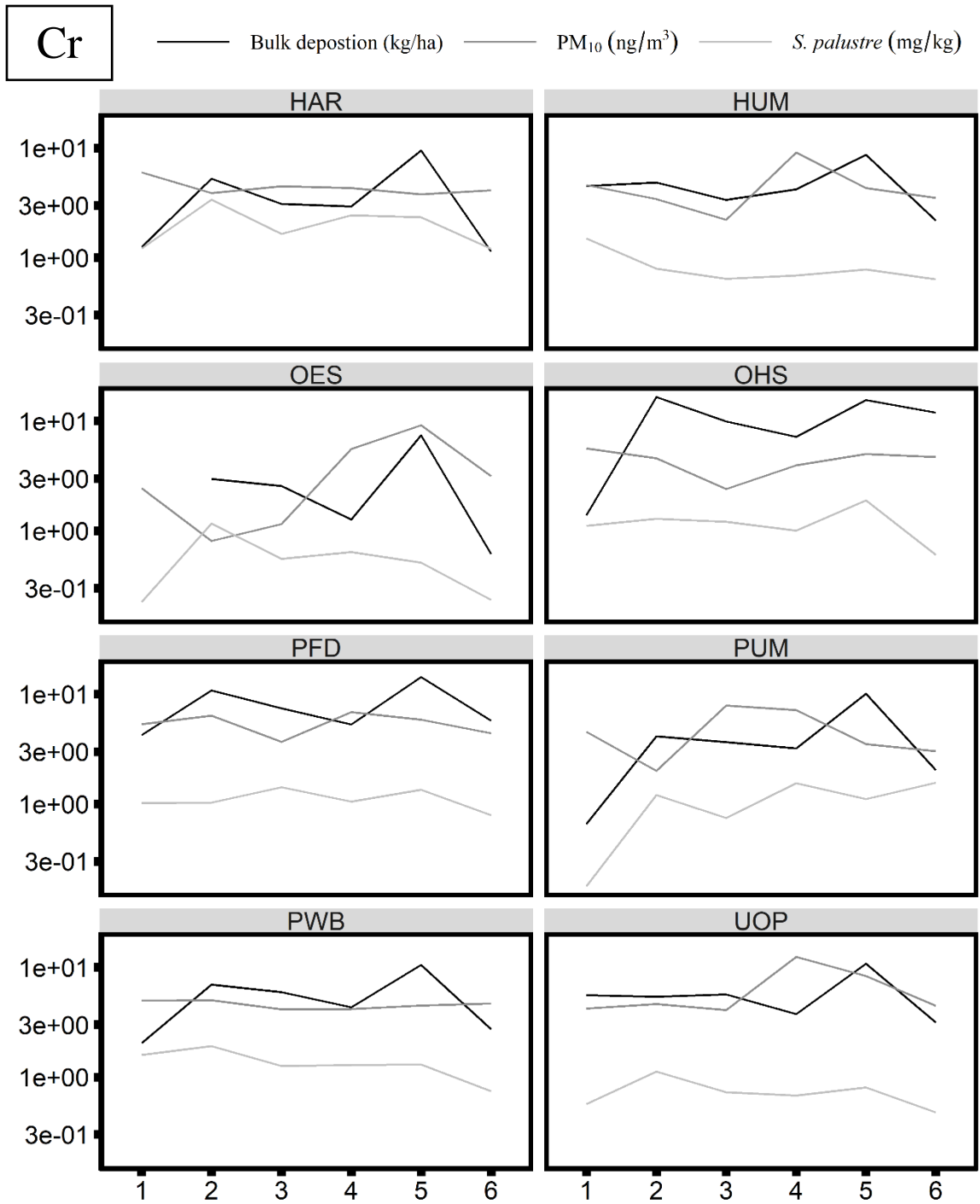
Figure S30. Timeseries showing Bulk deposition (mg/kg), ambient PM_{10} (ng/m^3) and *O. lyellii* tissue concertation (mg/kg) for barium separated by site over 6 sampling periods. The y-axis is log transformed for visual comparison and OES bulk deposition for sampling period 1 are omitted due to 0 values from no precipitation during that period.

Figure S31. Timeseries showing Bulk deposition (mg/kg), ambient PM_{10} (ng/m^3) and *S. palustre* tissue concertation (mg/kg) for aluminum separated by site over 6 sampling periods. The y-axis is log transformed for visual comparison and OES bulk deposition for sampling period 1 are omitted due to 0 values from no precipitation during that period.
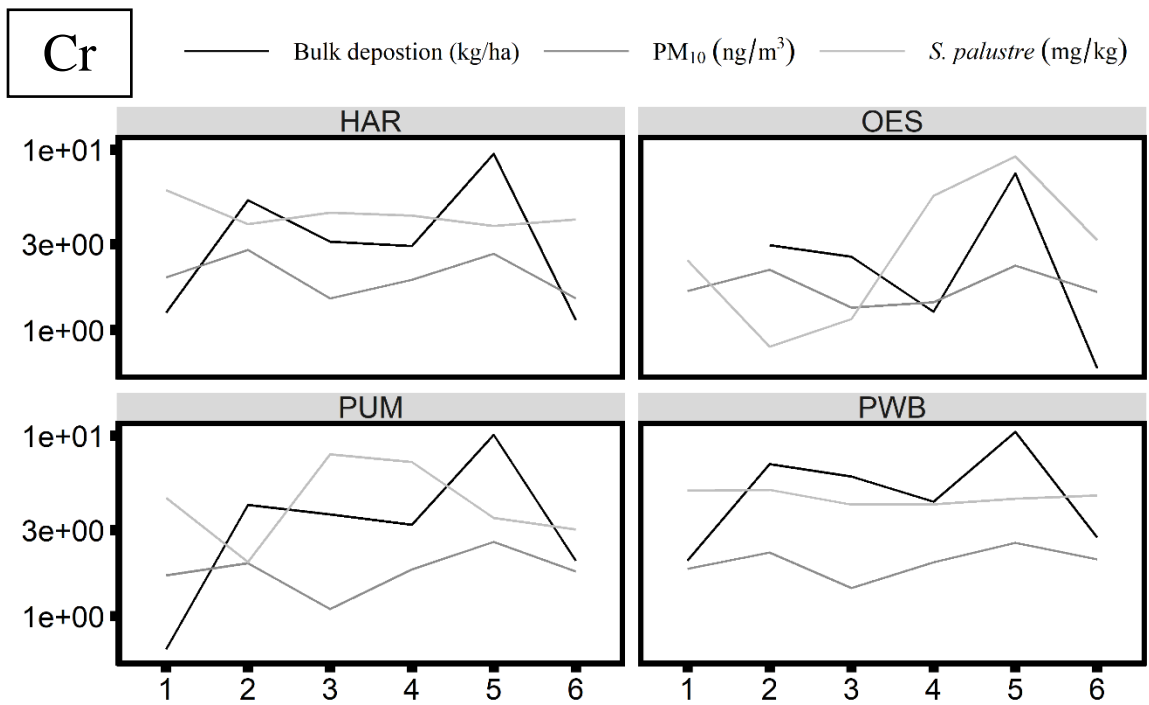
Figure S32. Timeseries showing Bulk deposition (mg/kg), ambient PM_{10} (ng/m³) and *O. lyellii* tissue concertation (mg/kg) for aluminum separated by site over 6 sampling periods. The y-axis is log transformed for visual comparison and OES bulk deposition for sampling period 1 are omitted due to 0 values from no precipitation during that period.
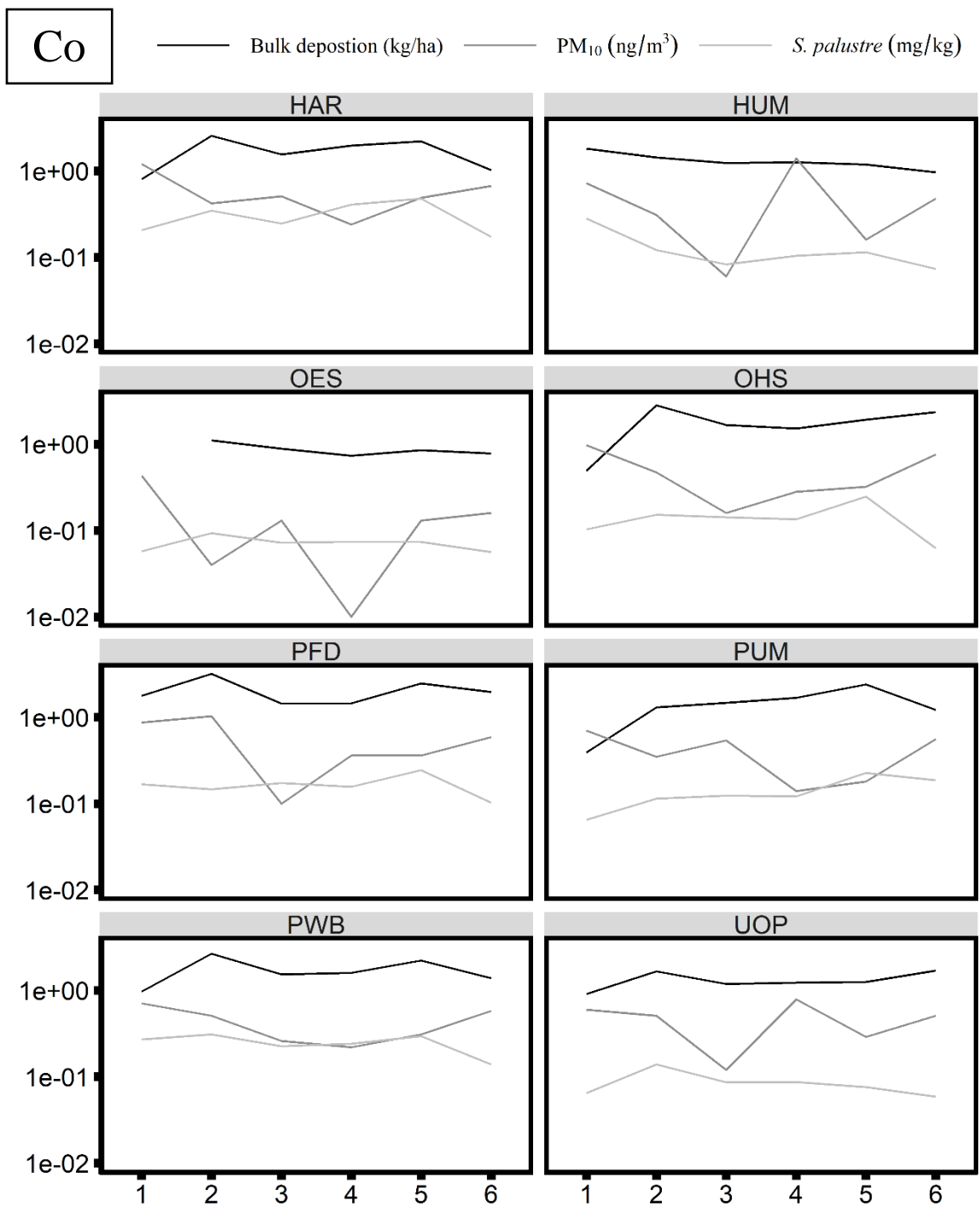
Figure S33. Timeseries showing Bulk deposition (mg/kg), ambient PM_{10} (ng/m^3) and *S. palustre* tissue concertation (mg/kg) for titanium separated by site over 6 sampling periods. The y-axis is log transformed for visual comparison and OES bulk deposition for sampling period 1 are omitted due to 0 values from no precipitation during that period.

Figure S34. Timeseries showing Bulk deposition (mg/kg), ambient PM_{10} (ng/m³) and *O. lyellii* tissue concertation (mg/kg) for titanium separated by site over 6 sampling periods. The y-axis is log transformed for visual comparison and OES bulk deposition for sampling period 1 are omitted due to 0 values from no precipitation during that period.
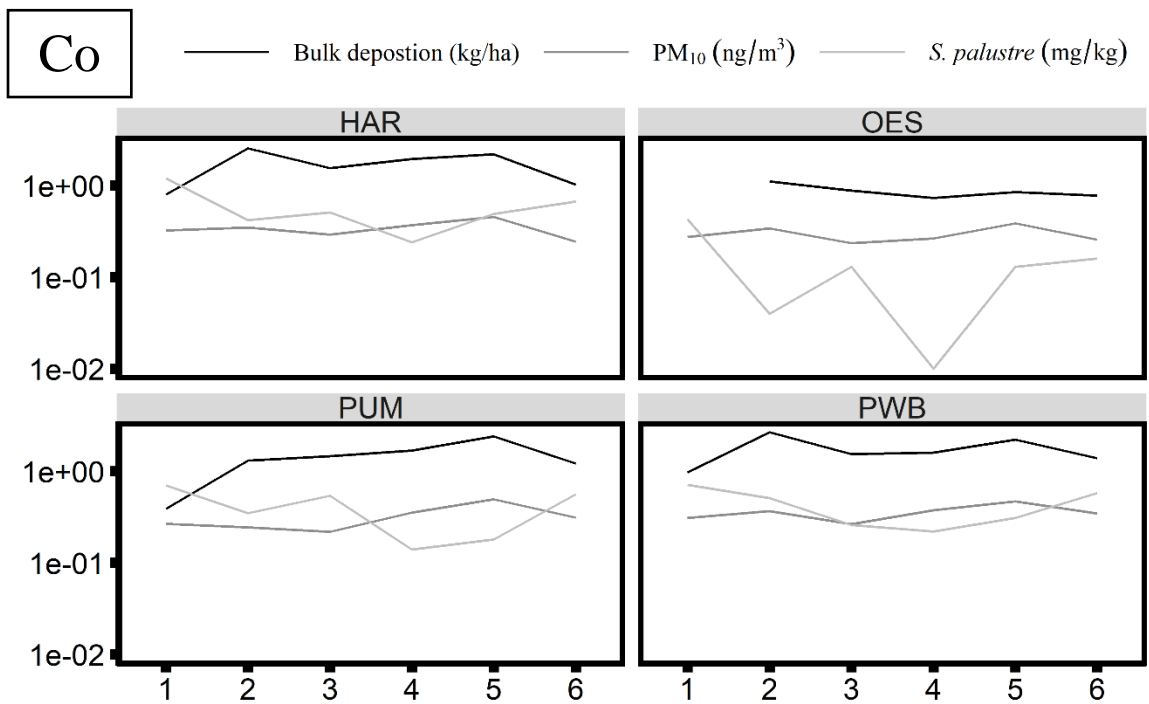
Figure S35. Timeseries showing Bulk deposition (mg/kg), ambient PM_{10} (ng/m³) and *S. palustre* tissue concertation (mg/kg) for chromium separated by site over 6 sampling periods. The y-axis is log transformed for visual comparison and OES bulk deposition for sampling period 1 are omitted due to 0 values from no precipitation during that period.
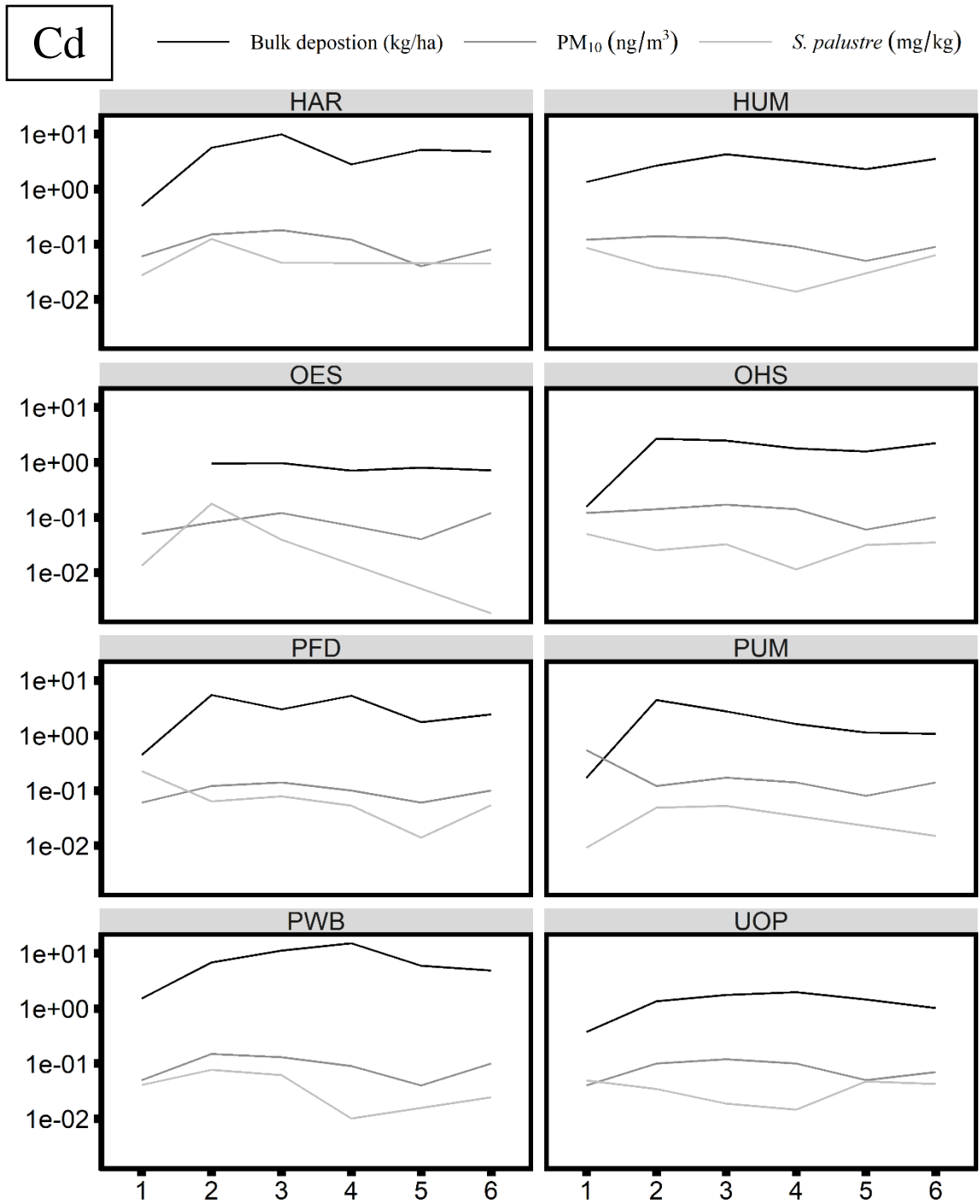
Figure S36. Timeseries showing Bulk deposition (mg/kg), ambient PM_{10} (ng/m³) and *O. lyellii* tissue concertation (mg/kg) for chromium separated by site over 6 sampling periods. The y-axis is log transformed for visual comparison and OES bulk deposition for sampling period 1 are omitted due to 0 values from no precipitation during that period.

Figure S37. Timeseries showing Bulk deposition (mg/kg), ambient PM$_{10}$ (ng/m^3) and *S. palustre* tissue concertation (mg/kg) for cobalt separated by site over 6 sampling periods. The y-axis is log transformed for visual comparison and OES bulk deposition for sampling period 1 are omitted due to 0 values from no precipitation during that period.
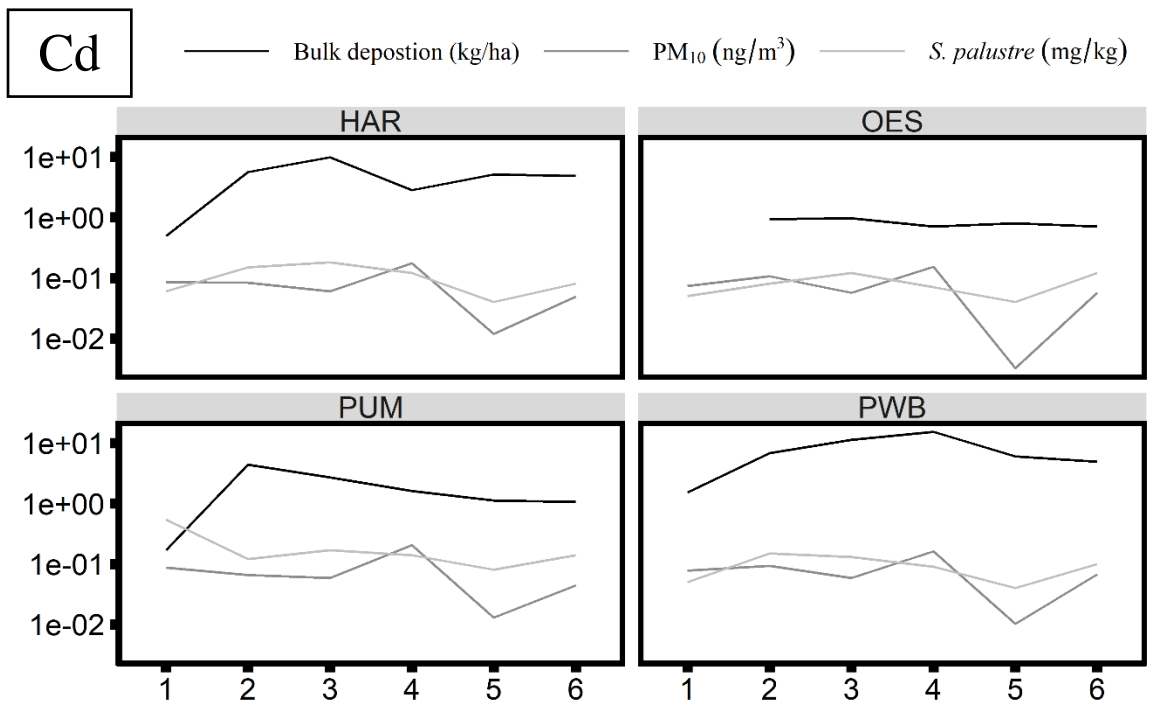
Figure S38. Timeseries showing Bulk deposition (mg/kg), ambient PM_{10} (ng/m³) and *O. lyellii* tissue concertation (mg/kg) for cobalt separated by site over 6 sampling periods. The y-axis is log transformed for visual comparison and OES bulk deposition for sampling period 1 are omitted due to 0 values from no precipitation during that period.

Figure S39. Timeseries showing Bulk deposition (mg/kg), ambient PM$_{10}$ (ng/m^3) and *S. palustre* tissue concertation (mg/kg) for cadmium separated by site over 6 sampling periods. The y-axis is log transformed for visual comparison and OES bulk deposition for sampling period 1 are omitted due to 0 values from no precipitation during that period.
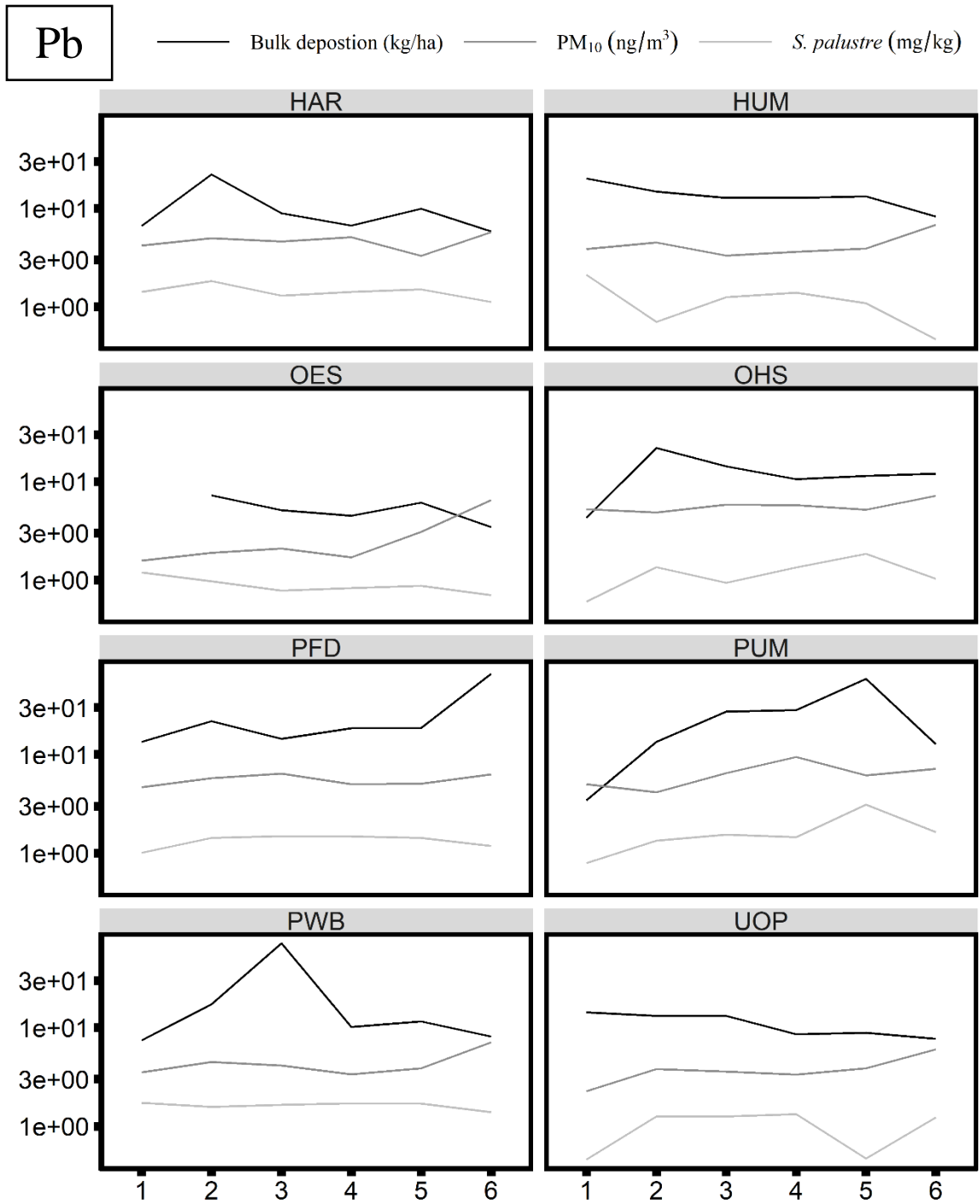
Figure S40. Timeseries showing Bulk deposition (mg/kg), ambient PM_{10} (ng/m^3) and *O. lyellii* tissue concertation (mg/kg) for cadmium separated by site over 6 sampling periods. The y-axis is log transformed for visual comparison and OES bulk deposition for sampling period 1 are omitted due to 0 values from no precipitation during that period.
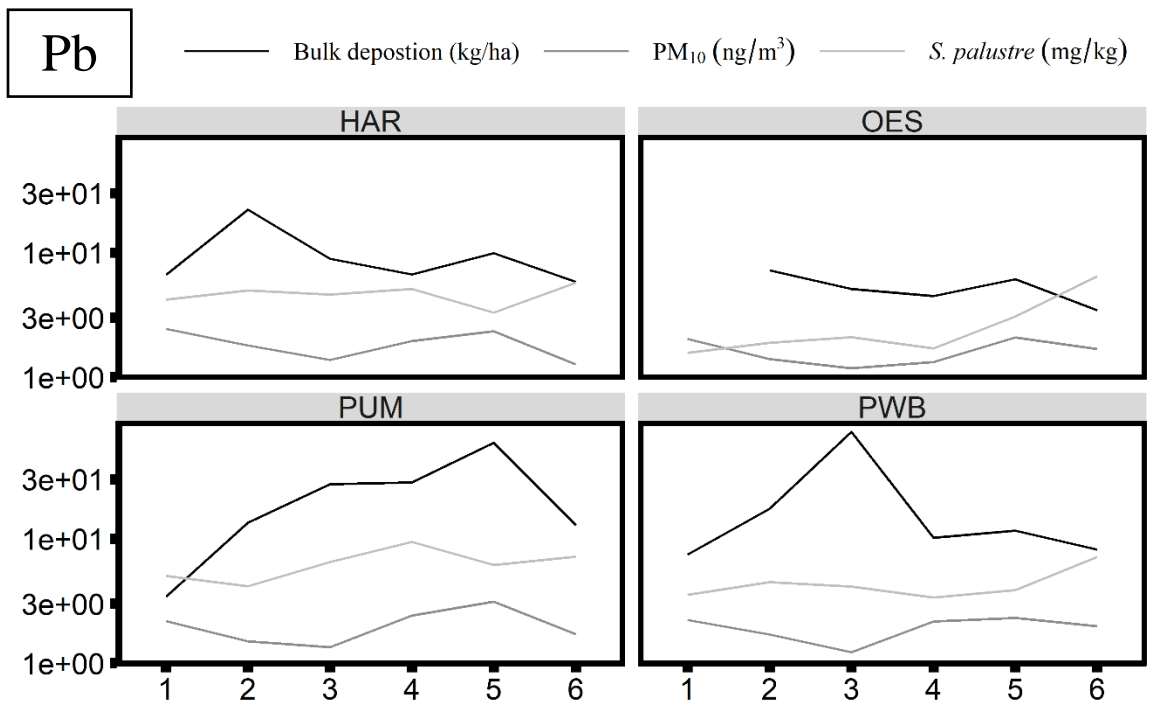
Figure S41. Timeseries showing Bulk deposition (mg/kg), ambient PM_{10} (ng/m³) and *S. palustre* tissue concertation (mg/kg) for lead separated by site over 6 sampling periods. The y-axis is log transformed for visual comparison and OES bulk deposition for sampling period 1 are omitted due to 0 values from no precipitation during that period.

Figure S42. Timeseries showing Bulk deposition (mg/kg), ambient PM_{10} (ng/m^3) and *O. lyellii* tissue concertation (mg/kg) for lead separated by site over 6 sampling periods. The y-axis is log transformed for visual comparison and OES bulk deposition for sampling period 1 are omitted due to 0 values from no precipitation during that period.
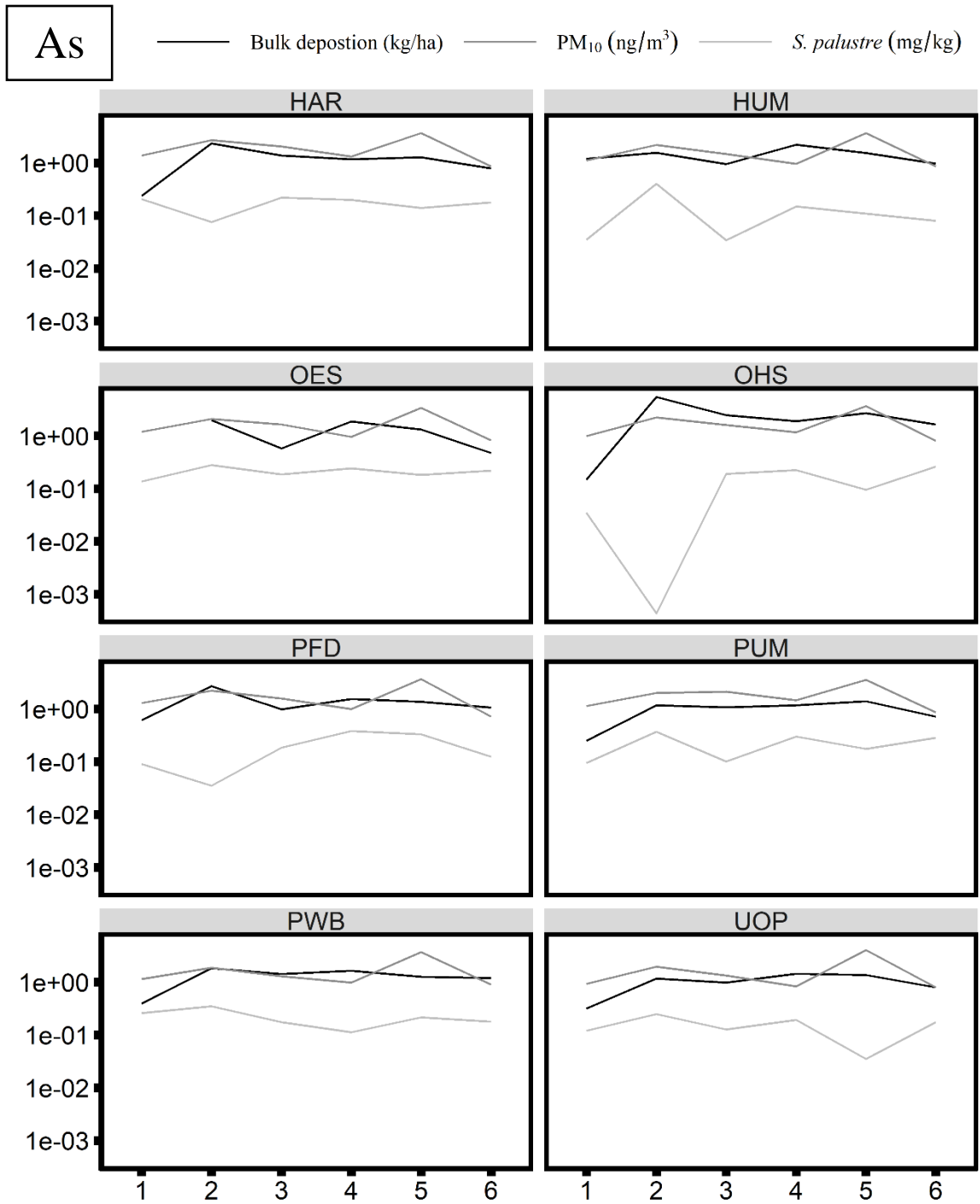
Figure S43. Timeseries showing Bulk deposition (mg/kg), ambient PM_{10} (ng/m³) and *S. palustre* tissue concertation (mg/kg) for arsenic separated by site over 6 sampling periods. The y-axis is log transformed for visual comparison and OES bulk deposition for sampling period 1 are omitted due to 0 values from no precipitation during that period.
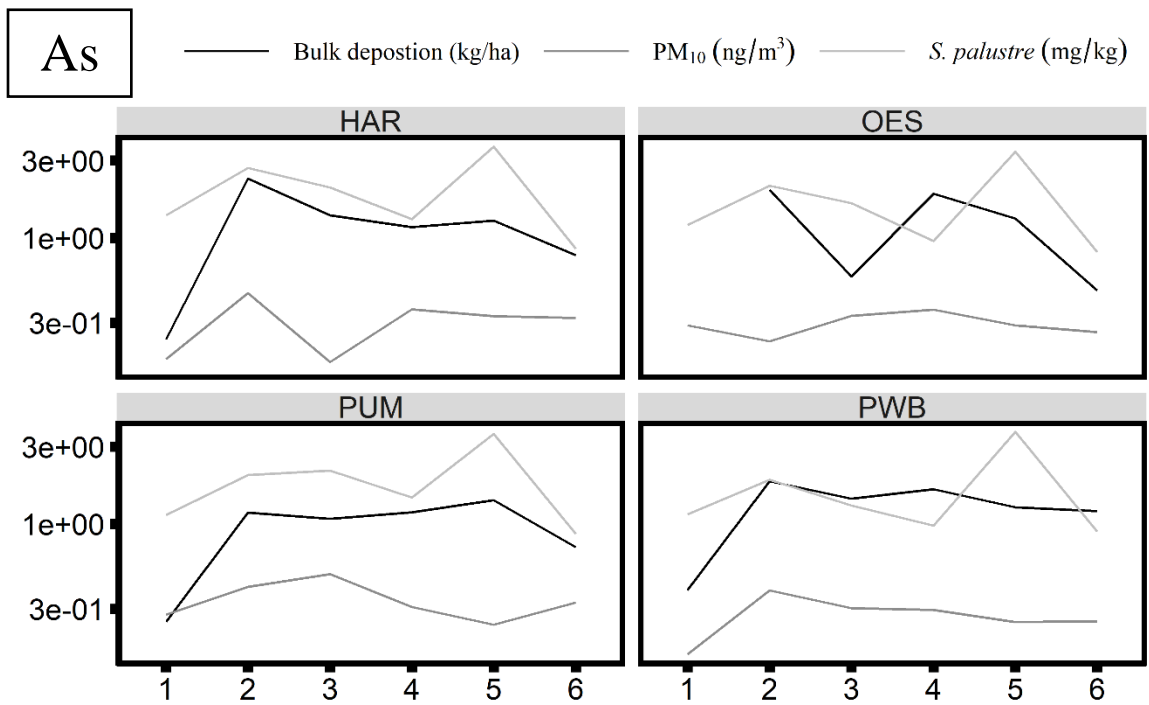
Figure S44. Timeseries showing Bulk deposition (mg/kg), ambient PM_{10} (ng/m^3) and *O. lyellii* tissue concertation (mg/kg) for arsenic separated by site over 6 sampling periods. The y-axis is log transformed for visual comparison and OES bulk deposition for sampling period 1 are omitted due to 0 values from no precipitation during that period.